Intravitreal formulations targeting the retinal vasculature in posterior segment eye diseases

Veurink, Marieke

UNIVERSITÉ DE GENÈVE

Section des Sciences Pharmaceutiques

FACULTÉ DES SCIENCES
Professeur Robert Gurny
Professeur Leonardo Scapozza

Section de Médecine Clinique
Département des Neurosciences Cliniques

FACULTÉ DE MÉDECINE
Professeur Constantin J. Pournaras

Intravitreal Formulations Targeting the Retinal Vasculature in Posterior Segment Eye Diseases

THÈSE

présentée à la Faculté des sciences de l'Université de Genève
pour obtenir le grade de Docteur ès sciences, mention sciences pharmaceutiques

par

Marieke VEURINK

de

Rheden (Les Pays-Bas)

Thèse n° 4528

GENÈVE
Atelier d'impression Repromail
2013

UNIVERSITÉ DE GENÈVE

Section des Sciences Pharmaceutiques

FACULTÉ DES SCIENCES
Professeur Robert Gurny
Professeur Leonardo Scapozza

Section de Médecine Clinique
Département des Neurosciences Cliniques

FACULTÉ DE MÉDECINE
Professeur Constantin J. Pournaras

Intravitreal Formulations Targeting the Retinal Vasculature in Posterior Segment Eye Diseases

THÈSE

présentée à la Faculté des sciences de l'Université de Genève
pour obtenir le grade de Docteur ès sciences, mention sciences pharmaceutiques

par

Marieke VEURINK

de

Rheden (Les Pays-Bas)

Thèse n° 4528

GENÈVE
Atelier d'impression Repromail
2013

UNIVERSITÉ
DE GENÈVE

FACULTÉ DES SCIENCES

Doctorat ès sciences
Mention sciences pharmaceutiques

Thèse de *Madame Marieke VEURINK*

intitulée :

" Intravitreal Formulations Targeting the Retinal Vasculature in Posterior Segment Eye Diseases "

La Faculté des sciences, sur le préavis de Messieurs R. GURNY, professeur honoraire et directeur de thèse (Section des sciences pharmaceutiques), L. SCAPOZZA, professeur ordinaire et co-directeur de thèse (Section des sciences pharmaceutiques), C. POURNARAS, professeur honoraire et co-directeur de thèse (Hôpitaux Universitaires de Genève - Clinique d'ophtalmologie – Genève, Suisse), Y. KALIA, docteur (Section des sciences pharmaceutiques), F. MUNIER, professeur (Jules-Gonin Eye Hospital – Lausanne, Suisse), A. O. URTTI, professeur (University of Helsinki – Faculty of Pharmacy – Centre for Drug Research – Helsinki, Finland), et C.G. WILSON, professeur (Strathclyde Institute of Pharmacy and Biomedical Sciences – Glasgow, United Kingdom) et Madame B. LÜCKEL, docteure (Roche Partnering – Global Research and Technologies – Bâle, Suisse), autorise l'impression de la présente thèse, sans exprimer d'opinion sur les propositions qui y sont énoncées.

Genève, le 1er février 2013

Thèse - 4528 -

Le Doyen, Jean-Marc TRISCONE

N.B. - La thèse doit porter la déclaration précédente et remplir les conditions énumérées dans les "Informations relatives aux thèses de doctorat à l'Université de Genève".

To my parents

Acknowledgments

I would like to express my sincere gratitude to Prof. Robert Gurny, Prof. Constantin J. Pournaras and Prof. Leonardo Scapozza for supervising this work.

Robert, thanks to you I was able to start my PhD here in Geneva. Thank you for all the support that you have given me in these five years, for your advice and encouragement. You always had time for a discussion and more than once you were able to convince me to look at things in a "more positive" way. Thank you for that! Moreover, you created a scientific environment in which there were many opportunities to go to conferences and courses, which I enjoyed very much.

Prof. Pournaras, thank you for accepting this collaboration. I greatly appreciated working with you and your team, learning a lot from the ophthalmic point of view during our discussions, which I always considered as very valuable, coming from a totally different background.

Leonardo, I am grateful for the way that you have taken me up in your group. You have made me feel very welcome and the "Italian atmosphere" in your group was very refreshing for a girl from the north like me. I very much enjoyed working with you and learning about modeling.

I would like to warmly thank the jury-members Prof. Francis Munier, Prof. Arto Urtti, Prof. Clive Wilson, Dr. Barbara Lückel and Dr. Yogeshvar Kalia, for having accepted to evaluate this thesis and for their valuable comments.

A big thank you to the whole team of the Vitreo-Retinal Unit at the HUG: Georgios, Stratos, Ioannis and Manu for all their help with the *in vivo* experiments. Nicole, a special thanks to you for being my personal "bridge" between the two departments!

My gratitude also goes to Maren Hennig and Prof. Arnd Heiligenhaus from the St. Franziskus Hospital in Münster, Germany for the pleasant collaboration.

I am extremely grateful to Dr. Michael Möller, Dr. Lutz Asmus, Dr. Béatrice Kaufmann, Dr. Yvonne Westermaier, Dr. Thomas Riis Johannessen, Sylvie Guinchard, Dr. Cinzia Stella and Dr. Cyrus Tabatabay for the fantastic collaboration. I greatly appreciated your help and know-how in the different projects and stages of this thesis. Without you it would not have been possible to finish this work, so many thanks to all of you!!

I thank the groups FABIP, FATEC and FABIO for the nice atmosphere in the lab. It was a real pleasure for me being here these five years! Karine, Gaëlle, Gesine, Florence M., Amandine, Claudia and Sarra: thanks to all of you for the great time we had during dinners, beers, and aerobic or yoga sessions! A special thanks goes to Nawal and Maria, my dear coffee/lunch friends, for being there for me during the last couple of years!

My old and new office buddies Marta, Ludmila, Ivana, Gianpaolo and Leo: it has been a pleasure for me sharing an office with you guys! Thanks for the discussions (scientific or sometimes more philosophical), the good laughs, and especially to Marta and Ludmila for teaching me to speak French!

Myrtha, thank you for your organizational skills, for your endless patience, for introducing me to the English Drama Society, and most of all for your great sense of humor!

And then some final words in Dutch:

Es, dank je voor je geweldige gevoel voor humor, voor je luisterend oor en voor de vele tripjes die je de afgelopen vijf jaren hierheen hebt gemaakt! Je bent en blijft m'n lievelingszus!

Pap en mam, dank jullie wel voor alles! Zonder jullie had ik dit nooit bereikt. Ik kan me geen fijnere ouders wensen!

Christian, je bent er altijd voor me. Dank je voor je relativeringsvermogen, je steun en bovenal voor wie je bent!

Table of Contents

Introduction

Drug delivery to the posterior segment of the eye presents a challenge, due to its isolated structure.[1,2] The eye is built up out of several layers, some of them avascular, which serve as barriers to protect its sensitive inner environment. Because of these barriers, the posterior segment is difficult to reach, limiting drug administration to this part of the eye.[1] Thus, conditions in which the retinal vasculature and tissues are affected are generally difficult to treat and often lead to vision loss.[2] To achieve therapeutically effective drug concentrations at the retinal tissues, different routes of administration have been investigated, including systemic, topical, periocular and intravitreal drug delivery.[1] The first three routes often fail to deliver sufficiently high drug concentrations to the posterior segment, due to the fact that the drug has to penetrate the corneoscleral or blood-ocular barrier.[3,4] Since intravitreal administration delivers the drug directly in the vitreous humor, thereby avoiding the passage of these barriers, this approach is the most straight-forward.[5] Moreover, local treatment of posterior segment diseases avoids the occurrence of side-effects that are often associated with systemic administration.[3,4] Different intraocular systems have been explored, of which intravitreal injections are the most widely used. However, a challenge that emerges from injecting small molecules into the vitreous humor is their rapid clearance from the eye.[1] Thus, to maintain therapeutic drug levels after a single injection of drug in solution, frequent re-injections are required.[3] This may affect patient compliance and increase the risk of cataract formation, retinal detachment and endophthalmitis.[3]

To improve the therapeutic efficacy of intravitreal injections, several strategies have been assessed. For instance, nano- and microparticles are able to keep the drug at the target site over a period of weeks up to months, and they are administered as conventional intravitreal injection.[6,7] By changing their size or polymer composition, the residence time of the drug can be modified, in order to meet the clinical need.[6] Disadvantage of these systems is the fact that they can lead to vitreous clouding.[6,7] Intravitreal implants are another option to increase the duration of drug action, since they release the

drug in a sustained manner, up to years.[6,8] However, most of these implants need to be placed surgically and if they are non-biodegradable, they also need to be removed from the eye, which makes this technology invasive and costly.[8]

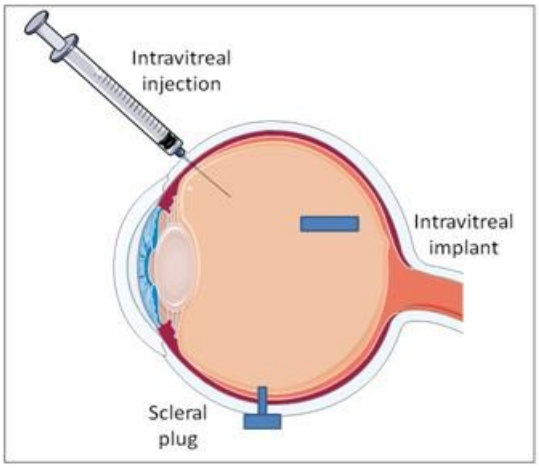

Figure 1. *Examples of intravitreal routes of administration.*

The present work investigates two alternative concepts to improve the therapeutic efficacy of intravitreal formulations and to reduce the number of intravitreal injections that is needed for an optimal therapeutic effect on the retinal vasculature. Both formulations are intended for intravitreal injection targeting the retinal vasculature. In the first part, the use of injectable and biodegradable polymer systems for the sustained release of small molecules to the retinal tissues is examined. The second part describes the combination of therapeutic antibodies with corticosteroids, aiming at the development of a stable, intravitreal combo-formulation. The idea behind this combination is that multiple injections are avoided and the interval between repetitive intravitreal injections may be prolonged, because of a synergistic effect. An attempt is made to select therapeutically inactive excipients that can be added to the antibody formulation as stabilizing agents, in order to improve the stability of the protein drug and consequently its therapeutic efficacy.

The oxygen consumption in the retina is higher than in any other tissue.[9] To comply with these high demands, oxygen and nutrients are transported to the different retinal layers in two ways: the outer

layers are in contact with the choroidal vasculature and the inner layers are nurtured by the retinal circulation.[9] When ischemic microangiopathies occur in the inner retina, the decrease in blood flow will result in the deprivation of nutrients and oxygen to certain parts of the retinal tissues.[10,11] To compensate for the hypoxia, these tissues will start over-expressing vascular endothelial growth factor A (VEGF-A), thereby stimulating uncontrolled angiogenesis, i.e. the growth of blood vessels from pre-existing vessels.[10,12] Moreover, increased VEGF-A levels induce a rise in vascular permeability,[10,12] which may lead to the development of macular edema or retinal hemorrhages,[12] thus contributing to visual impairment. Common retinal vascular diseases are diabetic retinopathy and retinal vein occlusive diseases.[13] Both are associated with VEGF-A up-regulation[14,15] and often lead to vision loss or even blindness, due to neovascularization, vascular leakage and retinal ischemia.[13] Current pharmacotherapy targeting these diseases focuses on inhibition of the secondary effects caused by angiogenesis, not on the underlying occlusive pathology.[14,15]

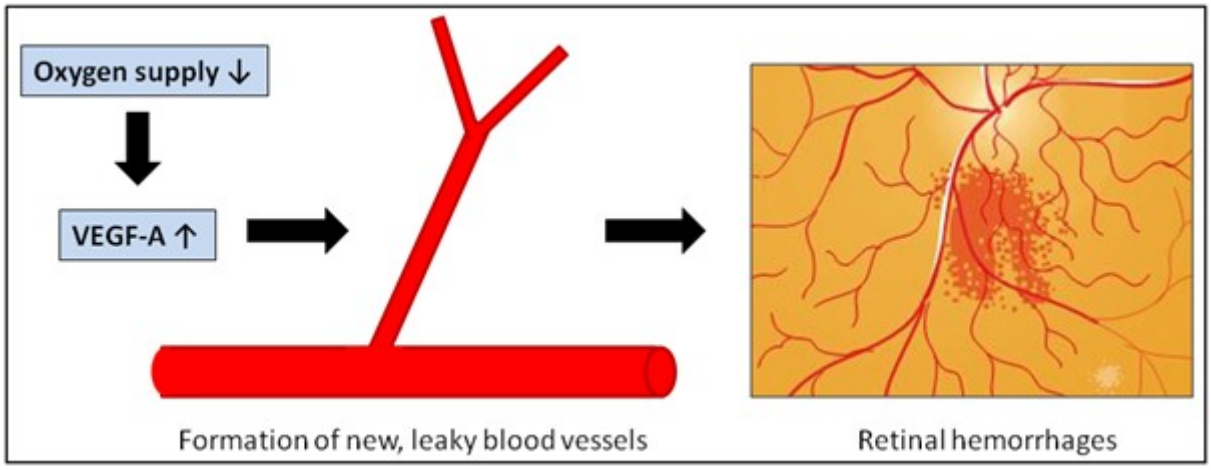

Figure 2. *Schematic representation of VEGF-A upregulation, angiogenesis and the secondary effects following hypoxia.*

In this work, an intervention earlier in the cascade is envisaged through the administration of vasodilative compounds, which might be able to overcome the initial retinal vascular occlusion.[16,17] This would ideally prevent over-expression of VEGF-A, thereby avoiding the formation of new leaky blood vessels and the subsequent secondary effects. The selected molecules are BQ123 and L-lactate,

both being able to cause vasodilation of the retinal arteries[16,17] and thus potential candidates for the treatment of vaso-occlusive diseases. The former is a cyclic pentapeptide that inhibits binding of the potent vasoconstrictor endothelin-1 to the endothelin$_A$ receptor, thereby preventing the contraction of smooth muscles cells.[18] The latter is an endogenous substance that probably causes vasodilation through stimulation of NO-synthase.[19] The subsequent increased concentration of NO will lead to activation of guanylyl cyclase and eventually to the opening of k_{ATP} channels, which will cause vasodilation.[19] Since the vasodilative effect after a single injection of L-lactate or BQ123 is short-lived,[16,17] the rationale of the first part of this work is to formulate these small molecules in a suitable drug delivery system for intravitreal injection (see Part A, Chapters 1 and 2 of the present thesis).

Whereas Part A focuses on intraocular formulations for the prevention of angiogenesis, the aim of Part B (see Chapters 3, 4 and 5) is to improve the stability of existing antibody formulations, which inhibit angiogenesis and increased permeability of the blood vessels. As described before, VEGF-A plays a major role in this process. Four principal isoforms of VEGF-A can be distinguished, among which $VEGF_{165}$ is predominant. VEGF-A binds to its receptors VEGFR1 and VEGFR2, which are both expressed on the surface of vascular endothelial cells. It has been suggested that only VEGFR2 mediates angiogenesis and increased permeability.[20] To inhibit VEGF-A from binding to VEGFR2, VEGF-A neutralizing agents have been developed.

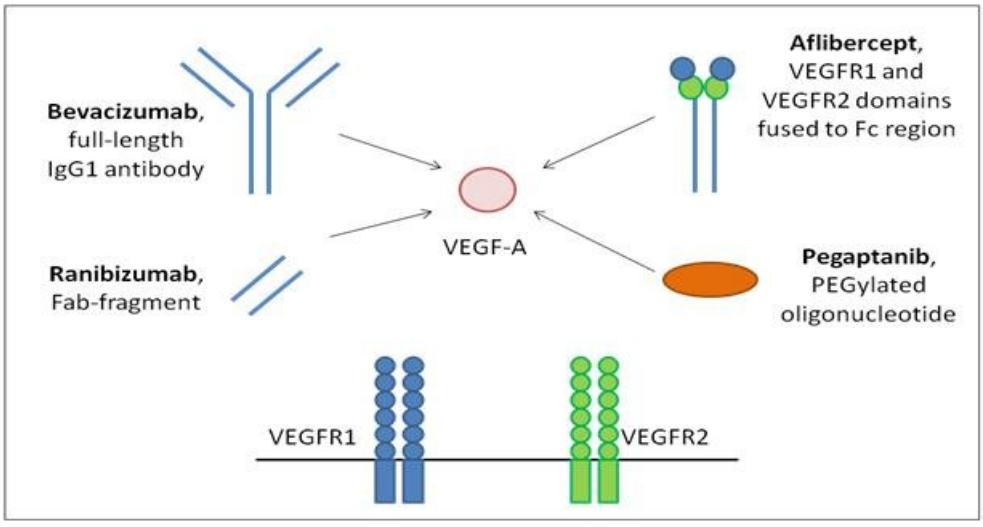

Figure 3. *VEGF-A neutralizing agents.*

The first to be registered for the treatment of a retinal vascular disease, i.e. wet age-related macular degeneration, was pegaptanib (Macugen®). This PEGylated nucleotide specifically binds to $VEGF_{165}$, thus preventing its binding to the receptor. Pegaptanib is unable to increase visual acuity, although its administration delays the loss in vision.[21] The monoclonal antibody bevacizumab (Avastin®) and its Fab-fragment ranibizumab (Lucentis®) are more effective. They are able to improve vision, since they bind to all VEGF-A isoforms, instead of only to $VEGF_{165}$.[22] Only ranibizumab has been approved for the treatment of various retinal vascular diseases, bevacizumab is on the market for the systemic treatment of different forms of cancer.[22] Nonetheless, it has been widely used off-label for intravitreal injection and has shown a similar efficacy as ranibizumab.[23] Recently, a new anti-VEGF agent has been approved by the FDA. Aflibercept (Eylea®), also known as VEGF Trap-Eye, is a fusion protein in which the Fc region of an IgG1 antibody is combined with parts of VEGFR1 and VEGFR2.[24] Aflibercept has a higher binding affinity for VEGF than ranibizumab and therefore, the duration of action can be prolonged compared to ranibizumab injections, while the clinical effect stays equivalent.[24]

Alongside anti-VEGF agents, corticosteroids are widely used for treatment of retinal vascular diseases, since they reduce vascular permeability and down-regulate VEGF-A.[15] Several groups have reported co-administration of bevacizumab with a corticosteroid,[25-27] with as incentive a potential synergistic effect, since angiogenesis and inflammation are believed to be interdependent processes. To our knowledge, however, possible interactions between the antibody and the anti-inflammatory drug have never been taken into account. Since therapeutic antibody formulations are prone to aggregation,[28] such interactions may influence the stability of the protein drug, potentially leading to reduced efficacy or immunogenicity problems. Hence, aggregation should be prevented whenever possible. Therefore, the aim of part B is the development of stable antibody formulations for intravitreal injection. This is achieved through the development of a formulation in which the antibody is combined with a corticosteroid or through the identification of therapeutically inactive excipients that act as stabilizing agents.

To summarize, the objective of the present thesis is the development of formulations for intravitreal injection that are targeting the retinal vasculature. The focus of Part A lies on prevention of angiogenesis, through the sustained release of vasoactive compounds that are able to overcome retinal vascular occlusions. Injectable and biodegradable polymer systems, based on α-hydroxy acids, are investigated as carriers or prodrugs for this application. Part B aims at improvement of existing formulations that act against VEGF-A, thus inhibiting angiogenesis. Therapeutic antibodies are combined with corticosteroids or with small therapeutically inactive excipients. Goal of the former is a stable combo-formulation that might cause a synergistic effect, purpose of the second is to prevent aggregate formation in the antibody formulation.

References

1. Trimawithana TR, Young S, Bunt CR, Green C, Alany RG. Drug delivery to the posterior segment of the eye. *Drug Discov Today* 2011; 16: 270-277.

2. Duvvuri S, Majumdar S, Mitra AK. Drug delivery to the retina: challenges and opportunities. *Expert Opin Biol Ther* 2003; 3: 45-56.

3. Herrero-Vanrell R, Refojo MF. Biodegradable microspheres for vitreoretinal drug delivery. *Adv Drug Deliv Rev* 2001; 52: 5-16.

4. Velez G, Whitcup SM. New developments in sustained release drug delivery for the treatment of intraocular disease. *Br J Ophthalmol* 1999; 83: 1225-1229.

5. Eljarrat-Binstock E, Pe'er J, Domb AJ. New techniques for drug delivery to the posterior eye segment. *Pharm Res* 2010; 27: 530-543.

6. Short BG. Safety evaluation of ocular drug delivery formulations: techniques and practical considerations. *Toxicol Pathol* 2008; 36: 49-62.

7. Del Amo EM, Urtti A. Current and future ophthalmic drug delivery systems: a shift to the posterior segment. *Drug Discov Today* 2008; 13: 135-143.

8. Lavik E, Kuehn MH, Kwon YH. Novel drug delivery systems for glaucoma. *Eye* 2011; 25: 578-586.

9. Robinson JC. Ocular anatomy and physiology relevant to ocular drug delivery, in: A.K. Mitra, Ophthalmic drug delivery systems Vol. 58, Marcel Dekker Inc., New York, 1993, pp. 29-57.

10. Pournaras CJ, Rungger-Brändle E, Riva CE, Hardarson H, Stefansson E. Regulation of retinal blood flow in health and disease. *Prog Retin Eye Res* 2008; 27: 284-330.

11. Stitt AW, O'Neill CL, O'Doherty MT, Archer DB, Gardiner TA, Medina RJ. Vascular stem cells and ischaemic retinopathies. *Prog Retin Eye Res* 2011; 30: 149-166.

12. Witmer AN, Vrensen GFJM, Van Noorden CJF, Schlingemann RO. Vascular endothelial growth factors and angiogenesis in eye disease. *Prog Retin Eye Res* 2003; 22: 1-29.

13. Zhang K, Zhang L, Weinreb RN. Ophthalmic drug discovery: novel targets and mechanisms for retinal diseases and glaucoma. *Nat Rev Drug Discov* 2012; 11: 541-559.

14. Hahn P, Fekrat S. Best practices for treatment of retinal vein occlusion. *Curr Opin Ophthalmol* 2012; 23: 175-181.

15. Rechtman E, Harris A, Garzozi HJ, Ciulla TA. Pharmacologic therapies for diabetic retinopathy and diabetic macular edema. *Clin Ophthalmol* 2007; 1: 383-391.

16. Stangos AN, Petropoulos IK, Pournaras JA, Mendrinos E, Pournaras CJ. The vasodilatory effect of juxta-arteriolar microinjection of endothelinA receptor inhibitor in healthy and acute branch retinal vein occlusion minipig retinas. *Invest Ophthalmol Vis Sci* 2010; 51: 2185-2190.

17. Mendrinos E, Petropoulos IK, Mangioris G, Tsilimbaris MK, Papadopoulou DN, Geka A, Pournaras CJ. Vasomotor effect of intravitreal juxta-arteriolar injection of L-lactate on the retinal arterioles after acute branch retinal vein occlusion in minipigs. *Invest Ophthalmol Vis Sci* 2011; 52: 3215-3220.

18. Ihara M, Ishikawa K, Fukuroda T, Saeki T, Funabashi K, Fukami T, Suda H, Yano M. In vitro biological profile of a highly potent novel endothelin (ET) antagonist BQ-123 selective for the ET_A receptor. *J Cardiovasc Pharmacol* 1992; 20: S11-S14.

19. Hein TW, Xu W, Kuo L. Dilation of retinal arterioles in response to lactate: role of nitric oxide, guanylyl cyclase, and ATP-sensitive potassium channels. *Invest Ophtalmol Vis Sci* 2006; 47: 693-699.

20. Ferrara N, Hillan KJ, Gerber HP, Novotny W. Discovery and development of bevacizumab, an anti-VEGF antibody for treating cancer. *Nat Rev Drug Discov* 2004; 3: 391-400.

21. Gragoudas ES, Adamis AP, Cunningham ET Jr, Feinsod M, Guyer DR. VEGF inhibition study in ocular neovascularization clinical trial group. *N Engl J Med* 2004; 351: 2805-2816.

22. Ciulla TA, Rosenfeld PJ. Antivascular endothelial growth factor therapy for neovascular age-related macular degeneration. *Curr Opin Ophthalmol* 2009; 20: 158-165.

23. Davis J, Olsen TW, Stewart M, Sternberg P Jr. How the comparison of age-related macular degeneration treatments trial results will impact clinical care. *Am J Ophthalmol* 2011; 152: 509-514.

24. Ohr M, Kaiser PK. Intravitreal aflibercept injection for neovascular (wet) age-related macular degeneration. *Expert Opin Pharmacother* 2012; 13: 585-591.

25.Ahmadieh H, Taei R, Riazi-Esfahani M, Piri N, Homayouni M, Daftarian N, Yaseri M. Intravitreal bevacizumab versus combined intravitreal bevacizumab and triamcinolone for neovascular age-related macular degeneration. *Retina* 2011; 31: 1819-1826.

26. Augustin AJ, Puls S, Offermann I. Triple therapy for choroidal neovascularization due to age-related macular degeneration: Verteporfin PDT, bevacizumab and dexamethasone. *Retina* 2007; 27: 133-140.

27. Bakri SJ, Couch SM, McCannel CA, Edwards AO. Same-day triple therapy with photodynamic therapy, intravitreal dexamethasone, and bevacizumab in wet age-related macular degeneration. *Retina* 2009; 29: 573-578.

28. Wang W, Nema S, Teagarden D. Protein aggregation – pathways and influencing factors. *Int J Pharm* 2010; 390: 89-99.

Design and *in vitro* assessment of L-lactic acid-based copolymers as prodrug and carrier for intravitreal sustained L-lactate release to reverse retinal arteriolar occlusions

Marieke Veurink[1], Lutz Asmus[1], Maren Hennig[2], Béatrice Kaufmann[1], Lena Bagnewski[2], Arnd Heiligenhaus[2], Efstratios Mendrinos[3], Constantin J. Pournaras[3], Robert Gurny[1], Michael Möller[1]

[1]School of Pharmaceutical Sciences, University of Geneva, University of Lausanne, 1211, Geneva, Switzerland; [2]Department of Ophthalmology at St. Franziskus Hospital, Muenster, Germany; [3]Department of Ophthalmology, Geneva University Hospitals, 1211, Geneva, Switzerland

Published in: European Journal of Pharmaceutical Sciences, 2013; 49: 233-240

Ophthalmic conditions in which the retinal vasculature is obstructed generally lead to vision loss. Administration of the vasodilator L-lactate might offer a treatment strategy by restoring the blood flow, but unfortunately its effect after single intravitreal injection is short-lived. This study describes a concept in which the sustained release of L-lactic acid from a biodegradable copolymer system is investigated. The 50:50 (n/n) copolymer system, composed of L-lactic acid and L,D-2-hydroxyoctanoic acid, is a viscous injectable that will form an intravitreal drug depot. Hydrolysis of the copolymer will automatically lead to the release of L-lactic acid, which will convert to L-lactate at physiological pH, thereby providing a carrier and pro-drug in one. *In vitro* and *ex vivo* release studies demonstrate an L-lactic acid release over several weeks. Biocompatibility of the co-polymer and its degradation products is shown on a human retinal pigment epithelial cell line and on *ex vivo* retinal tissues. A low molecular weight copolymer (1200 g/mol) with low polydispersity has promising properties with a constant release profile, good biocompatibility and injectability.

Keywords: L-lactate, retinal vasodilation, biocompatibility, biodegradable copolymers, sustained release, intravitreal injection.

INTRODUCTION

Many sight threatening ophthalmic conditions cause obstruction of the retinal vasculature. Such posterior segment diseases might be treated by administration of vasodilative drugs, which restore the blood flow in the obstructed vessels. The retinal vasculature lacks autonomic innervations[1] and therefore, retinal blood flow is most probably controlled locally through the release of vasoactive substances by the retinal tissues.[2] Although the exact mechanism of retinal vasodilation has not been fully elucidated, the endogenous compound L-lactate is involved in this mechanism because its intravenous administration results in dilation of retinal vessels.[3] Moreover, intravitreal injections of L-lactate in mini-pigs induce vasodilation of retinal arteries both in healthy eyes and in eyes in which acute branch retinal vein occlusion is evoked.[4-6] Based on these observations and on the fact that L-lactate is an endogenous substance present in the eye, it is envisaged a potential drug candidate for the treatment of posterior segment diseases in which the retinal vasculature is obstructed. However, one major disadvantage of a single intravitreal injection of an L-lactate solution is its limited duration of action of approximately 15 minutes.[4] This is due to the fact that elimination from the eye depends on the size of the molecule, resulting in short half-lives for molecules like L-lactate (Mw 89 Da) with a molar mass < 500 Da. Consequently, frequent injections are necessary to maintain therapeutic drug levels.[7] In order to prolong the therapeutic effect, a sustained intraocular release system is envisaged, ideally releasing L-lactate over a period of several weeks. The therapeutic benefit of such a system would be an immediate intervention to overcome the vascular obstruction, thereby preventing angiogenesis and giving time to plan further surgery.

For a suitable intraocular sustained release formulation, several challenges and limitations should be taken into account. First, the volume of injection is linearly related to the intraocular pressure (IOP),[8] limiting the formulation volume that can be administered. Currently used volumes do not exceed 0.1 ml per injection.[9] Second, posterior segment diseases are difficult to treat because of the layer-like structure of the eye, which serves as protection barrier for the sensitive inner environment, reducing its accessibility to drugs. The most successful routes of administration are intravitreal injections and implants that are placed in the vitreous humor or sutured onto the sclera.[10,11] The advantage of

implants is that they offer a sustained release of drugs over a prolonged period of time, up to years. However, drawbacks of most implants that are currently on the market, like Vitrasert® and Retisert®, include high costs and invasiveness, due to the fact that they need to be surgically introduced in the vitreous.[12] Furthermore, they are not biodegradable and eventually need to be removed from the eye. Thus, to avoid invasiveness and high costs associated with surgery, we opt for a sustained release formulation that can be administered by conventional intravitreal injection, keeping the injection volume low to prevent an undesirable rise in IOP.

The sustained release of L-lactic acid from a polymer built up with L-lactic acid subunits, like poly(L-lactic acid) (PLA), is selected as a starting point for the sustained release formulation. The idea behind this choice is the fact that L-lactic acid, being a subunit of the polymer chain, will be released automatically through hydrolysis of the ester bonds, directly forming free L-lactate at physiological pH. Therefore, such a polymer system may serve as a carrier and a prodrug in one. However, PLA is a solid, which is degrading too slowly for a sufficient release. To change the polymer from a solid into a viscous injectable, plasticizers may be added.

Herein, the concept of an L-lactic acid based copolymer system is investigated, in which 50% (n/n) of the methyl groups of PLA are substituted by hexylgroups, serving as internal plasticizers.[13] The result is a viscous biodegradable copolymer system, poly(L-lactic acid-*co*-L,D-2-hydroxyoctanoic acid) that in theory meets the requirements for the intravitreal sustained release of L-lactic acid, being:

1) a viscous injectable suitable for conventional intravitreal injection.
2) an L-lactate prodrug/carrier system that forms a drug depot in the vitreous humor, releasing L-lactic acid upon hydrolysis of the copolymer.

The degradation and degradation profile of poly(2-hydroxyoctanoic acid) by hydrolysis were demonstrated in earlier work by Trimaille et al.[14] *In vitro* and *ex vivo* investigations are performed, aiming at the development of a system that is biocompatible with retinal tissues, releases therapeutic doses of L-lactic acid and is injectable by intravitreal injection.

MATERIALS

2-hydroxypropionic acid (L-lactic acid), 3,6-dimethyl-1,4-dioxane-2,5-dione (dilactide) and sodium L-lactate were obtained from Sigma Aldrich (St. Louis, USA). 2-hydroxyoctanoic acid was synthesized as described by Trimaille et al.[14]

METHODS

Polymerization and formulation preparation

Polymerization and purification of the random-order poly(L-lactic acid-*co*-L,D-2-hydroxyoctanoic acid) copolymers were performed as described for hexylsubstituted poly(lactic acid) by Asmus et al.,[13] whereby L-lactic acid was reacted with 2-hydroxyoctanoic acid in a 50:50 molar ratio. In short, a melt polycondensation was performed at 150°C under vacuum leading to a quantitative yield. At this reaction temperature, preservation of the L-form of lactic acid is expected.[15] In the case of low polydisperse copolymers, monomers and short oligomers were removed by precipitation into cold 1 M sodium bicarbonate solutions followed by decantation and drying under vacuum. The molecular weight (M_w) and polydispersity index (PDI) (M_w/M_n) of the copolymers were determined by gel permeation chromatography. A calibration was done with 8 polystyrene standards (PSS, Mainz, Germany) with known M_w and M_n. A Waters 515 HPLC pump, Waters 410 injector, Styragel HR 1-4 columns and Waters 2414 refractive index detector (Waters Corporation, Milford, USA) were used with tetrahydrofuran as continuous phase.

Three copolymer systems were compared:

1) 50:50 n/n poly(L-lactic acid-*co*-L,D-2-hydroxyoctanoic acid), M_w of 1200 g/mol, PDI of 1.5
2) 50:50 n/n poly(L-lactic acid-*co*-L,D-2-hydroxyoctanoic acid), M_w of 1400 g/mol, PDI of 2.6
3) 50:50 n/n poly(L-lactic acid-*co*-L,D-2-hydroxyoctanoic acid), M_w of 2500 g/mol, PDI of 1.5
    a. With 5% of additional sodium L-lactate
    b. With 10% of additional sodium L-lactate

Sodium L-lactate incorporation into the copolymer was achieved by cryomilling (SPEX 6700 freezer/mill, SPEX SamplePrep, Metuchen, USA) during 5 minutes.

Injectability

The injectability of the copolymers was tested *in vitro*, using a 1 ml Tuberculin syringe (Norm-Ject, Henke-Sass, Wolf GmbH, Tuttlingen, Germany) with a 21-gauge needle (0.8 mm x 25 mm) (BD Medical, Franklin Lakes, USA). All formulations were warmed to 37°C and 100 µl of copolymer were injected into sodium phosphate buffer to mimic an application in clinic with minimal discomfort for the patient and to exclude an influence of the temperature on viscosity.[13] Injectability was considered sufficient if the formulation could be manually pushed through the 21-gauge needle.

***In vitro* and *ex vivo* L-lactic acid release studies**

Study design

L-lactic acid release from the different copolymers was studied over time *in vitro*. A quantity of 100 µl of copolymer, equivalent to the quantity that would be used *in vivo*, was placed in 25 ml 150 mM sodium phosphate buffer at pH 7. This buffer strength and volume were chosen to maintain a constant pH, which simulates the ocular buffering capacity. Because of the good solubility of L-lactic acid at pH 7, sink conditions were met during all studies. The release tests were performed at 37°C under light shaking conditions during the entire study period. Samples of 50 µl of release medium were taken at different time points to measure the amount of released L-lactic acid; this volume was replaced by fresh medium after each sample collection. A similar study was carried out in porcine vitreous humor with 0.2% sodium azide to avoid bacterial growth (*ex vivo* tests), in order to study the influence of enzymes on the release rate.

Sample analysis

The amount of L-lactic acid released from the copolymers was quantified by ultra performance liquid chromatography (UPLC Acquity system, Waters Corporation, Milford, USA) coupled with UV detection at 210 nm. Chromatographic separation was accomplished at 25°C using an Acquity HSS T3 column (1.8 µm, 2.1x50 mm). A phosphate buffer at pH 2.5 was used as mobile phase with a flow rate of 0.2 ml/min. In a first step of method development, standard solutions of L-lactic acid and of dilactide were injected separately to assess their retention time, showing a clear baseline separation

between the two peaks. Thereafter, the copolymer was subjected to stress conditions (1 hour in phosphate buffer at pH 1.9) and analyzed. The L-lactic acid peak was identified in the stressed sample, having an identical retention time as the L-lactic acid standard solution. Since endogenous L-lactic acid is already present in the *ex vivo* vitreous humor, L-lactic acid was quantified in a blank vitreous humor sample and subtracted from the other samples to obtain the concentration of L-lactic acid that was released from the system. The final degradation product of poly(2-hydroxyoctanoic acid), 2-hydroxyoctanoic acid, was quantified by UPLC, using an Acquity BEH C18 column (1.7µm, 2.1 x 50 mm) at 40°C. An 80:20 (v/v) mixture of phosphate buffer pH 2.5 and isopropanol was applied as mobile phase at 0.3 ml/min. All samples were acidified to pH 2.0 ± 0.2 before analysis and a sample volume of 6 µl was injected. Data are presented as mean ± standard deviation (SD).

Ex vivo biocompatibility studies

Biocompatibility with ARPE-19 cells

The biocompatibility of 2-hydroxyoctanoic acid and L-lactic acid was tested on a human retinal pigment epithelial cell line (ARPE-19 cells). The ARPE-19 cells were cultured for 3 days and viability of the cells was determined by performing a 3-(4,5-dimethylthiazol-2-yl)-2,5-diphenyltetrazolium bromide test (MTT-test) (n=5).[16] L-lactic acid concentrations ranged from 0.5 mM to 500 mM (in water), and 2-hydroxyoctanoic acid concentrations from 0.1 mM to 100mM (in ethanol). Results were compared with the blank solutions, e.g. water in the case of L-lactic acid and ethanol for 2-hydroxyoctanoic acid. The viability of ARPE-19 cells in medium was normalized to 100%. The viability of the cells exposed to L-lactic acid, 2-hydroxyoctanoic acid, water or ethanol was calculated based on the medium control (100% viability). Statistical differences were calculated using a paired t-test ($p<0.05$).

Biocompatibility with post mortem porcine eyes

Porcine eyes were provided by a slaughterhouse and used immediately. The anterior segment and vitreous body were carefully removed to access the retinal tissues. The biocompatibility of the two degradation products of the copolymer, L-lactic acid and 2-hydroxyoctanoic acid, was investigated by

placing 100 µl of the substance in direct contact with the retinal tissues, in concentrations ranging from 1 mM to 300 mM in 75% (v/v) aqueous ethanol. A positive and a negative control were always placed on a part of the same eye. The positive control, a highly concentrated 300 mM 2-hydroxy octanoic acid in a 75% (v/v) aqueous ethanol solution caused formation of white stains on the retinal tissues, whereas the negative control of 75% (v/v) aqueous ethanol solution did not show any adverse events. The three copolymer formulations were tested as well, again by placing 100 µl in direct contact with the retinal tissues. Effects on the retina were observed by visual inspection over a period of 1.5 hours. In parallel, the posterior segments that were placed in contact with above mentioned substances were fixed with 4% v/v formaldehyde in phosphate buffer for histological examination of the retinal tissues. The fixed tissues were embedded in paraffin and cut in serial sections of 7 µm. Thereafter, five sections were stained with hematoxilin and eosin using a standard protocol.

RESULTS AND DISCUSSION

The aim of this paper is to study a concept in which L-lactic acid is released in a controlled way through the degradation of an L-lactic acid based copolymer system. The envisaged application of the formulation is an easy intravitreal injection, forming a single copolymer droplet in the vitreous humor that serves as a drug depot for L-lactic acid, which will directly convert to L-lactate at physiological pH. L-lactate is selected since it is an endogenous substance, which causes vasodilation of the retinal arteries after single injection. The proposed underlying mechanism of action for the vasodilative effect is an L-lactate dependent activation of nitric oxide synthase (NOS). The production of nitric oxide causes activation of guanylyl cyclase and a subsequent opening of k_{ATP} channels, leading to vasodilation.[17] Since maintaining a vasodilative response over a prolonged period of time is the goal of the novel formulation, L-lactate needs to be able to activate NOS repeatedly, to reproduce its vasodilative effect on the same retinal vessels. An *ex vivo* study by Hein et al.[17] reported on the vasomotor action of different L-lactate concentrations on isolated retinal arterioles. Recurrent exposure of these arterioles to L-lactate resulted in vasodilation without loss in effect,[17] confirming that L-lactate indeed is able to dilate the retinal vessels repeatedly.

Injectability

The 50:50 n/n poly(L-lactic acid-*co*-L,D-2-hydroxyoctanoic acid) copolymer was selected as the optimal formulation for an injectable system that releases sufficient amounts of L-lactic acid. This selection was based on tests with copolymers with varying molar ratios between L-lactic acid and 2-hydroxyoctanoic acid. A higher ratio of L-lactic acid increased the viscosity of the copolymer, leading to difficulties in injectability. Lowering the amount of L-lactic acid in the system decreased its viscosity; however it also led to a decreased L-lactic acid dose that was released (results not shown). Thus, the 50:50 molar ratio is the optimal compromise between good injectability and sufficient L-lactic acid dosing. A second property that influences the injectability of the system is the polydispersity of the copolymer: a copolymer with higher PDI contains short oligomer chains and is therefore less viscous than a system with lower PDI. For this reason, two copolymers with comparable molecular weights but with different polydispersity indices were included in the study. Finally, the choice for low molecular weight copolymers was based on the fact that they are less viscous and therefore easier to inject than higher molecular weight polymers.[13]

A summary of the injectability data is presented in Table 1. The copolymers without additional free sodium L-lactate were injectable through the 21-gauge needle, and settled as a single bubble on the bottom of the vial. The choice for using a 21-gauge needle, being a large diameter for intravitreal injection, was justified by the fact that a similar needle size (22-gauge) is used in clinics for the injection of Ozurdex®.[18] The incorporation of free sodium L-lactate in the formulation caused a rise in viscosity, which made injection difficult. A way to solve this problem may be the incorporation of a low percentage of external plasticizer, like *N*-methyl-2-pyrrolidone, which is widely accepted for parenteral formulations.[19] However, since this study aims at the development of a copolymer formulation with as few excipients as possible, the use of external plasticizers was not considered in the current work. In future formulation development, needle size and syringe dimensions could be adjusted towards smaller gauge needles.

Table 1. *Summary on biocompatibility, L-lactic acid release and injectability of the different poly(L-lactic acid-co-L,D-2-hydroxyoctanoic acid) copolymers.*

Type of copolymer (M_W, PDI)	Biocompatibility (*ex vivo* porcine eyes)	Therapeutically effective dose released*	Injectability
1) 50:50 n/n copolymer, (1200 g/mol, 1.5)	 Good	Yes	Good
2) 50:50 n/n copolymer, (1400 g/mol, 2.6)	 Adverse Events	Yes	Good
3) 50:50 n/n copolymer, (2500 g/mol, 1.5) + 5% or 10% free L-lactate	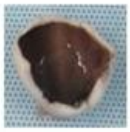 Good	Only over the first 48 hours	Insufficient

**Based upon extrapolation of data from Brazitikos et al.*[4]

In vitro and *ex vivo* L-lactic acid release

In vitro L-lactic acid release from pure poly(L-lactic acid-co-L,D-2-hydroxyoctanoic acid)

An *in vitro* release study was performed to compare two 50:50 n/n poly(L-lactic acid-*co*-L,D-2-hydroxyoctanoic acid) copolymers with similar molecular weights but different polydispersity indices (Formulations 1 and 2). The pH of the release medium was kept at 7.0 ± 0.2 during the study, which is similar to the pH of human vitreous humor (pH 7.0-7.4).[20] Such constant pH is important, to avoid accelerated hydrolysis of the copolymer due to a decrease in pH caused by the release of L-lactic acid and 2-hydroxyoctanoic acid. Figure 1 depicts the release profiles, presented as milligrams of L-lactic acid released per day. For the formulation with the higher PDI, an initial burst release of 10.5 mg L-lactic acid was observed during the first day, corresponding to 30.3 ± 0.1% of the total amount of L-lactic acid present. Thereafter, an almost linear release was detected, resulting in an amount between 1 and 3 mg of L-lactic acid released per day. The copolymer with the lower polydispersity released L-lactic acid much slower and without an initial burst: a constant release of around 0.9 mg L-lactic acid released per day was observed. In both *in vitro* studies, the hydrophobic drug depot remained present as a single droplet over the complete study duration. Therefore, clearance as such is not expected, since the droplet is much too big to cross the retinal barriers. The pronounced burst release of the

copolymer with high PDI results from the larger amount of small oligomers present. These small oligomers are soluble in the buffer solutions, and degrade faster to monomer entities, thus promoting interaction with the surrounding water towards release and dissolution of the L-lactic acid. When the water soluble oligomers were removed beforehand from this polymer, leading to a copolymer with a lower PDI, no burst occurred. The zero order release indicates that L-lactic acid is released from the copolymer by pure surface degradation of the depot droplet.

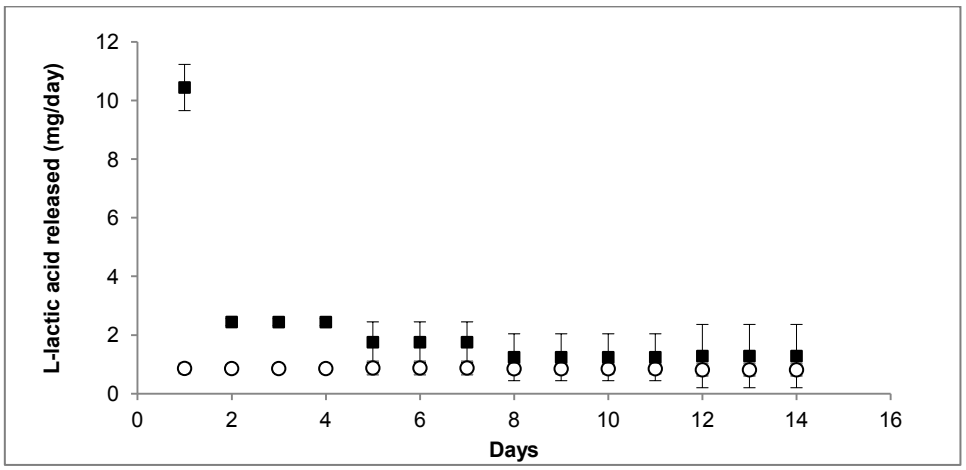

Figure 1. *Influence of polydispersity on the in vitro release of L-lactic acid (mg/day). Dissolution media: 150 mM sodium phosphate buffer, pH 7; n=6 (2 separate vials, 3 analyses per vial per time point); mean values ± SD are presented. 100% release corresponds to 37 mg L-lactic acid.*

○ = copolymer with low polydispersity, MW 1200 g/mol, PDI 1.5;

■ = copolymer with high polydispersity, MW 1400 g/mol, PDI 2.6

In vitro L-lactic acid release from poly(L-lactic acid-co-L,D-2-hydroxyoctanoic acid) with incorporated sodium L-lactate

The initial burst release as observed for the high polydisperse copolymer might be advantageous in the treatment of vascular obstruction: occlusion of the retinal vasculature is an event requiring immediate intervention and therefore a fast initial release of L-lactic acid is envisioned. However, the burst obtained with the high polydisperse copolymer cannot be controlled easily. Therefore, an alternative strategy was explored to obtain a similar release behavior; an additional extent of sodium L-lactate was added to the low polydisperse copolymer matrix-drug.

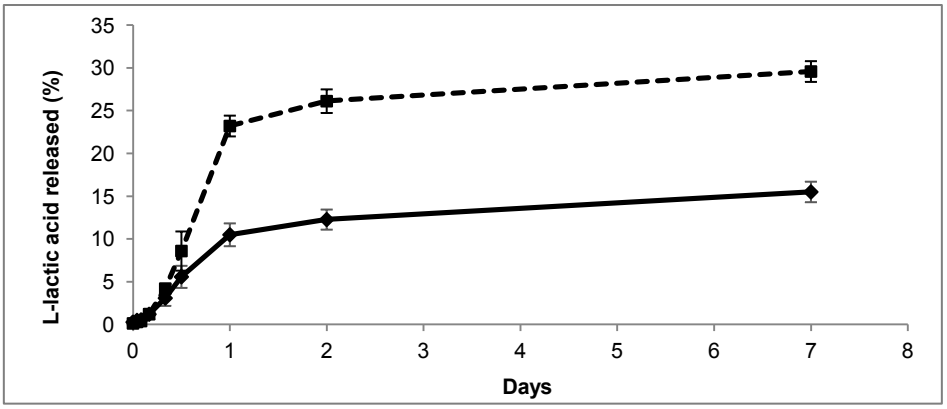

Figure 2. *Influence of the percentage of additional sodium L-lactate on the in vitro release of L-lactic acid. Dissolution media: 150 mM sodium phosphate buffer, pH 7; n=9 (3 separate vials, 3 analyses per vial per time point); mean percentages ± SD are presented. 100% release corresponds to 41 mg L-lactate for the formulation with 5% additional L-lactate and to 47 mg for the 10% formulation.*

… copolymer with 10% additional sodium L-lactate, MW 2500 g/mol, PDI 1.5

— copolymer with 5% additional sodium L-lactate, MW 2500 g/mol, PDI 1.5

For the copolymer formulations containing 5% or 10% free L-lactate, respectively, an initial burst release was observed (Figure 2). This burst almost completely depended on the amount of free L-lactate that is present and not on hydrolysis of the copolymer. For the 5% formulation, 10.5 ± 1.3% L-lactic acid was released in the first 24 hours, corresponding to 4.3 mg. The release from day 1 up to day 7 was much slower: only an additional 5% of L-lactic acid was released, leading to a final amount of 6.4 mg L-lactic acid after 7 days. A similar release profile was observed for the 10% formulation: an initial burst could be distinguished on the first day, releasing 23.2 ± 1.2% or 10.9 mg L-lactic acid. Thereafter, the release rate depended on the degradation of the copolymer; after 7 days 29.6 ± 1.2% or 13.9 mg was present in the release media. Since the burst does not depend on hydrolysis of the copolymer, but on the amount of incorporated sodium L-lactate, it can be controlled by the percentage of free L-lactate that is added, allowing adaption to the clinical need.

Estimated required dose versus amount released in vitro

In order to estimate the required L-lactic acid dose that should be released per day to maintain a therapeutic effect, results published by Bratizikos et al.[4] were used. In a mini pig model, a vasodilative effect was observed after a single juxta arteriolar injection of 0.2 µl 0.5M L-lactate, corresponding to

an amount of 0.01 mg. The effect was maintained for around 15 minutes, with a maximal vasodilative effect between 3 and 6 minutes after injection. Based on these results, the required L-lactate dose per day was calculated to be 0.85 mg of L-lactate needed per day to maintain a vasodilative effect. Of course, it should be taken into account that these calculations were based upon a single injection. Since the general advantage of sustained release systems is avoidance of "peak and valley" drug levels following bolus injection,[21] it might be possible that lower amounts of L-lactate will be sufficient to maintain the therapeutic effect.

The calculated values were compared to the amounts of L-lactic acid released from the different copolymers. The two pure copolymers (Formulations 1 and 2) without additional sodium L-lactate both released amounts of L-lactic acid equivalent to the estimated 0.85 mg per day. This leads to the assumption that sufficient amounts are released to maintain a therapeutic effect during 14 days. The formulations with 5% or 10% incorporated sodium L-lactate (Formulation 3) released adequate amounts during the first 48 hours to achieve and maintain therapeutic doses. Thereafter, the average daily release was around 0.3 mg L-lactic acid per day for both formulations, which probably will not be enough to meet the therapeutic demand. However, the copolymer that was used for incorporation has an M_w of 2500 g/mol: decreasing the M_w will augment the rate at which L-lactic acid is released due to hydrolysis of the copolymer. Certainly, these assumptions are based on estimations and they need to be confirmed *in vivo*.

Ex vivo L-lactate release from pure poly(L-lactic acid-co-L,D-2-hydroxyoctanoic acid)

To determine whether the release rate is influenced by the presence of enzymes in vitreous humor, an *ex vivo* release study with the high PDI formulation was undertaken (Formulation 2). Comparing the release of L-lactic acid in vitreous humor and in phosphate buffer demonstrated a similar release profile, as is depicted in Figure 3. Thus, it is postulated that the degradation rate of the copolymer in vitreous humor is not substantially influenced by enzymes like esterases. This finding is of clinical importance, since it implies that the L-lactic acid release rate will not be majorly affected by inter-patient variability in enzyme activity.

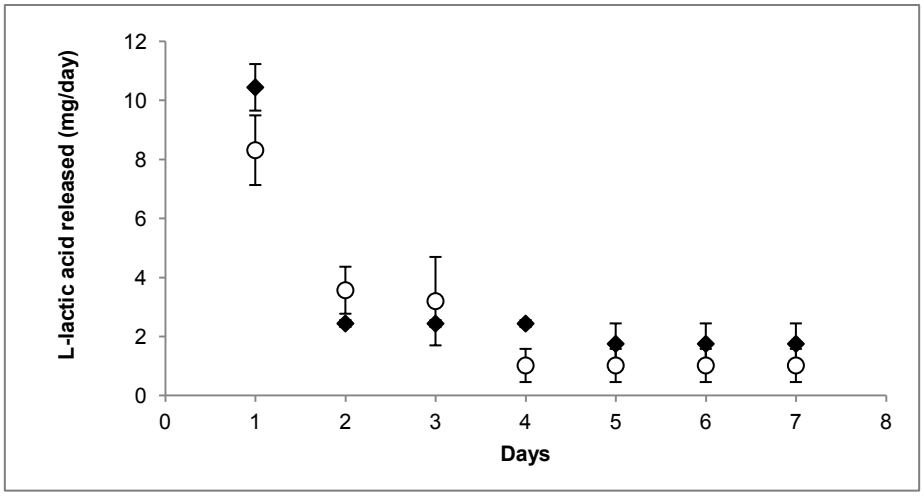

Figure 3. *Influence of release medium on the L-lactic acid release (mg/day). In vitro release: 150 mM sodium phosphate buffer, pH 7; n=6 (2 separate vials, 3 analyses per vial per time point). Ex vivo release: porcine vitreous humor; n=9 (3 separate vials, 3 analyses per vial per time point). Mean values ± SD are presented. 100% release corresponds to 37 mg L-lactic acid.*

♦ *= copolymer in phosphate buffer, MW 1400 g/mol, PDI 2.6;*

○ *= copolymer in vitreous humor, MW 1400 g/mol, PDI 2.6*

In addition to the release of L-lactic acid, the concentration of the other monomer subunit of the copolymer, free 2-hydroxyoctanoic acid, was measured. As expected for a 50:50 (n/n) poly(L-lactic acid-*co*-L,D-2-hydroxyoctanoic acid) copolymer with random distribution of the two monomers in the polymer chain, the release of 2-hydroxyoctanoic acid was similar to that of L-lactic acid (results not shown), since both degradation products are released in parallel. Since the general aim of the release studies was to show a proof of concept for the release of L-lactic acid from the "all in one" system, we limited the study to the initial release phase of 1-2 weeks for these different systems. Further investigations need to include long-term release studies, in order to characterize the complete degradation profile of this prodrug system.

In vitro and *ex vivo* biocompatibility studies

Biocompatibility of poly(L-lactic acid-co-L,D-2-hydroxyoctanoic acid) degradation products with ARPE-19 cells

Since the biodegradable poly(L-lactic acid-*co*-L,D-2-hydroxyoctanoic acid) will be hydrolysed in the vitreous humor, the *ex vivo* biocompatibility of its two degradation products, L-lactic acid and 2-

hydroxyoctanoic acid, was investigated by performing MTT tests on ARPE-19 cells (Figure 4). Up to 5 mM L-lactic acid the cell viability remained at 90%, whereas a 50 mM L-lactic acid concentration caused significant reduction in cell viability compared to the control. For 2-hydroxyoctanoic acid, 90% cell viability was observed up to 1 mM. At higher concentrations, e.g. 10 mM and 100 mM 2-hydroxyoctanoic acid, the viability of the cells was significantly reduced compared to the control. Thus, both the endogenous L-lactic acid and 2-hydroxyoctanoic acid show a comparable biocompatibility with the ARPE-19 cells. These results indicate that the rate of degradation of the copolymers and its local concentrations need to be controlled in order to ensure a biocompatible intraocular formulation. The fact that too high concentrations of degradation products of biodegradable polymers may cause adverse events was reported earlier by Ignatius and Claes.[22] The *in vitro* toxicity of the degradation products of poly(DL-lactide) and poly(L-lactide-*co*-glycolide), e.g. L-lactic acid and glycolic acid, was investigated by performing an MTT test on BALB 3T3 cells. Reduced cell viability was observed when the cells were exposed to too high concentrations of L-lactic acid and glycolic acid.[22]

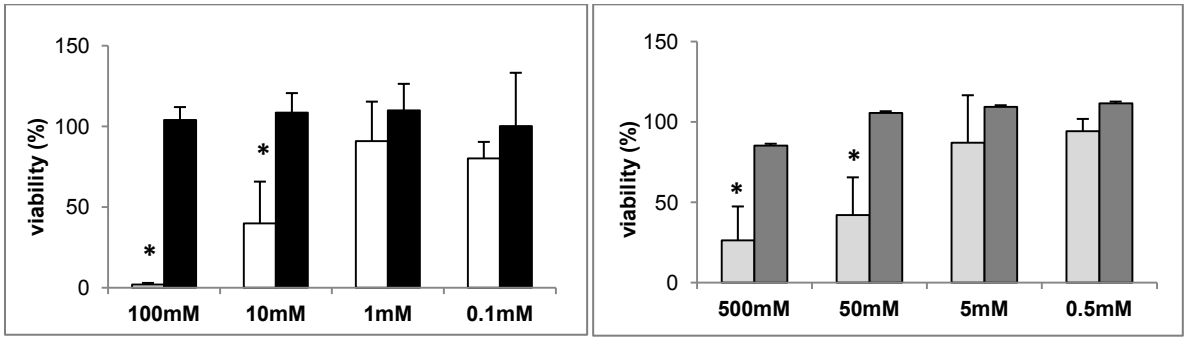

Figure 4. *Biocompatibility of 2-hydroxyoctanoic acid and L-lactic acid with ARPE-19 cells. Cell viability was investigated by performing an MTT-test. Mean percentage ± SD is presented (n=5). *Significantly different compared to control (paired t-test; p<0.05).*

□ = *2-hydroxyoctanoic acid (in ethanol)*

■ = *ethanol (control)*

■ = *L-lactic acid (in water)*

■ = *water (control)*

Biocompatibility of poly(L-lactic acid-co-L,D-2-hydroxyoctanoic acid) and its degradation products with ex vivo porcine retinal tissues

As an orthogonal model for the MTT test on ARPE-19 cells, the effects of the degradation products on *ex vivo* porcine retinal tissues were also investigated, allowing a quick indication of their biocompatibility with the intact retinal tissues within their natural surrounding environment. After being placed in direct contact with the retinal tissues, concentrations up to 5 mM 2-hydroxyoctanoic acid and 10 mM L-lactic acid demonstrated good biocompatibility (Table 2). Higher concentrations of both degradation products caused the formation of white stains on the retinal tissues directly after application, indicating adverse events on the retinal tissue. In line with these observations, the histological study showed an edematous ganglion cell layer with reduced amount of ganglion cells on the retinal tissues that were in contact with high concentrations of L-lactic acid and 2-hydroxyoctanoic acid. In contrast, no abnormalities were observed at low concentrations (Figure 5). Hence, these data confirm the results that are observed on the ARPE-19 cells.

Table 2. *Tissue compatibility of the monomers from poly(L-lactic acid-co-L,D-2-hydroxyoctanoic acid), L-lactic acid and 2-hydroxyoctanoic acid, on isolated porcine retinal tissues.*

Molecule	Structure	Concentration at which no adverse events occur[a]	Adverse events at high local concentrations[b]
L-lactic acid (L-2-hydroxypropanoic acid)	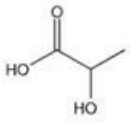		
L,D-2-hydroxyoctanoic acid	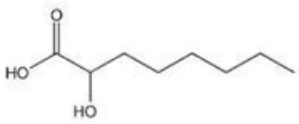		

[a] *Good biocompatibility is observed for a direct application of 100 µl 10 mM L-lactic acid and 5 mM 2-hydroxyoctanoic acid (in 75% (v/v) aqueous ethanol).*

[b] *Application of higher concentrations (100 µl 300 mM L-lactic acid or 2-hydroxyoctanoic acid) leads to white staining of the retinal tissues.*

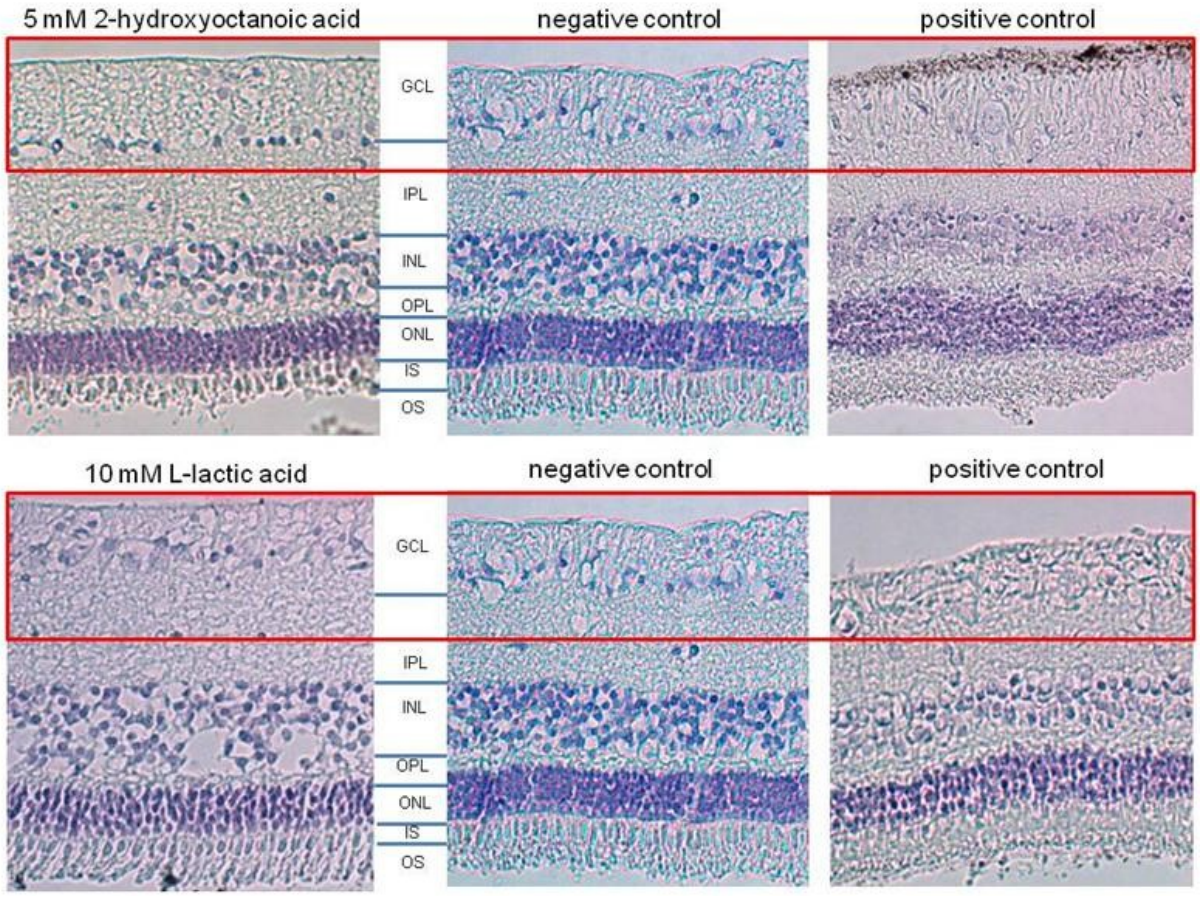

Figure 5. *Histology after direct contact of the porcine retinal tissues with monomers from poly(L-lactic acid-co-L,D-2-hydroxyoctanoic acid). Good biocompatibility is observed for 10 mM L-lactic acid and 5 mM 2-hydroxyoctanoic acid in 75% (v/v) aqueous ethanol compared to the negative control (75% (v/v) aqueous ethanol). A reduced number in ganglion cells and edema of the ganglion cell layer are observed after contact with the highly concentrated positive controls, e.g. 300 mM L-lactic acid and 2-hydroxyoctanoic acid. Different cell layers are visible: ganglion cell layer (GCL), inner plexiform layer (IPL), inner nuclear layer (INL), outer plexiform layer (OPL), outer nuclear layer (ONL), inner segments (IS) and outer segments (OS).*

For the copolymer formulation, this means that the presence of high amounts of small oligomers should be avoided in order to comply with ocular concentrations that do not exceed 5 mM for 2-hydroxyoctanoic acid or 10 mM in the case of L-lactic acid. Based upon the envisioned use as an intravitreal injection, a volume of 100 µl 50:50 (n/n) copolymer into 4 ml vitreous humor is foreseen, which is the approximate volume of the human eye.[23] From these values it can be calculated that a maximum of 3.7 mg of L-lactic acid and 3.2 mg of 2-hydroxyoctanoic acid may be released and present at a given time point; higher amounts might lead to adverse reactions.

Comparing these estimations with the data obtained from the release studies, it is hypothesized that the copolymer with a low polydispersity will show good biocompatibility with the *ex vivo* retinal tissues, as well as the low polydisperse copolymers with additional sodium L-lactate. In contrast, the high polydisperse copolymer contains a higher ratio of shorter oligomer chains, which degrade faster to monomer entities and therefore it is expected that this formulation will tend to have adverse events on the retinal tissues. The hypothesis was confirmed by placing all copolymer formulations in direct contact with the retinal tissues: necrotic effects were observed for the high polydisperse copolymer, whereas the low polydisperse copolymers with and without additional sodium L-lactate showed an excellent biocompatibility (Table 1).

Direct placement of the copolymer on the *ex vivo* retinal tissues to study their biocompatibility has its limitations and the above discussed results should be considered as a first indication. First of all, this model only allows studying the immediate effect. Besides, a turnover of intravitreal fluids takes place *in vivo*, leading to fast clearance of the degradation products, due to the fact that both L-lactic acid and 2-hydroxyoctanoic acid have a molecular weight < 500 Da.[7] Furthermore, the position of the copolymer is envisaged centrally in the vitreous humor, thereby avoiding direct contact with the retinal tissues and thus differing from the *ex vivo* experiment. Despite these constraints, the data show the general importance of controlling the degradation profile of polyester based systems and the local concentrations of their degradation products, while applying these formulations for intraocular use. These findings should not only be taken into account for our system, but also for formulations with well-known polymers like poly(lactic acid) (PLA) and poly(lactic-*co*-glycolic acid) (PLGA). However, when the limitations of these systems are acknowledged, successful development of a biocompatible polymer matrix is feasible. This is illustrated by the example of the intraocular implant Ozurdex®, which is a PLGA copolymer that shows good biocompatibility and has been widely used in clinic. Although some adverse events have been reported after intravitreal administration of this implant, they all were related to the intravitreal injection and not associated with the copolymer matrix.[24]

CONCLUSIONS

The suitability of an "all in one" concept for the sustained release of L-lactic acid from a biodegradable poly(L-lactic acid-*co*-L,D-2-hydroxyoctanoic acid) injectable copolymer for intravitreal application was investigated. The viscous liquid system forms a drug depot upon injection and acts as prodrug and carrier in one. A sustained release of L-lactic acid from the different systems over a period up to 14 days was achieved. The novel copolymer formulations can be easily adapted to the clinical need, through the addition of free sodium L-lactate for a direct onset of the therapeutic effect. Good *ex vivo* biocompatibility with the retinal tissues was accomplished for copolymer formulations in which shorter oligomer chains that can quickly degrade to monomers are absent. To conclude, a fundamental understanding of such a copolymer formulation and its degradation profile is needed to develop suitable intraocular systems: The presented poly(L-lactic acid-*co*-L,D-2-hydroxyoctanoic acid) formulation with low polydispersity and low molecular weight shows the most promising characteristics with a zero order release profile, good biocompatibility and injectability. Although the results need to be confirmed *in vivo*, these data demonstrate the potential of these copolymers for the intravitreal sustained release of L-lactic acid.

ACKNOWLEDGMENTS

The authors wish to thank Dr. S. Wasmuth for providing the ARPE-19 cells, Prof. Dr. M. Rohrbach for his support in interpreting the histology data and the Swiss National Science Foundation for their financial support (#320030-122190).

REFERENCES

1. Ye X, Laties AM, Stone RA. Peptidergic innervations of the retinal vasculature and optic nerve head. *Invest Ophthalmol Visual Sci* 1990; 31: 1731-1737.

2. Brown SM, Jampol LM. New concepts of regulation of retinal vessel tone. *Arch Ophthalmol* 1996; 114: 199-204.

3. Garhöfer G, Zawinka C, Resch H, Menke M, Schmetterer L, Dorner GT. Effect of intravenous administration of sodium-lactate on retinal blood flow in healthy subjects. *Invest Ophthalmol Visual Sci* 2003; 44: 3972-3976.

4. Brazitikos PD, Pournaras CJ, Munoz JL, Tsacopoulos M. Microinjection of L-lactate in the preretinal vitreous induces segmental vasodilation in the inner retinal of miniature pigs. *Invest Ophthalmol Visual Sci* 1993; 34: 1744-1752.

5. Mendrinos E, Petropoulos IK, Mangioris G, Papadopoulou DN, Stangos AN, Pournaras CJ. Lactate-induced retinal arteriolar vasodilation implicates neuronal nitric oxide synthesis in minipigs. *Invest Ophthalmol Visual Sci* 2008; 49: 5060-5066.

6. Mendrinos E, Petropoulos IK, Mangioris G, Tsilimbaris MK, Papadopoulou DN, Geka A, Pournaras CJ. Vasomotor effect of intravitreal juxta-arteriolar injection of L-lactate on the retinal arterioles after acute branch retinal vein occlusion in minipigs. *Invest Ophthalmol Visual Sci* 2011; 52: 3215-3220.

7. Trimawithana TR, Young S, Bunt CR, Green C, Alany RG. Drug delivery to the posterior segment of the eye. *Drug Discov Today* 2011; 16: 270-277.

8. Pallikaris IG, Kymionis GD, Ginis HS, Kounis GA, Tsilimbaris MK. Ocular rigidity in living human eyes. *Invest Ophthalmol Visual Sci* 2005; 46: 409-414.

9. Bakri SJ, Pulido JS, McCannel CA, Hodge DO, Diehl N, Hillemeier J. Immediate intraocular pressure changes following intravitreal injections of triamcinolone, pegaptanib, and bevacizumab. *Eye* 2009; 23: 181-185.

10. Shah SS, Denham LV, Elison JR, Bhattacharjee PS, Clement C, Huq T, Hill JM. Drug delivery to the posterior segment of the eye for pharmacologic therapy. *Expert Rev Ophthalmol* 2010; 5: 75-93.

11. Duvvuri S, Majumdar S, Mitra AK. Drug delivery to the retina: challenges and opportunities. *Expert Opin Biol Ther* 2003; 3: 45-56.

12. Lavik E, Kuehn MH, Kwon YH. Novel drug delivery systems for glaucoma. *Eye* 2011; 25: 578-586.

13. Asmus LR, Gurny R, Möller M. Solutions as solutions – Synthesis and use of a liquid polyester excipient to dissolve lipophilic drugs and formulate sustained-release parenterals. *Eur J Pharm Biopharm* 2011; 79: 584-591.

14. Trimaille T, Gurny R, Möller M. Poly(hexyl-substituted lactides): novel injectable hydrophobic drug delivery systems. *J Biomed Mater Res Part A* 2007; 80: 55-65.

15. Hiltunen K, Seppälä JV, Härkönen M. Effect of catalyst and polymerization conditions on the preparation of low molecular weight lactic acid polymers. *Macromolecules* 1997; 30: 373-379.

16. Mosmann TJ. Rapid colorimetric assay for cellular growth and survival: application to proliferation and cytotoxicity assays. *Immunol Methods 1983; 65: 55-63.*

17. Hein TW, Xu W, Kuo L. Dilation of retinal arterioles in response to lactate: role of nitric oxide, guanylyl cyclase, and ATP-sensitive potassium channels. *Invest Ophthalmol Visual Sci* 2006; 47: 693-699.

18. http://hcp.ozurdex.com/Clinical-Profile/Delivery-Technology

19. Dunn R. Application of the ATRIGEL® implant drug delivery technology for patient-friendly, cost-effective product development. *Drug Delivery Technol* 2003; 3.

20. Swindle KE, Ravi N. Recent advances in polymeric vitreous substitutes. *Expert Rev Ophthalmol* 2007; 2: 255-265.

21. Einmahl S, Capancioni S, Schwach-Abdellaoui K, Möller M, Behar-Cohen F, Gurny R. Therapeutic applications of viscous and injectable poly(ortho esters). *Adv Drug Delivery Rev* 2001; 53: 45-73.

22. Ignatius AA, Claes LE. In vitro biocompatibility of bioresorbable polymers: poly(L, DL-lactide) and poly(L-lactide-co-glycolide). *Biomaterials* 1996; 17: 831-839.

23. Robinson JC. Ocular anatomy and physiology relevant to ocular drug delivery, in: Mitra, A.K. (Ed.), Ophthalmic drug delivery systems. Marcel Dekker Inc., New York 1993, pp. 29-57.

24. Haller JA, Bandello F, Belfort R, Blumenkranz MS, Gillies M, Heier J, Loewenstein A, Yoon YH, Jacques ML, Jiao J, Li XY, Whitcup SM, Ozurdex Geneva Study Group. Randomized, sham-controlled trial of dexamethasone intravitreal implant in patients with macular edema due to retinal vein occlusion. *Ophthalmology* 2010; 117: 1134-1146.

Development of an intravitreal peptide (BQ123) sustained release system based on poly(2-hydroxyoctanoic acid) aiming at a retinal vasodilator response

Marieke Veurink[1], Georgios Mangioris[2], Béatrice Kaufmann[1], Lutz Asmus[1], Maren Hennig[3], Arnd Heiligenhaus[3], Robert Gurny[1], Michael Möller[1], Constantin J. Pournaras[2]

[1]School of Pharmaceutical Sciences, University of Geneva, University of Lausanne, 1211, Geneva, Switzerland; [2]Department of Ophthalmology, Geneva University Hospitals, 1211, Geneva, Switzerland; [3]Department of Ophthalmology at St. Franziskus Hospital, Muenster, Germany

Submitted to Investigative Ophthalmology & Visual Science

PURPOSE Development of a novel formulation for intravitreal administration, in which the endothelin$_A$ receptor antagonist BQ123 is incorporated in a biodegradable and injectable polymer drug delivery system, poly(2-hydroxyoctanoic acid), aiming at a prolonged retinal vasodilator response.

METHODS BQ123 0.2% and 1.0% (w/w) were incorporated in poly(2-hydroxyoctanoic acid) by cryomilling, leading to a homogenous mixture that could be easily injected through a 25-gauge needle. *In vitro* release profiles were obtained in porcine vitreous humor (n=6). The *ex vivo* biocompatibility was studied by placing the formulation in direct contact with porcine retinal tissues and performing histology. In a pilot *in vivo study*, the change in retinal vessel diameter of mini pigs (n=2) was followed over 3 hours after intravitreal injection of the formulation, as well as the release of BQ123 from the polymer system up to 7 days (n=6). Quantification of BQ123 in the vitreous humor and in the remaining polymer depot was performed after vitrectomy and enucleation, respectively.

RESULTS *In vitro*, a zero order release profile was obtained, releasing up to 91% of BQ123 within 7 days. Histology on the porcine retinal tissues showed good *ex vivo* biocompatibility. *In vivo*, a vasodilative response was observed over the whole duration of the study, with a retinal vessel diameter increase from 14% after 15 minutes, up to 39% after 3 hours. Compared to a single BQ123 injection, this is a 6-fold prolongation of the duration. At t=3h, the BQ123 concentration in the vitreous humor was 0.7 ± 0.2 µg/ml, followed by 1.5 ± 1.0 µg/ml and 1.1 ± 0.8 µg/ml after 3 and 7 days, respectively. 39.9 ± 6.0 % of BQ123 was still present in the polymer depot at t=7d.

CONCLUSIONS The results show that intravitreal injection of this drug delivery system leads to a fast onset and prolonged vasodilative response, as well as to the release of BQ123 over 7 days, suggesting a therapeutic potential in the management of retinal ischemic conditions.

Keywords: biodegradable polymers, retinal vasodilation, endothelin$_A$ receptor antagonist, injectable sustained release system.

INTRODUCTION

Retinal vein occlusion (RVO) and diabetic retinopathy are sight-threatening conditions, for which no successful treatment exists to date.[1,2] In the US alone, 4.1 million patients were estimated to have diabetic retinopathy in 2004, of which 0.9 million were vision threatening.[3] Due to a predicted increase in prevalence of diabetes mellitus, forecasts suggest that these numbers will triple in the coming 40 years.[4] Retinal vein occlusions are another important cause of visual impairment due to retinal vascular conditions: worldwide, an estimated 16 million people suffer from vision loss due to a form of retinal vein occlusion.[5] Current pharmacotherapy is targeting the secondary effects of these disorders, without addressing the cause of the obstruction of the retinal blood vessels, or the prevention of the retinal ischemia.[1,6] Therefore, there is a need to explore alternative strategies, which interfere in an earlier stage of the disease and focus on overcoming the vascular occlusion.

A possible approach is the inhibition of the potent vasoconstrictor endothelin-1 (ET-1) that has been associated with both diabetic retinopathy[7,8] and RVO.[9] ET-1 causes vasoconstriction of the retinal arteries and a reduction in retinal blood flow, predominantly through activation of smooth muscle endothelin$_A$ (ET_A) receptors.[10] The selective ET_A receptor antagonist BQ123 is a small cyclic peptide that inhibits the vasoconstrictor effect of ET-1 on retinal blood flow.[11] Moreover, intravitreal injection of BQ123 caused vasodilation in both healthy mini pig eyes and eyes in which branch retinal vein occlusion was evoked.[12] Thus, the peptide offers promising characteristics as a therapeutic agent for treatment of diseases in which the retinal arterioles are restricted.[12,13] However, the vasodilative effect is short-lived and reaches its maximum of 30% dilation already after 6 minutes, followed by a rapid decline in dilation.[12] To prolong the duration of action, the development of a BQ123 sustained release system is envisaged that slowly releases therapeutic doses of the peptide over a prolonged period of time. The clinical interest of such a system would be to maintain the arteriolar perfusion, in order to prevent vision loss due to the retinal ischemia.

Poly(2-hydroxyoctanoic acid) was selected for the formulation of such a sustained release system.[14,15] In contrast to solid poly(lactide) (PLA) based delivery systems, poly(2-hydroxyoctanoic acid) is a viscous liquid at room temperature[15] and can be administered as a conventional intravitreal injection, thereby avoiding invasive and expensive surgery associated with ocular implants.[16] In addition, this polyester is completely degradable by hydrolysis in an aqueous environment like the vitreous humor. The drug release is governed by diffusion and degradation of the polymer matrix, respectively. Furthermore, incorporation of the therapeutic agent is achieved by simply mixing drug and polymer, without the need of heat or additional solvents.[15] This is beneficial for a peptide like BQ123, since it prevents the possible occurrence of stability issues.

The aim of this study was to develop a formulation that forms a drug depot in the vitreous humor upon injection, which continuously releases BQ123 over a period of 7 days. The envisaged formulation requires being injectable by conventional intravitreal injection and biocompatible with the ocular tissues. Besides, since tissue damage was found to occur within hours after experimentally induced branch retinal vein occlusion,[17] the formulation should cause an immediate vasodilative effect. The loading of BQ123 should be sufficient to reach therapeutic levels over a period of 7 days, taking in consideration that only a small volume of the formulation can be injected to avoid a rise in intraocular pressure.[18] To assess whether these requirements are met, the release of BQ123 from the formulation and the degradation of free BQ123 were studied *in vitro* in porcine vitreous humor. Furthermore, the biocompatibility of the formulation was tested by placing the polymer in direct contact with *ex vivo* retinal tissues and performing histology on the tissues. Finally, an *in vivo* proof of concept was performed in mini pigs to investigate: (i) whether the formulation is able to cause a vasodilative effect on the retinal arterioles and (ii) whether it releases therapeutic doses of BQ123 over a period of 7 days. This animal model was chosen, since mini pig arterioles show close similarities with human ones.[19]

METHODS

Preparation of the formulation

Synthesis of 2-hydroxyoctanoic acid was first described by Trimaille et al.[14] In the present study, poly(2-hydroxyoctanoic acid) was prepared by melt polycondensation at 150°C under vacuum as reported by Asmus et al.[15] Molecular weight (M_w) and polydispersity index (PDI, M_w/M_n) were determined by gel permeation chromatography (GPC). A Waters 515 HPLC pump, Waters 410 injector, Styragel HR 1-4 columns and Waters 2414 refractive index detector (Waters Corporation, Milford, USA) were used with THF as the continuous phase. Calibration was performed using polystyrene standards (PSS, Mainz, Germany). The same batch of poly(2-hydroxyoctanoic acid) was used for all experiments. Two different percentages of BQ123 (Peptide 2.0, Chantilly, USA) were incorporated in the polymer formulation by cryomilling (SPEX 6700 freezer/mill, SPEX SamplePrep, Metuchen, USA) during 5 minutes, i.e. 0.2% and 1.0% w/w BQ123 in poly(2-hydroxyoctanoic acid). The final formulations were stored at -20°C.

Ex vivo biocompatibility

Fresh porcine eyes were obtained from a slaughterhouse and the anterior segment and vitreous humor were carefully removed to access the retinal tissues. 50 µl of poly(2-hydroxyoctanoic acid) were placed in direct contact with the retinal tissues (n = 2) and the effects were visually observed over 1.5 hours. A positive control (300 mM 2-hydroxyoctanoic acid monomer in 75% v/v aqueous ethanol[20]) was put on a part of the same eye. In parallel, 50 µl of polymer were placed in direct contact with the retinal tissues, whereafter the posterior segment was fixed in 4% v/v formaldehyde in phosphate buffer for histological examination. As negative control, a part of the posterior segment was fixed without polymer. After embedding the fixed tissues in paraffin and cutting them in serial sections of 7 µm, five sections were stained with hematoxilin and eosin following a standard protocol.

***In vitro* BQ123 release and BQ123 stability in the release medium**

The BQ123 release from the polymer was measured over time by placing 50 µl of the 0.2% BQ123 in poly(2-hydroxyoctanoic acid) formulation in 2 ml porcine vitreous humor with 0.2% sodium azide to avoid bacterial growth (n = 6 separate vials). These volumes were chosen to simulate the *in vivo* study in mini pigs. Vials were stored under light shaking conditions at 37°C for 7 days, and 50 µl samples of vitreous humor were taken at different time points to measure the amount of BQ123 released from the delivery system. After each sample collection, the sample volume was replaced by fresh vitreous humor.

The results of the BQ123 release study might be influenced by the fact that the released BQ123 degrades with time. To measure the rate at which BQ123 degrades in vitreous humor, 100 µg of free BQ123 was placed in a vial with vitreous humor (n = 2 separate vials) and stored under the same conditions as the polymer formulation. This amount of free BQ123 was chosen since the polymer depot used in the *in vitro* study contains 100 µg of BQ123 as well. The amount present at t_0 was considered as 100%.

Quantification of BQ123 in the vitreous humor was performed by HPLC (1200 Series, Agilent Technologies, Basel, Switzerland) on a C18 Waters Symmetry column (4.6 x 30 mm, 3.5 µm) with fluorimetric detection at experimentally determined wavelengths of 278 nm (excitation) and 348 nm (emission). The temperature was maintained at 35°C and the flow rate at 1.5 ml/min. A mixture of water and acetonitrile was used as mobile phase in gradient mode, with 20% acetonitrile at the start of elution, increasing to 40% at 2 minutes and back to 20% at 4 minutes. Each sample was diluted 1:1 with water and injected in triplicate with an injection volume of 5 µl. All values are presented as mean ± standard deviation (SD).

The release profile was corrected for degradation in vitreous humor using the following equations:

$$BQ123_{corrected} = \left(\frac{100}{BQ123_{non-degraded}}\right) * BQ123_{measured}$$

$$BQ123_{non-degraded} = -20.051\,t + 100$$

in which:

- t is the time point expressed in days;
- $BQ123_{measured}$ is the percentage of BQ123 that is released from the polymer depot and measured in the release medium;
- $BQ123_{non\text{-}degraded}$ is the percentage of free BQ123 that is still present in the medium;
- $BQ123_{corrected}$ is the released percentage of BQ123 after correction for degradation.

The degradation profile follows a zero-order kinetic during these first three days, with a coefficient of determination (r^2) of 0.955, after t=3d the percentage of BQ123 stays stable. Therefore, the second equation was only applied for the time points between t0 and t=3d, for later time points the $BQ123_{non\text{-}degraded}$ value was fixed at 40%.

***In vivo* BQ123 release and retinal vasodilation**

The study was performed on 5 mini pigs (Göttingen breed, Arare Animal Facility, Geneva, Switzerland) with a weight varying from 10 to 12 kg. All experiments were conducted conform to the ARVO statement for Use of Animals in Ophthalmic and Vision Research and were approved by the local veterinary authorities of Geneva (#1004/3419/2R). The animals were prepared as described in previous work,[21] receiving an intramuscular injection of 3 ml (15 mg) midazolanum maleate (Dormicum®, Roche Pharma, Reinach, Switzerland), 3 ml (120 mg) azaperone (Stresnil®, Janssen Pharmaceutica, Beerse, Belgium), and 1 ml (0.5 mg) atropine as premedication.

In two of the mini pigs, the retinal vasodilative effect was monitored during 3 hours after intravitreal injection of 0.2% BQ123 in poly(2-hydroxyoctanoic acid). The pigs were anaesthetized with 2 to 3 mg ketamine hydrochloride (Ketalar®, Parke-Davis, Zurich, Switzerland) injected into an ear vein. Thereafter, they were intubated and artificially ventilated as previously described.[21] After removal of the eyelids, detachment of the bulbar conjunctiva and cleaning of the sclera, a metal ring was sutured around the limbus to fix the globe. A sclerotomy was performed 2 to 3 mm posterior to the limbus and a contact lens was placed on the cornea. An operating microscope (Carl Zeiss Meditec, GmbH, Oberkuchen, Germany) was used to observe the fundus. 50 µl of the 0.2% BQ123 in poly(2-hydroxyoctanoic acid) formulation were injected centrally in the vitreous humor with a Hamilton 250 µl syringe (Hamilton Bonaduz AG, Bonaduz, Switzerland) and a 25-gauge needle. The retinal arteriolar diameter was monitored over a period of 3 hours with a retinal vessel analyzer (RVA, Imedos GmbH, Jena, Germany). Measurements were performed before injection and thereafter every 15 minutes. At the same time, arterial oxygen partial pressure (PaO_2), carbon dioxide pressure ($PaCO_2$), and pH were measured in blood from the femoral artery with a blood gas analyzer (Labor-systeme Flükiger AG, Menziken, Switzerland) and controlled over the duration of the study. After 3 hours, the animal was sacrificed; the eye was enucleated and stored immediately at -20°C.

The remaining three pigs received an intravitreal injection of 1% BQ123 in poly(2-hydroxyoctanoic acid) in both eyes and vitreous humor samples were taken 3 and 7 days after injection, to determine the BQ123 concentration in vitreous humor. The 1% formulation was selected to ensure sufficiently high BQ123 concentrations in the vitreous humor for quantification after 7 days. The mini pigs were surveyed on a daily base over the duration of the study. At t_0, the premedication protocol as described above was followed and thereafter, 50 µl of the 1% BQ123 in poly(2-hydroxyoctanoic acid) formulation were injected centrally in the vitreous humor of each eye with a Hamilton 250 µl syringe (Hamilton Bonaduz AG, Bonaduz, Switzerland) and a 25-gauge needle. After three days, the animals were submitted to the same premedication protocol, before being anaesthetized with 2 to 3 mg ketamine hydrochloride (Ketalar®, Parke-Davis, Zurich, Switzerland) injected into an ear vein. A vitrectomy (without activation of the infusion line) was performed to remove approximately 100 µl of

vitreous humor from both eyes, in order to quantify the amount of free BQ123 present in the eye. Attention was paid not to touch the polymer depot during this procedure. The vitreous humor samples were stored immediately at -20°C. After 7 days, the animals were sacrificed; the eyes were enucleated and stored at -20°C.

Sample analysis

The BQ123 concentration was determined in the obtained vitreous humor samples, as well as in the enucleated eyes. For the former, the vitreous humor was diluted with water (1:1) before analysis by HPLC with fluorescence detection as described for the *in vitro* release study. For the latter, the complete vitreous humor with the polymer droplet was separated from the rest of the eye and its total mass was weighed. Two different samples were prepared. For the first sample, the polymer droplet and a small part of the surrounding vitreous humor were removed to quantify the amount of BQ123 that was still present in the polymer bubble. The polymer droplet was completely dissolved in 1 ml isopropanol, thereafter, 9 ml water were added. The sample was centrifuged and the supernatant was filtered with a 0.22 µm filter. Secondly, to quantify the amount of BQ123 released from the bubble, the remaining vitreous humor was carefully homogenized and thereafter centrifuged and filtered (0.22 µm). Both samples were diluted 1:1 with water before analysis by HPLC with fluorescence detection. All values are presented as mean ± standard deviation (SD).

RESULTS

Characteristics of the formulation

The poly(2-hydroxyoctanoic acid) used in the present study had a molecular weight (M_w) of 3300 g/mol and a polydispersity index (PDI, M_w/M_n) of 1.4. A homogeneous mixture of BQ123 incorporated in the polymer was obtained by cryomilling. The formulations were easily injectable through a 25-gauge needle into the central vitreous humor, as tested and stated by the handling ophthalmologist.

***Ex vivo* biocompatibility**

The biocompatibility of the polymer formulation with the retinal tissues was investigated on *ex vivo* porcine eyes. Upon visual inspection, no adverse events were observed after placement of poly(2-hydroxyoctanoic acid) in direct contact with the retinal tissues, whereas the positive control caused white stains on the retinal tissues (Figure 1A). Histology also showed that the retinal layers remained unaffected upon direct contact with the polymer: no differences were observed between the untreated retinal tissues and the ones that were in contact with the formulation (Figure 1B).

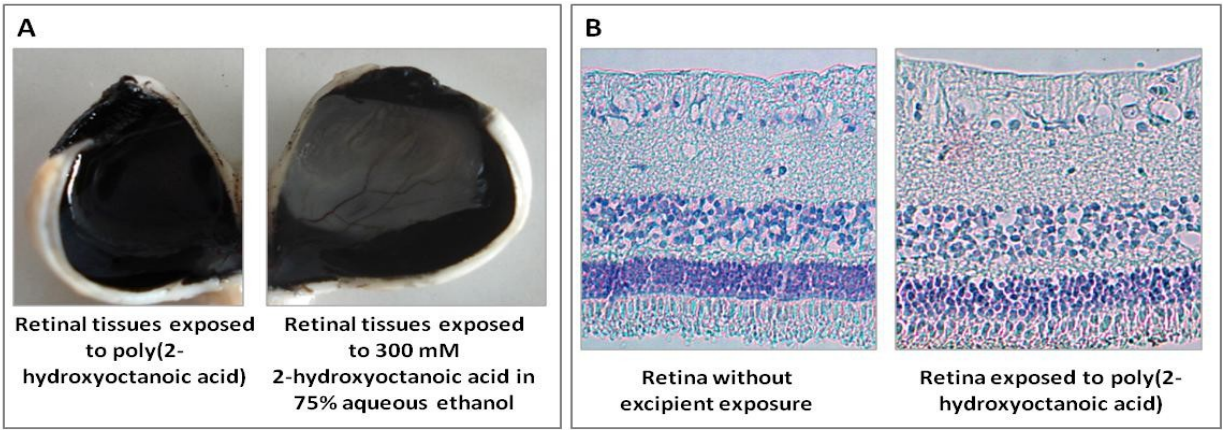

Figure 1. *Ex vivo BQ123 biocompatibility.* ***(A)*** *Poly(2-hydroxyoctanoic acid) (left) in direct contact with the retinal tissues does not lead to adverse events. As positive control, high concentrations of 2-hydroxyoctanoic acid in 75% v/v aqueous ethanol (300 mM) are causing white stains on the retinal tissues due to a damaged ganglion cell layer (right), as was observed by histology in earlier work.*[20] ***(B)*** *Histology of the retinal tissues shows good biocompatibility of poly(2-hydroxyoctanoic acid) (right). No differences were observed on the tissues compared to the non-polymer exposed retinal tissues (left).*

***In vitro* BQ123 release and BQ123 stability in the release medium**

The *in vitro* release of BQ123 from the polymer formulation over a period of 10 days showed an initial burst release during the first hours, followed by a constant release up to 55 ± 15% at day 10 (Supplementary Data Figure S1A). However, these amounts may practically be higher considering that free BQ123 degrades over time in vitreous humor. The degradation profile of free BQ123 in vitreous humor release medium demonstrated that around 60% of the initially present BQ123 degraded within

the first 3 days and that a residual 40% of intact peptide was measurable up to 7 days (Supplementary Data Figure S1B). Therefore, the BQ123 release profile was corrected for degradation of free BQ123, revealing an almost complete release after 7 days (Supplementary Data Figure S1C). The corrected release profile is depicted in Figure 2, demonstrating an amount between 13 and 17 µg of BQ123 released per day from the polymer depot.

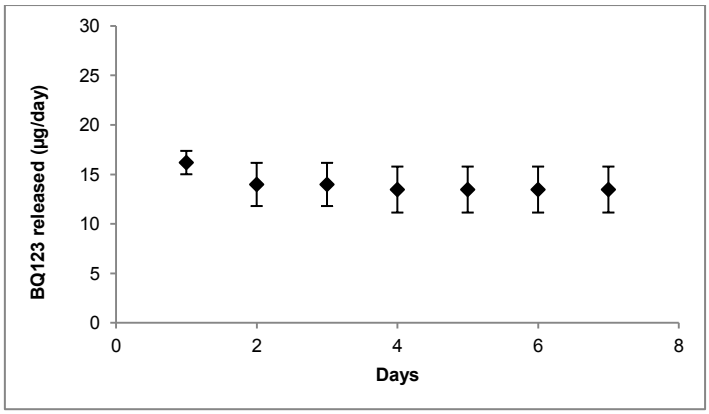

Figure 2. *In vitro BQ123 release from poly(2-hydroxyoctanoic acid) in porcine vitreous humor, presented in µg/day (mean ± SD, n=18: 6 vials, 3 analyses per vial). Data are derived from a correction of the release profile for the degradation of free BQ123 in vitreous humor.*

In vivo BQ123 release and retinal vasodilation

The retinal vasodilator response after intravitreal injection of the BQ123 depot is depicted in Figure 3. A clear vasodilation was observed and remained present over the whole study period (Figure 4). The onset of the vasodilative effect already occurred in the first 15 minutes with a vessel diameter increase of 14%. Thereafter, a continuous rise was distinguished, up to 39% after 3 hours. Figure 5 shows the BQ123 concentration in the vitreous humor at the time points 3 hours, 3 days and 7 days, being 0.7 ± 0.2 µg/ml, 1.5 ± 1.0 µg/ml, and 1.1 ± 0.8 µg/ml, respectively. After 7 days, 40 ± 6% of the total amount of BQ123 that was injected still remained in the polymer depot, corresponding to 193.3 ± 29.2 µg of BQ123. The drug depot stayed clearly visible over 7 days and was well tolerated during the complete study; no adverse events were observed.

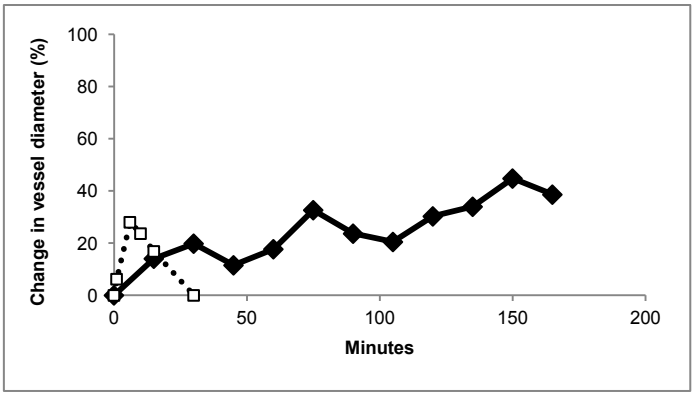

Figure 3. *Rapid onset of vasodilative effect after intravitreal injection of the polymer drug depot in mini pigs (black curve). The change in vessel diameter (mean, n=2) was measured with a retinal vessel analyzer after injection of 50 µl 0.2% BQ123 in poly(2-hydroxyoctanoic acid). The vessel diameter that was measured directly before injection was considered as baseline. In comparison, the change in vessel diameter after a single intravitreal dose of BQ123 (30 µl, 0.61 µg/ml) (black dashed curve) is short-lived, based upon Stangos et al.*[12]

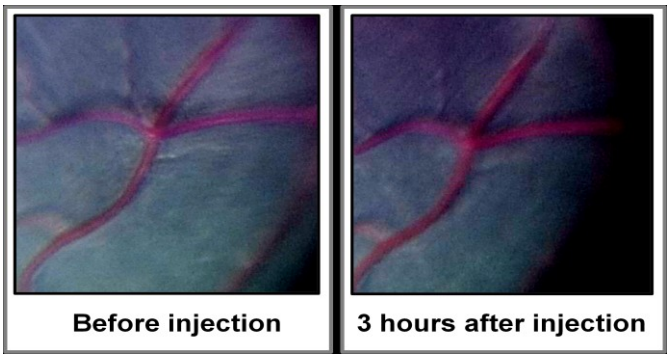

Figure 4. *Retinal arteriolar diameter changes in a mini pig. Comparison of the arterioles before injection (left) and 3 hours after injection of 50 µl 0.2% BQ123 in poly(2-hydroxyoctanoic acid) (right) demonstrates a visible vasodilative effect. The same magnification was used for both pictures.*

DISCUSSION

It has been shown earlier that BQ123 elicits a strong, but unfortunately short-lived,[12] vasodilative response on the retinal arterioles. This work aimed at the development of an easily injectable intravitreal sustained release system for BQ123 that is biocompatible with the retinal tissues and that is able to induce an immediate vasodilative effect, in order to overcome the acute obstruction. The therapeutic potential of this formulation is a direct pharmacological effect, in order to improve the oxygen and nutrient supply to the retinal tissues.

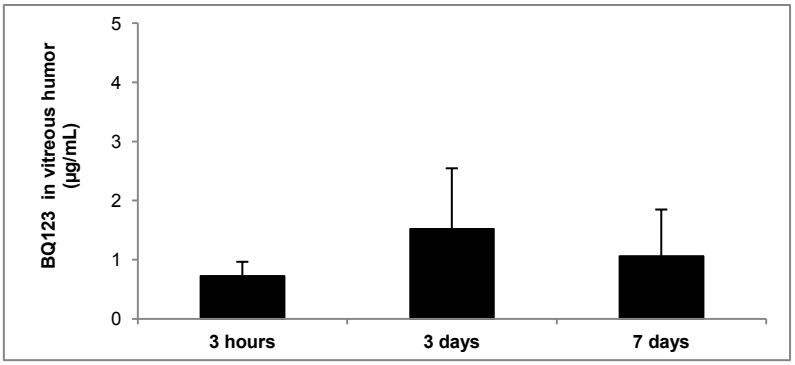

Figure 5. *In vivo BQ123 concentration (µg/ml) in mini pig vitreous humor upon intravitreal injection of BQ123 in poly(2-hydroxyoctanoic acid). Concentrations are presented as mean ± SD. Two different formulations were used: t=3h is the concentration upon injection of 0.2% BQ123 w/w in poly(2-hydroxyoctanoic acid) (n=6, 2 separate eyes, 3 analyses per eye), t=3d and t=7d upon injection of 1% BQ123 w/w in poly(2-hydroxyoctanoic acid) (n=18, 6 separate eyes, 3 analyses per eye).*

The injectable and biodegradable poly(2-hydroxyoctanoic acid) was selected as a potential drug delivery system, since this very hydrophobic polymer forms immediately after injection a single droplet drug depot in the vitreous humor that will be hydrolysed over time in the aqueous environment, comparable to the injectable polymer poly(ortho ester) (POE) described earlier.[22] To assess the biocompatibility of poly(2-hydroxyoctanoic acid), a preliminary *ex vivo* study was conducted, revealing good biocompatibility with the retinal tissues upon visual inspection and upon histological examinations of the retinal cell layers. During the *in vivo* study in mini pigs, good biocompatibility of the system with the ocular tissues was observed over a period of 7 days. No adverse events were distinguished. Of course, the present work only provides information on the short-term biocompatibility of the system with the retinal tissues and therefore, further studies need to investigate the long-term effects.

The *in vitro* release results demonstrated the ability of the system to release BQ123 in a controlled manner over a period of 7 days. The initial burst is beneficial, since it leads to an immediate onset of the vasodilative arteriolar response. Despite the observed burst, the overall release up to 7 days showed a high correlation for linear regression: a coefficient of determination of 0.98 was found for the non-corrected release profile and of 0.99 when correction for BQ123 degradation was taken into

account. Thus, the main release profile follows a zero order kinetic, leading to a release between 13 and 17 µg of BQ123 per 24 hours. The amount of BQ123 released is sufficient to maintain a vasodilator response on the retinal arterioles, based on an extrapolation of an *in vivo* study by Stangos et al.[12] This study was selected, since the same animal model was used as for our novel sustained release formulation. Upon a single dose of 30 µl BQ123 (0.61 µg/ml), corresponding to an amount of 18.3 ng, a clear vasodilative effect was observed that remained up to 15 minutes, which was the end point of the study.[12] However, extrapolation of the curve leads to the assumption that the effect will have disappeared completely after 30 minutes. This extremely short vasodilative response is in accordance with another study, in which a single intravitreal injection of different concentrations of BQ123 caused an increase in retinal blood flow in a rat model.[8] In this study, a maximum was reached after 5 minutes and return to baseline within 15 minutes, independent on the concentration of BQ123 injected.[8] Based on the hypothesis that 18.3 ng of BQ123 triggers an effect for 30 minutes in mini pigs, it can be calculated that around 0.9 µg would be necessary to maintain a therapeutic effect over 24 hours. Our initial *in vitro* results show that sufficient amounts were released over a period of 7 days. The aims of the following *in vivo* study were (i) to verify whether the formulation would immediately release sufficient amounts of BQ123 in order to evoke a vasodilative response and (ii) to investigate whether the system releases therapeutic doses of BQ123 over a period of 7 days. An immediate vasodilative effect is of valuable clinical importance, since occlusion of the retinal arterioles leads to a severe drop in oxygen supply to the retinal tissues, or tissue hypoxia in case of post-BRVO retinal ischemia.[23,24] This hypoxia will induce an upregulation of VEGF, causing angiogenesis and increased vascular permeability.[25] In a rat model, Kaur et al. demonstrated that already after 3 hours of hypoxia, VEGF concentrations were significantly elevated.[26] Moreover, 4 hours after experimentally induced branch retinal vein occlusion in a mini pig, the ganglion cell layer showed oedema and necrosis.[17] It is therefore relevant to develop a system that directly overcomes the occlusion.

An important parameter that distinguishes *in vivo*- from *in vitro*- release studies is the fact that clearance of the drug occurs. Although to our knowledge, BQ123 clearance from the vitreous humor

has not been investigated, a fast clearance is nonetheless expected based on the low molecular weight of the peptide (610 g/mol).[27] Therefore, it is probable that the amount of BQ123 quantified in the vitreous humor at t=3h, t=3d and t=7d is lower than the amount of BQ123 that was released *in vitro*. Nevertheless, the BQ123 vitreous concentration was sufficient to evoke an almost immediate vasodilative effect, which was maintained over 3 hours. Compared with a single injection of BQ123, this is a six-fold increase in duration. Earlier work on the same animal model showed that injection of a physiologic saline solution does not lead to any differences in the retinal vessel diameter, demonstrating that the vasodilative effect is not induced by the injection itself.[12]

At t=3h, a BQ123 concentration of 0.7 ± 0.2 µg/ml in the vitreous humor led to an increase of 40% in retinal vessel diameter. Thereof, since the BQ123 concentrations at t=3d and t=7d are in the same order of magnitude (1.5 ± 1.0 µg/ml, and 1.1 ± 0.8 µg/ml, respectively), we postulate that these values will be sufficient to maintain the vasodilative effect over a period of one week. Since 40% of BQ123 still remained in the formulation droplet after 7 days, a longer duration of the vasodilative effect with this delivery system can be envisaged. Based on these preliminary *in vivo* results, poly(2-hydroxyoctanoic acid) seems an adequate system for the sustained release of BQ123. Further investigations will be initiated regarding the long term efficacy of the formulation in future studies.

To summarize, this work was intended as an initial and pivotal investigation of poly(2-hydroxyoctanoic acid) as an intraocular carrier. It demonstrates that the system is a promising drug delivery system for intravitreal application. Good injectability and biocompatibility are observed, as well as an *in vitro* zero order release of BQ123 from the polymer system over a period of 7 days. The *in vivo* data show that the system immediately releases therapeutic doses of BQ123, causing a six-fold increase in the duration of the vasodilative effect compared to a single intravitreal injection. Moreover, a sustained release of therapeutic doses of BQ123 over a period of 7 days was observed in mini pigs. In conclusion, the data present a proof of concept for the *in vivo* sustained release of BQ123 from poly(2-hydroxyoctanoic acid), which may eventually result in the development of a therapeutic system for treatment of retinal ischemic conditions.

ACKNOWLEDGMENTS

The authors wish to thank Nicole Gilodi and Manuel Jorge Costa for their help with the *in vivo* experiments, Marcel Kohler of the "Service de toxicologie de l'environnement bâti" for making available the HPLC with fluorescence detection and the Swiss National Science Foundation for financial support (#320030-122190).

REFERENCES

1. Hahn P, Fekrat S. Best practices for treatment of retinal vein occlusion. *Curr Opin Ophthalmol* 2012; 23: 175-181.

2. Curtis TM, Gardiner TA, Stitt AW. Microvascular lesions of diabetic retinopathy: Clues towards understanding pathogenesis? *Eye* 2009; 23: 1496-1508.

3. Kempen JH, O'Colmain BJ, Leske MC, Haffner SM, Klein R, Moss SE, Taylor HR, Hamman RF, Eye Diseases Prevalence Research Group. The prevalence of diabetic retinopathy among adults in the United States. *Arch Ophthalmol* 2004; 122: 552-563.

4. Saaddine JB, Honeycutt AA, Venkat Narayan KM, Zhang X, Klein R, Boyle JP. Projection of diabetic retinopathy and other major eye diseases among people with diabetes mellitus. United States, 2005-2050. *Arch Ophthalmol* 2008; 126: 1740-1747.

5. Rogers S, McIntosh RL, Cheung N, Lim L, Wang JJ, Mitchel P, Kowalski JW, Nguyen H, Wong TY, International Eye Disease Consortium. The prevalence of retinal vein occlusion: Pooled data from population studies from the United States, Europe, Asia, and Australia. *Ophthalmology* 2010; 117: 313-319.

6. Rechtman E, Harris A, Garzozi HJ, Ciulla TA. Pharmacologic therapies for diabetic retinopathy and diabetic macular edema. *Clin Ophthalmol* 2007; 1: 383-391.

7. Deng D, Evans T, Mukherjee K, Downey D, Chakrabarti S. Diabetes-induced vascular dysfunction in the retina: Role of endothelins. *Diabetologia* 1999; 42: 1228-1234

8. Takagi C, Bursell SE, Lin YW, Takagi H, Duh E, Jiang Z, Clermont AC, King GL. Regulation of retinal hemodynamics in diabetic rats by increased expression and action of endothelin-1. *Invest Ophthalmol Vis Sci* 1996; 37: 2504-2518.

9. Iannaccone A, Letizia C, Pazzaglia S, Vingolo EM, Clemente G, Pannarale MR. Plasma endothelin-1 concentrations in patients with retinal vein occlusions. *Br J Ophthalmol* 1998; 82: 498-503.

10. Hein TW, Ren Y, Yuan Z, Xu W, Somvanshi S, Nagaoka T, Yoshida A, Kuo L. Functional and molecular characterization of the endothelin system in retinal arterioles. *Invest Ophthalmol Vis Sci* 2009; 50: 3329-3336.

11. Polak K, Petternel V, Luksch A, Krohn J, Findl O, Polska E, Schmetterer L. Effect of endothelin and BQ123 on ocular blood flow parameters in healthy subjects. *Invest Ophthalmol Vis Sci* 2001; 42: 2949-2956

12. Stangos AN, Petropoulos IK, Pournaras JA, Mendrinos E, Pournaras CJ. The vasodilatory effect of juxta-arteriolar microinjection of endothelinA receptor inhibitor in healthy and acute branch retinal vein occlusion minipig retinas. *Invest Ophthalmol Vis Sci* 2010; 51: 2185-2190.

13. Mendrinos E, Petropoulos IK, Mangioris G, Papadopoulou DN, Pournaras CJ. Intravitreal L-arginine injection reverses the retinal arteriolar vasoconstriction that occurs after experimental acute branch retinal vein occlusion. *Exp Eye Res* 2010; 91: 205-210.

14. Trimaille T, Gurny R, Möller M. Poly(hexyl-substituted lactides): Novel injectable hydrophobic drug delivery systems. *J Biomed Mater Res A* 2007; 80: 55-65.

15. Asmus LR, Gurny R, Möller M. Solutions as solutions - synthesis and use of a liquid polyester excipient to dissolve lipophilic drugs and formulate sustained-release parenterals. *Eur J Pharm Biopharm* 2011; 79: 584-591.

16. Lavik E, Kuehn MH, Kwon YH. Novel drug delivery systems for glaucoma. *Eye* 2011; 25: 578-586.

17. Donati G, Kapetanios A, Dubois-Dauphin M, Pournaras CJ. Caspase-related apoptosis in chronic ischaemic microangiopathy following experimental vein occlusion in mini-pigs. *Acta Ophthalmol* 2008; 86: 302-306.

18. Pallikaris IG, Kymionis GD, Ginis HS, Kounis GA, Tsilimbaris MK. Ocular rigidity in living human eyes. *Invest Ophthalmol Vis Sci* 2005; 46: 409-414.

19. Beauchemin ML. The fine structure of the pig's retina. *Albrecht Von Graefes Arch Klin Exp Ophthalmol* 1974; 190: 27-45.

20. Veurink M, Asmus L, Hennig M, Kaufmann B, Bagnewski L, Heiligenhaus A, Mendrinos E, Pournaras CJ, Gurny R, Möller M. Design and in vitro assessment of L-lactic acid-based copolymers as prodrug and carrier for intravitreal sustained L-lactate release to reverse retinal arteriolar occlusions. *Submitted to European Journal of Pharmaceutical Sciences.*

21. Pournaras CJ, Riva CE, Tsacopoulos M, Strommer K. Diffusion of O2 in the retina of anesthetized miniature pigs in normoxia and hyperoxia. *Exp Eye Res* 1989; 49: 347-360.

22. Einmahl S, Ponsart S, Bejjani RA, D'Hermies F, Savoldelli M, Heller J, Tabatabay C, Gurny R, Behar-Cohen F. Ocular biocompatibility of a poly(ortho ester) characterized by autocatalyzed degradation. *J Biomed Mater Res A* 2003; 67: 44-53.

23. Alder VA, Ben-Nun J, Cringle SJ. PO_2 profiles and oxygen consumption in cat retina with an occluded retinal circulation. *Invest Ophthalmol Vis Sci* 1990; 31: 1029-1034.

24. Pournaras CJ, Tsacopoulos M, Strommer K, Gilodi N, Leuenberger PM. Experimental retinal branch vein occlusion in miniature pigs induces local tissue hypoxia and vasoproliferative microangiopathy. *Ophthalmology* 1990; 97: 1321-1328.

25. Witmer AN, Vrensen GFJM, Van Noorden CJF, Schlingemann RO. Vascular endothelial growth factors and angiogenesis in eye disease. *Prog Retin Eye Res* 2003; 22: 1-29.

26. Kaur C, Foulds WS, Ling EA. Hypoxia-ischemia and retinal ganglion cell damage. *Clin Ophthalmol* 2008; 2: 879-889.

27. Trimawithana TR, Young S, Bunt CR, Green C, Alany RG. Drug delivery to the posterior segment of the eye. *Drug Discov Today* 2011; 16: 270-277.

SUPPLEMENTARY MATERIAL

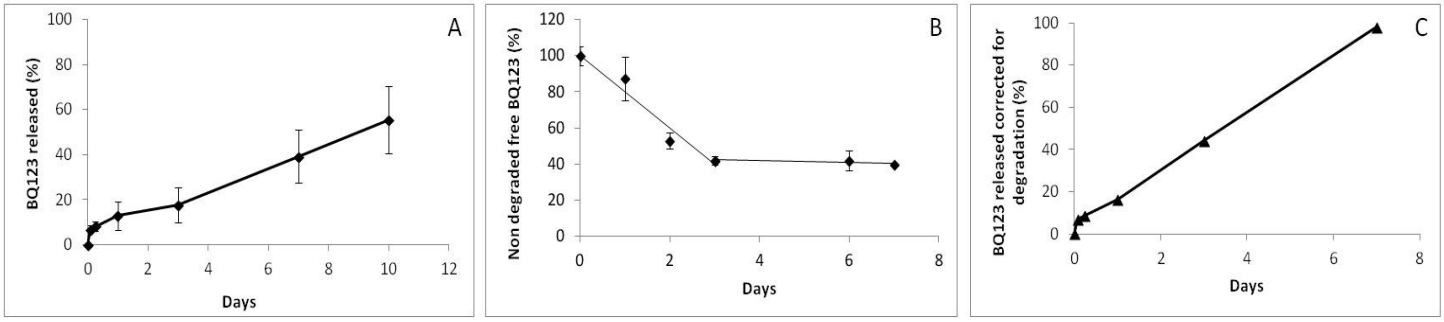

Figure S1. *In vitro BQ123 release and degradation in porcine vitreous humor* ***(A)*** *Non corrected release of BQ123 from the polymer (mean ± SD, n=18: 6 vials, 3 analyses per vial). 100% release corresponds to 100 µg BQ123.* ***(B)*** *Degradation of free BQ123 (mean ± SD, n=6: 2 vials, 3 analyses per vial). 100% non-degraded free BQ123 corresponds to 100 µg BQ123. A linear regression with a coefficient of determination of 0.955 is observed for the first 3 days of the curve, thereafter degradation stops and the amount of BQ123 present remains at 40%.* ***(C)*** *BQ123 release corrected for degradation (mean), derived from* ***(A)*** *and* ***(B)*** *following the equation as presented in Methods.*

Association of ranibizumab (Lucentis®) or bevacizumab (Avastin®) with dexamethasone and triamcinolone acetonide: An *in vitro* stability assessment

Marieke Veurink[1], Cinzia Stella[1], Cyrus Tabatabay[2], Constantin J. Pournaras[2] and Robert Gurny[1]

[1] Department of Pharmaceutics and Biopharmaceutics, School of Pharmaceutical Sciences, University of Geneva, University of Lausanne, CH-1211 Geneva 4, Switzerland, [2] Department of Ophthalmology, Geneva University Hospitals, Geneva, Switzerland

Published in: European Journal of Pharmaceutics and Biopharmaceutics, 2011; 78: 271-277

The *in vitro* stability of monoclonal antibodies used for age-related macular degeneration, ranibizumab and bevacizumab, was investigated. The aggregation profile of the antibodies was compared, alone and after association with dexamethasone sodium phosphate or triamcinolone acetonide. Commercial formulations of ranibizumab and bevacizumab were dialysed into three different buffers. After dialysis, samples were stored at 4ºC, 25ºC and 40ºC during 35 days, alone and in combination with dexamethasone sodium phosphate, triamcinolone acetonide phosphate solution or triamcinolone acetonide suspension. Combined formulations based on both commercial formulations were investigated as well. The aggregation state of the antibodies was measured by multi-angle light scattering (MALS) after separation by asymmetrical flow field-flow fractionation (AFFF) or size-exclusion chromatography (SEC). Ranibizumab results to be more stable than bevacizumab, alone and in combination with dexamethasone sodium phosphate or triamcinolone acetonide. Elevation in concentration, pH and temperature causes a decrease in stability of both antibodies. The association of triamcinolone acetonide phosphate solution with either ranibizumab or bevacizumab is observed to be the least stable combination of all samples tested. Dexamethasone sodium phosphate was shown to have a stabilizing effect on bevacizumab, although this is not the case for its combination with the commercial formulation Avastin®. The results demonstrate that the *in vitro* association of either ranibizumab or bevacizumab with dexamethasone sodium phosphate or triamcinolone acetonide suspension does not decrease the stability of these antibodies. Although ranibizumab is more stable than bevacizumab *in vitro*, further research has to point out how this affects their mechanism of action *in vivo*.

Keywords: monoclonal antibodies, asymmetrical flow field-flow fractionation, aggregation state, anti-inflammatory drugs, neovascular age-related macular degeneration.

INTRODUCTION

Ranibizumab (Lucentis®) is a humanized monoclonal antibody fragment with a molecular weight of 48 kiloDalton (kDa) that inhibits vascular endothelial growth factor (VEGF). It has been registered since 2006 for the treatment of neovascular age-related macular degeneration (AMD).[1,2] Bevacizumab (Avastin®) is a monoclonal humanized antibody with a molecular weight of 149 kDa that has a comparable mechanism of action, since ranibizumab is a fragment of the same antibody and currently, is widely used off-label for the treatment of AMD.[1] For ranibizumab a monthly injection is recommended to maintain therapeutically effective drug concentrations[3] and the same frequency is generally reported for bevacizumab injections.[2] Nevertheless, a reduced frequency of injections would be favourable because of patient discomfort and risk of complications.[4]

Combination therapy of VEGF-inhibitors with anti-inflammatory drugs such as dexamethasone or triamcinolone acetonide could possibly increase the therapeutic efficacy of the treatment. Anti-inflammatory drugs are well known for their positive effects on AMD,[5-8] with a different mechanism of action compared to VEGF-inhibitors.[9] Therefore, combination of the two drugs could lead to a synergistic effect. Several clinical trials report the co-administration of bevacizumab with triamcinolone acetonide or dexamethasone.[5,10-13] However, in these studies the possible interaction between bevacizumab and triamcinolone acetonide or dexamethasone has never been taken into account. The antibody-based formulation may aggregate, resulting in serious clinical side-effects, since protein aggregates can reduce the efficacy and enhance the immunogenicity of the protein drug.[14-17] Thus, formation of dimers, trimers or higher order oligomers should be prevented where possible.

The present study focuses on the *in vitro* compatibility of ranibizumab and bevacizumab with dexamethasone sodium phosphate, triamcinolone acetonide phosphate solution and triamcinolone acetonide suspension. The purpose is to investigate whether the monomeric native state of the antibodies is influenced by addition of these anti-inflammatory drugs. Samples are analysed by asymmetrical flow field-flow fractionation (AFFF). This analytical technique covers a large range of

detectable protein sizes, from protein monomers up to subvisible particles,[18] which makes it a good candidate for protein aggregation studies. As described by Demeule, AFFF offers the possibility to combine two methodologies:[19] in a first step hardly any mechanical stress is applied allowing the detection of loose aggregates, followed by a second step in which the different fractions of monomers and aggregates are separated.

MATERIALS AND METHODS

Four different series of samples were tested:

Series I.

To obtain a baseline, the aggregation state of both commercial formulations of ranibizumab (Lucentis®, Novartis Pharma Schweiz AG, Bern, Switzerland) and bevacizumab (Avastin®, Roche Pharma, Reinach, Switzerland) was analysed during 35 days of storage at 4ºC, 25ºC and 40ºC. For both formulations, three different sample containers were stored and for each container 2 analyses were carried out directly after preparation (t_0) and after 7, 14 and 35 days. Because of the low inter-sample variability over time shown in these analyses (CV≤0.5% for both ranibizumab and bevacizumab at all time points and temperatures), all other analyses were carried out in duplicate.

Series II.

Concentrations of 5, 10, 18 and 25 mg/ml ranibizumab and bevacizumab were prepared to study the influence of concentration on the aggregation state. Ranibizumab and bevacizumab were dialysed overnight (Pierce Slide-A-Lyzer Dialysis Cassette, Reactolab, Servion, Switzerland) into a 10 mM histidine buffer pH 5.5 and a 50 mM phosphate buffer pH 6.2, respectively, since these are the buffers used in the commercial products Lucentis® and Avastin®. NaCl was added to the buffers to obtain isotonicity. After dialysis, all samples were concentrated by centrifugation or diluted with buffer to concentrations of 5, 10, 18 and 25 mg/ml. Samples were stored during 35 days at 40ºC.

Series III.

The commercial products Lucentis® and Avastin® were associated with dexamethasone 21-phosphate disodium salt (Sigma-Aldrich, Lausanne, Switzerland), triamcinolone acetonide-21-phosphate dipotassium salt solution (Kenacort A solubile, Dermapharm AG Arzneimittel, Grünwald, Germany) or triamcinolone acetonide suspension (Kenacort A 40, Dermapharm AG Arzneimittel, Grünwald, Germany) to study the influence of a combined formulation on the stability of the antibody. Both antibodies were stored at 40ºC, alone and in combination with dexamethasone sodium phosphate, triamcinolone acetonide solution and triamcinolone acetonide suspension. Based on concentrations described in literature for combination therapy with bevacizumab the following combined formulations were selected:

i. 1.5 mg bevacizumab and 0.8 mg dexamethasone sodium phosphate[5]

ii. 1.25 mg bevacizumab and 2 mg triamcinolone acetonide[10-13] (solution and suspension)

iii. 0.6 mg ranibizumab and 0.8 mg dexamethasone sodium phosphate

iv. 0.5 mg ranibizumab and 2 mg triamcinolone acetonide (solution and suspension)

The dosage of ranibizumab in the combined formulation was chosen to be 2.5 times lower than that of bevacizumab, based on the difference in therapeutic dosage, which is 0.5 mg for ranibizumab compared to 1.25 mg for bevacizumab. The pH of the combined formulations was not adjusted after addition of the anti-inflammatory drugs, in order to stay as close as possible to the clinical studies mentioned earlier.

Series IV.

To evaluate the influence of anti-inflammatory drugs on the antibodies in different buffers and at different pH values, bevacizumab and ranibizumab were associated with dexamethasone 21-phosphate disodium salt, triamcinolone acetonide-21-phosphate dipotassium salt solution or triamcinolone acetonide suspension. Before addition of the anti-inflammatory drugs, both bevacizumab and ranibizumab were dialysed overnight in three different isotonic buffers to change the pH. For bevacizumab, 50 mM acetate buffer pH 5.0, 50 mM phosphate buffer pH 6.2 and 50 mM phosphate buffer pH 7.0 were used. For ranibizumab, 50 mM acetate buffer pH 5.0, 10 mM histidine buffer pH

5.5 and 50 mM phosphate buffer pH 7.0 were chosen. The buffer choice was based on a pH range and buffer capacity that is tolerated by the eye and that is acceptable for the stability of the antibodies.[20,21] A phosphate buffer pH 6.2 and histidine buffer pH 5.5 were selected because these buffers are used in the commercial products Avastin® and Lucentis®, respectively.

After dialysis, bevacizumab was analysed at a concentration of 19 mg/ml (pH 5.0=19.8 mg/ml, pH 6.2=19.2 mg/ml, pH 7.0=18.7 mg/ml) and ranibizumab at 6 mg/ml (pH 5.0=6.8 mg/ml, pH 5.5= 5.9 mg/ml, pH 7.0=6.4 mg/ml). Both antibodies were stored at 4ºC, 25ºC and 40ºC, alone and in combination with dexamethasone sodium phosphate, triamcinolone acetonide solution and triamcinolone acetonide suspension. The ratio antibody:anti-inflammatory drug was the same as described in Series III. Again, no pH adjustments were made after addition of the anti-inflammatory drug, to mimic the clinical studies in which the combinations were applied.

Sample analysis

Samples with a sample volume of 0.5 µl for all bevacizumab samples and 1.0 µl for all ranibizumab samples were analysed directly after preparation (t_0) and after 7, 14 and 35 days. Before analysis, the samples containing triamcinolone acetonide suspension were filtered over a 0.2 µm filter to obtain a visible clear sample for measurement. The weight-averaged molar mass of the antibody fractions was measured by multi-angle light scattering (MALS) after separation by asymmetrical flow field-flow fractionation (AFFF) (Wyatt Technology Europe GmbH, Dernbach, Germany).[22-24] Since the molar masses of both Avastin® and Lucentis® are known, the data obtained by MALS can be used to calculate the degree of aggregation. The concentrations of bevacizumab and ranibizumab were determined by UV spectroscopy at 280 nm, based upon an extinction coefficient of 1.7 and 1.8 cm ml/mg, respectively. Data were collected and analysed with Astra software (Wyatt Technology Europe GmbH, Dernbach, Germany). The aggregation state was expressed as the percentage of monomers versus time. For the aggregated fraction a distinction was made between dimers, aggregates that are greater than or equal to trimers and higher order aggregates (≥ ten times $MW_{monomer}$). The mobile phase was the same as the buffer used for each analyzed formulation. To minimize mechanical stress applied

on the sample during analysis by focussing and cross-flow, samples were analysed without focussing and cross-flow in a first step. In a second step, focussing and cross-flow were applied in order to separate the fraction of monomers from any existing aggregates.

The samples containing the commercial products Avastin® and Lucentis® in combination with anti-inflammatory drugs (Series III) were analysed by Size Exclusion Chromatography as well, in order to have an orthogonal technique to double check the results obtained by AFFF. Both analyses (AFFF and SEC) were performed on the same samples. Separations were achieved on an Ultrahydrogel 120 (Lucentis® samples) and an Ultrahydrogel 250 column (Avastin® samples) (Waters, Milford, USA). The weight-averaged molar mass and concentrations of both antibodies were measured by MALS and UV spectroscopy, respectively. Analyses were carried out in isocratic conditions and at a temperature of 35ºC, using a 50 mM phosphate buffer as mobile phase.

RESULTS

Series I.

The commercial product Lucentis® is very stable at 4ºC, 25Cº and 40ºC (Figure 1A). As expected, a rise in temperature causes a small decrease in stability: even at 40ºC an average monomer percentage of 99.6 ± 0.3% (n=6) is observed after 35 days of storage. However, the small fractions of aggregates present are higher order aggregates. The commercial product Avastin® is less stable than Lucentis® (Figure 1B). At t=0, the average measured monomer percentage is 97.2 ± 0.1% (n=6). After 35 days of storage, this percentage decreases to 96.9 ± 0.2% (n=6) at 4ºC, 96.6 ± 0.1% (n=6) at 25Cº and 91.3 ± 0.5% (n=6) at 40ºC. The measured aggregates are present in the form of dimers.

Series II.

The comparison of ranibizumab and bevacizumab at 5, 10, 18 and 25 mg/ml also shows a higher stability for ranibizumab than for bevacizumab at all four concentrations (Figure 2A and 2B). A rise in concentration causes a stability decrease for both antibodies. After 35 days of storage at 40ºC, the average percentage of monomers is 99.8% (n=2) for a concentration of 5 mg/ml ranibizumab.

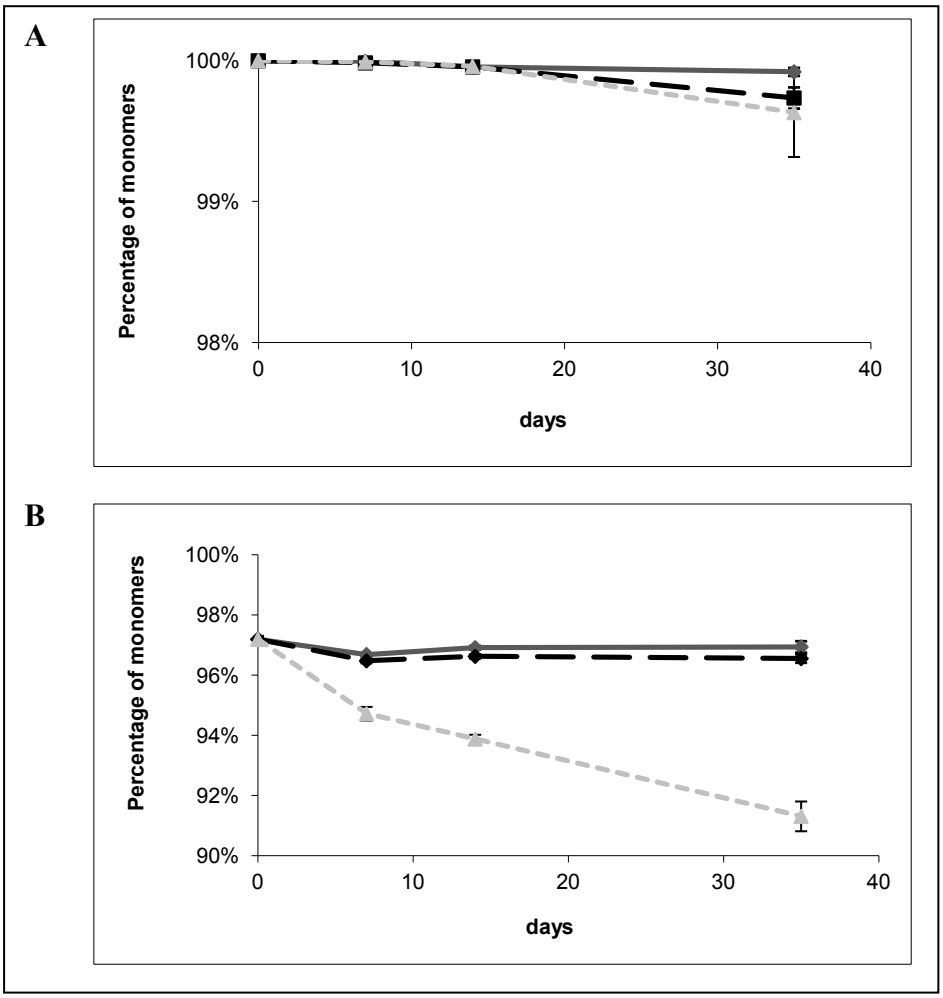

Figure 1. *Comparison of commercial products of ranibizumab and bevacizumab at different storage temperatures.* ***1A.*** *Upper figure represents the percentage of monomers of the commercial product of ranibizumab (Lucentis®) after storage at 4ºC (n=6, dark grey line), 25ºC (n=6, dashed black line) and 40ºC (n=6, dashed light grey line).* ***1B.*** *Lower figure represents the percentage of monomers of the commercial product of bevacizumab (Avastin®) after storage at 4ºC (n=6, dark grey line), 25ºC (n=6, dashed black line) and 40ºC (n=6, dashed light grey line).*

For concentrations of 10, 18 and 25 mg/ml ranibizumab this percentage rises to 98.2% (n=2), 97.0% (n=2) and 97.5% (n=2) respectively. For all concentrations, the aggregated fraction consists of dimers. 98.1% (n=2) of bevacizumab is found to be present as monomer at a concentration of 5 mg/ml after 35 days at 40ºC, compared to 97.2% (n=2) at 10 mg/ml, 92.9% (n=2) at 18 mg/ml and 92.8% (n=2) at 25 mg/ml. The concentration of 5 mg/ml demonstrates to contain only dimers in the aggregated fraction, the other concentrations contain dimers and a fraction ≥ trimers. After 35 days, a partial reversion to monomers is detected for the samples with concentrations of 5 mg/ml and 10 mg/ml (Figure 2B).

Almost no difference is observed between the samples with a concentration of 18 mg/ml and 25 mg/ml.

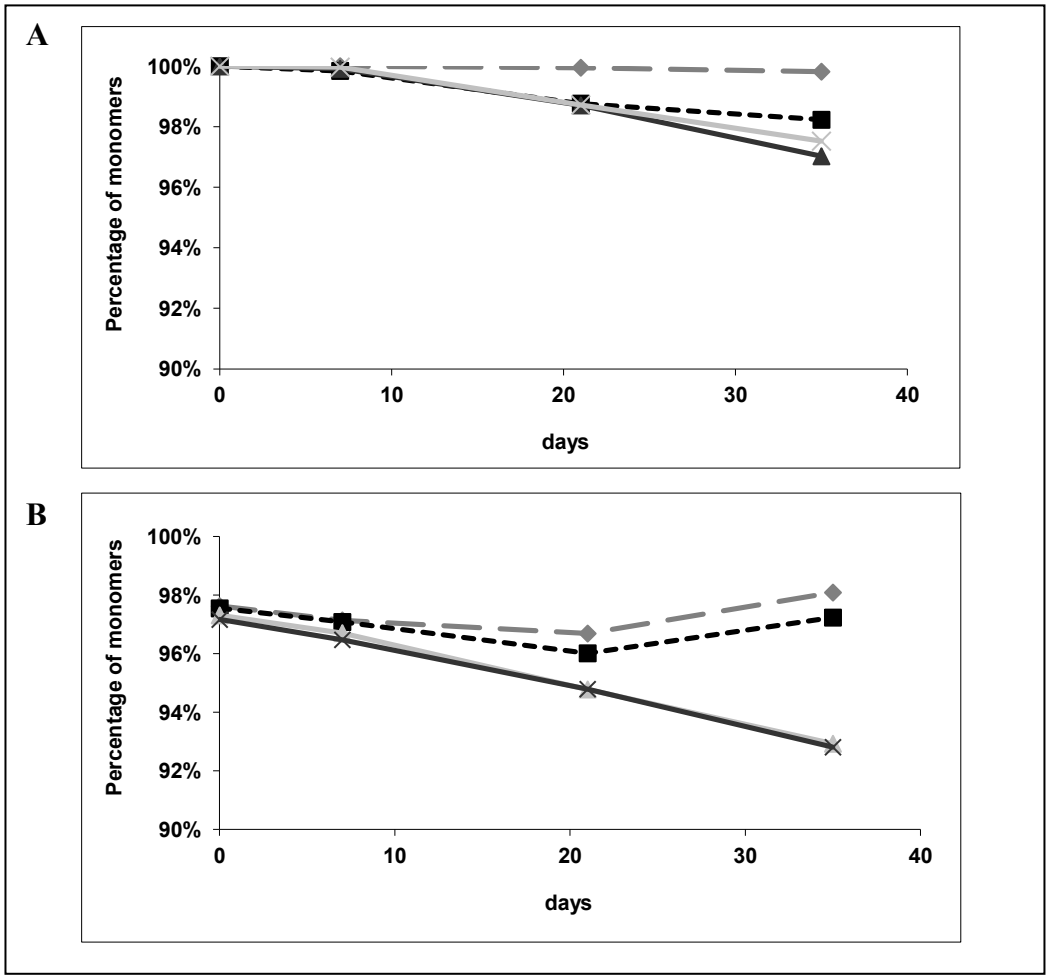

Figure 2. *Influence of concentration on the stability of ranibizumab and bevacizumab. The stability of both antibodies is tested at four different concentrations, stored at 40ºC.* ***2A.*** *Upper figure shows the average percentage of monomers (n=2) of ranibizumab 5 mg/ml (grey dashed line), ranibizumab 10 mg/ml (black dashed line), ranibizumab 18 mg/ml (dark grey line) and ranibizumab 25 mg/ml (light grey line), pH 5.5.* ***2B.*** *Lower figure shows the average percentage of monomers (n=2) of bevacizumab 5 mg/ml (grey dashed line), bevacizumab 10 mg/ml (black dashed line), bevacizumab 18 mg/ml (light grey line) and bevacizumab 25 mg/ml (dark grey line), pH 6.2.*

Series III.

Lucentis® commercial product, alone and in combination with dexamethasone sodium phosphate, triamcinolone acetonide phosphate solution and triamcinolone acetonide suspension

The commercial product Lucentis® stays stable over time after storage at 40ºC, alone and in combination with dexamethasone and triamcinolone acetonide suspension (Table 1A). After 35 days, monomer percentages of 99.5%, 99.3%, and 98.7% are observed by AFFF analysis for Lucentis® alone, in combination with dexamethasone and with triamcinolone acetonide suspension, respectively. For all three formulations, the aggregated fraction is present in the form of higher order aggregates. These results are confirmed by SEC analysis (Table 1B). The combined formulation of Lucentis® with triamcinolone acetonide solution is unstable, large visible aggregates were observed after 7 days storage. Therefore, this sample was not further analysed.

Table 1. *Comparison of the aggregation state of Lucentis® alone and as combined formulation.*

1A: *Results obtained by AFFF separation*[a,b]

	Lucentis	**Lucentis + Dexamethasone**	**Lucentis + Triamcinolone suspension**	**Lucentis + Triamcinolone solution**
Monomer	99.5 ± 0.1 %	99.3 ± 0.1 %	98.7 ± 0.1 %	Large visible aggregates
Dimer				
≥ Trimer	0.5 ± 0.1 %	0.7 ± 0.1 %		
Higher order aggregates			0.7 ± 0.1 %	

1B: *Results obtained by SEC separation*[a,b]

	Lucentis	**Lucentis + Dexamethasone**	**Lucentis + Triamcinolone suspension**	**Lucentis + Triamcinolone solution**
Monomer	99.7 ± 0.2 %	98.9 ± 0.2 %	99.35 ± 0.2 %	Large visible aggregates
Dimer				
≥ Trimer	0.3 ± 0.2 %	1.1 ± 0.2 %		
Higher order aggregates			1.1 ± 0.2 %	

[a] *Data are expressed as the percentage of monomers and aggregates ± SD (n=3).*

[b] *Samples are stored for 35 days at 40ºC.*

Avastin® commercial product, alone and in combination with dexamethasone sodium phosphate, triamcinolone acetonide phosphate solution and triamcinolone acetonide suspension

The combined formulation of Avastin® and triamcinolone acetonide phosphate solution shows large visible aggregates as well after 14 days of storage at 40ºC. The other combinations demonstrate a similar amount of aggregation as the Avastin® alone: after 35 days monomer percentages of 88.5%, 88.6% and 89.6% are detected for Avastin® alone, in combination with dexamethasone phosphate and with triamcinolone acetonide suspension, respectively. However, the aggregated fraction consists of only dimers for Avastin® alone and for the formulation containing triamcinolone acetonide suspension, whereas the combination with dexamethasone phosphate shows a fraction of dimers and a small fraction of higher order oligomers as well (Table 2A). The results are confirmed by SEC. The percentages of monomers for Avastin® and the combination with triamcinolone acetonide suspension are slightly lower than obtained by AFFF, however the aggregated fraction also contains dimers only.

Table 2. *Comparison of the aggregation state of Avastin® alone and as combined formulation.*

2A: *Results obtained by AFFF separation*[a,b]

	Avastin	**Avastin + Dexamethasone**	**Avastin + Triamcinolone suspension**	**Avastin + Triamcinolone solution**
Monomer	88.5 ± 0.4 %	88.6 ± 0.9 %	89.6 ± 3.6 %	
Dimer	11.5 ± 0.4 %	10.2 ± 0.8 %	10.4 ± 3.6 %	Large visible aggregates
≥ Trimer				
Higher order aggregates		1.2 ± 0.3 %		

2B: *Results obtained by SEC separation*[a,b]

	Avastin	**Avastin + Dexamethasone**	**Avastin + Triamcinolone suspension**	**Avastin + Triamcinolone solution**
Monomer	95.0 ± 0.3 %	88.3 ± 0.4 %	96.1 ± 0.1 %	
Dimer	5.0 ± 0.3 %		3.9 ± 0.1 %	Large visible aggregates
≥ Trimer				
Higher order aggregates		11.7 ± 0.4 %		

[a] *Data are expressed as the percentage of monomers and aggregates ± SD (n=3).*

[b] *Samples are stored for 35 days at 40ºC.*

For the formulation with dexamethasone phosphate a similar monomer percentage is found as by AFFF, however the fraction of aggregates consists only of higher order aggregates, probably because the dimer peak and the higher order oligomer peak are not separated (Table 2B).

Series IV.

Ranibizumab, alone and in combination with dexamethasone sodium phosphate, triamcinolone acetonide phosphate solution and triamcinolone acetonide suspension

Ranibizumab is observed to be very stable at all pH conditions (Table 3A). The sample of ranibizumab alone is least stable at pH 7, with an average monomer percentage of 98.7% (n=2) after 35 days of storage at 40ºC (Figure 3). On the other hand, at both pH 5.0 and pH 5.5, the sample shows a 100% monomer state during 14 days at all temperatures (data not shown). At 35 days, a monomer percentage > 99% is observed for these samples. For all three pHs, the aggregated fraction contains oligomers ≥ trimers.

Ranibizumab in association with dexamethasone sodium phosphate presents a similar degree of aggregation as ranibizumab alone under all three pH conditions tested at 4ºC and 25ºC. At 40ºC, the addition of dexamethasone causes a slightly higher aggregation at pH 5.0 and 5.5, i.e. from >99% of monomers to >95%. The measured aggregates are present as dimers. At pH 7.0 the aggregation profile of the combined sample at 40ºC is comparable to that of ranibizumab alone; both show monomer percentages > 98% and a fraction ≥ trimers after 35 days of storage at 40ºC.

The combination of ranibizumab with triamcinolone acetonide phosphate solution causes an increase in aggregation at all pH values compared to ranibizumab alone. The sample stored at pH 7, 40ºC presents the highest amount of aggregates (≥ trimers), with an average monomer percentage of 93.9% (n=2). At pH 5.0 and pH 5.5, monomer percentages of 96.7% (n=2, pH 5.0) and 98.7% (n=2, pH 5.5) are obtained after 35 days of storage at 40ºC. Oligomers ≥ trimers are detected as aggregated fraction. Ranibizumab combined with triamcinolone acetonide suspension also shows a higher aggregation at

pH 7.0 compared to ranibizumab alone, with an average monomer percentage of 95.9% (n=2). At pH 5.0 and 5.5, the aggregation state is similar to that of the ranibizumab sample. For all three pHs, the aggregated fraction is ≥ trimers.

Table 3. *Comparison of the aggregation state of ranibizumab (A) or bevacizumab (B) alone and as combined formulation.*

3A: *Percentages of monomers/aggregates for ranibizumab*[a,b]

	Ranibizumab			**Ranibizumab + Dexamethasone**			**Ranibizumab + Triamcinolone suspension**			**Ranibizumab + Triamcinolone solution**		
pH	**5**	**5.5**	**7**	**5**	**5.5**	**7**	**5**	**5.5**	**7**	**5**	**5.5**	**7**
Monomer	99.2%	99.5%	98.7%	95.5%	95.3%	98.8%	99.3%	99.4%	95.9%	96.7%	98.7%	93.9%
Dimer				4.5%	4.7%							
≥ Trimer	0.8%	0.5%	1.3%			1.2%	0.7%	0.6%	4.1%	3.3%	1.3%	6.1%

3B: *Percentages of monomers/aggregates for bevacizumab*[a,b]

	Bevacizumab			**Bevacizumab + Dexamethasone**			**Bevacizumab + Triamcinolone suspension**			**Bevacizumab + Triamcinolone solution**		
pH	**5**	**6.2**	**7**	**5**	**6.2**	**7**	**5**	**6.2**	**7**	**5**	**6.2**	**7**
Monomer	95.9%	87.5%	68.8%	94.4%	95.2%	95.6%	Large visible aggre-gates	84.2%	73.3%	96.5%	Large visible aggre-gates	60.6%
Dimer	4.1%	12.5%	27.2%	5.6%	4.8%	4.4%		15.8%	26.7%	3.5%		2.2%
≥ Trimer			4.0%									16.4%
Higher order aggregates												20.8%

[a] *Results are expressed as the average percentage of monomers and aggregates (n=2).*

[b] *Samples are stored for 35 days at 40ºC.*

Bevacizumab, alone and in combination with dexamethasone sodium phosphate, triamcinolone acetonide phosphate solution and triamcinolone acetonide suspension

After changing the pH from 6.2 to 5.0 by dialysis, the monomer percentage of the sample of bevacizumab alone rises from 98.3% (t_0, n=2) to 100% (n=2) after storage at 4ºC and 25ºC (Figure 4). This stabilization is not observed after 35 days of storage at 40ºC: an average monomer percentage of 95.9% (n=2) and 4.1% of dimers are measured. Storage at pH 6.2 and pH 7.0 results in monomer percentages of 87.5% (n=2) and 68.8% (n=2), respectively (Table 3B). The aggregated fraction

demonstrates only dimers for pH 6.2, whereas pH 7.0 contains dimers and a fraction of oligomers ≥ trimers.

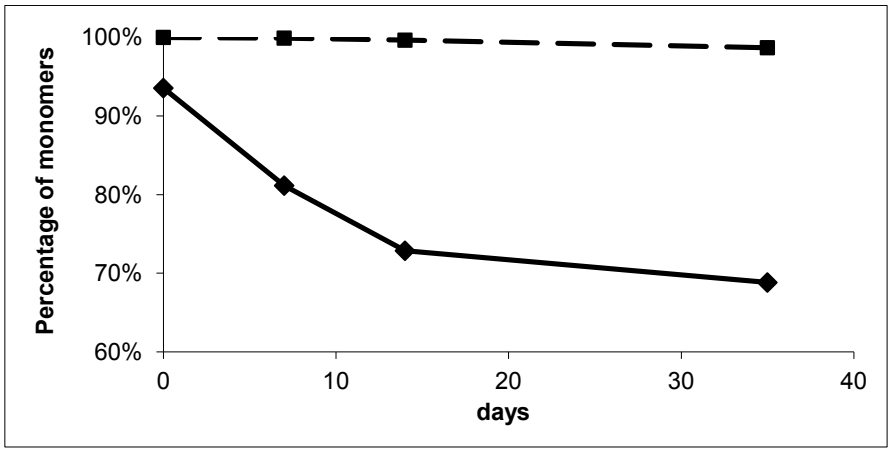

Figure 3. *Stability comparison of ranibizumab (dashed black line) and bevacizumab (black line) at pH 7.0, 40ºC. Analyses are carried out in duplicate; the average percentage of monomers of the two analyses is taken for both curves.*

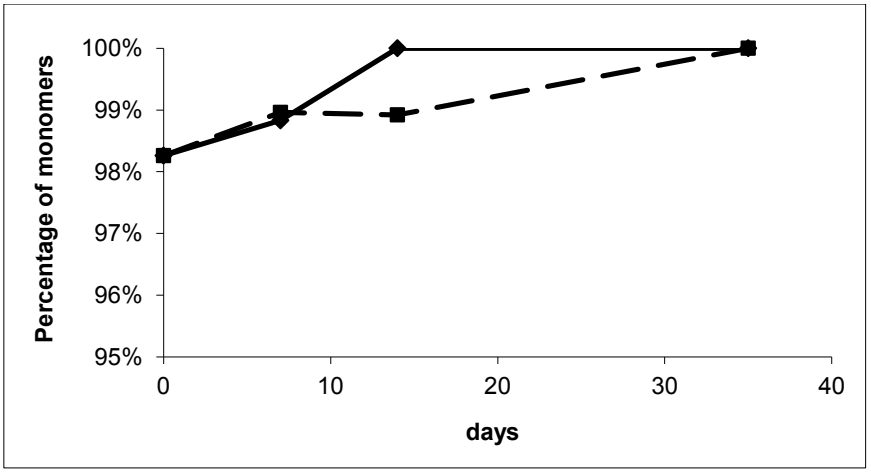

Figure 4. *Reversion back into monomers of bevacizumab in pH 5.0, after storage at 4ºC (black line) and 25ºC (dashed black line). Analyses are carried out in duplicate; the average percentage of monomers of the two analyses is taken for both curves.*

The association of bevacizumab with dexamethasone sodium phosphate causes a surprising stabilization of the antibody in comparison with the sample of bevacizumab alone (Figure 5). After 35 days of storage at 40ºC at pH 6.2 and pH 7.0, the combination sample shows average monomer percentages of 95.2% (n=2) for pH 6.2 and 95.6% (n=2) for pH 7.0. The effect is not observed at pH 5,

after 35 days at 40ºC, a monomer percentage of 94.4% (n=2) is measured. For all three pH conditions, the aggregated fraction consists of dimers.

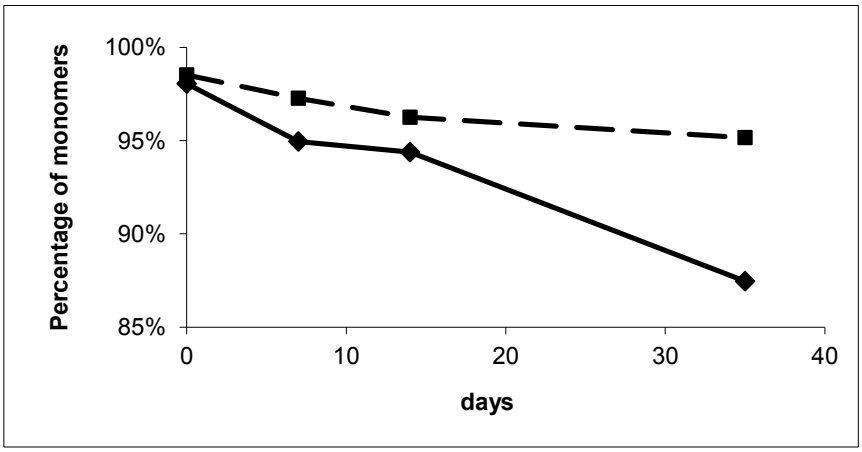

Figure 5. *Stabilizing effect of dexamethasone sodium phosphate on bevacizumab at pH 6.2, 40ºC. The monomer percentage of the sample of bevacizumab alone is represented by the black line and the combination sample of dexamethasone sodium phosphate and bevacizumab by the dashed black line. Analyses are carried out in duplicate; the average of the two analyses is taken for both curves.*

The combination of bevacizumab with triamcinolone acetonide phosphate solution is the least stable of all samples tested, with an average monomer percentage of 60.6% (n=2) at pH 7.0 after 35 days of storage at 40ºC. The aggregated fraction contains oligomers ≥ trimers and higher order aggregates. At pH 6.2, large visible aggregates are observed after 35 days of storage at 40ºC. After filtration over a 0.2 µm filter, neither monomers, nor aggregates are detected during AFFF analysis of the sample. Therefore, this sample is left out of the results. The most stable combination with triamcinolone acetonide phosphate solution is observed at pH 5.0, with an average monomer percentage of 96.5% (n=2) and 3.5% dimers after 35 days storage at 40ºC. The association of bevacizumab with triamcinolone acetonide suspension forms a visible precipitation at pH 5.0. The combination is filtered over a 0.2 µm filter prior to analysis. Analysis of the filtrate shows no detectable amount of monomers or aggregates and is therefore left out of the results. At pH 6.2 and pH 7.0, the amount of aggregation is similar to the one of bevacizumab alone and the aggregated fractions are both observed to be present as dimers.

DISCUSSION

The purpose of this study is to compare the stability of ranibizumab and bevacizumab alone and in combination with anti-inflammatory drugs. Percentages of monomers, dimers, trimers and higher order aggregates of both antibodies are measured to determine whether association with dexamethasone sodium phosphate and triamcinolone acetonide influences the aggregation state of these proteins. Since aggregates have been observed to cause severe side-effects,[14-17] these results are of great importance for clinical use.

A difference in stability is already observed between both commercial products; for Lucentis®, an average monomer percentage of 99.6 ± 0.3% (n=6) is measured after 35 days of storage at 40ºC, compared to 91.3 ± 0.5% (n=6) for Avastin®. The stability difference might be explained by the fact that the concentration of ranibizumab is approximately 2.5 times lower than that of bevacizumab: aggregation processes can be concentration dependent[21,25] and therefore, a more concentrated formulation may result in a higher state of aggregation. To exclude the possibility that ranibizumab is more stable because of its lower concentration in comparison to bevacizumab, the aggregation state of both antibody samples is compared at concentrations of 5, 10, 18 and 25 mg/ml. As expected, both antibodies show a decrease in stability after increasing the concentration. However, a comparison of ranibizumab and bevacizumab at the same concentration shows a higher stability for ranibizumab at all four concentrations (Figure 2A and 2B). Thus, the fact that bevacizumab is 2.5 times more concentrated than ranibizumab cannot totally explain the difference in stability.

The pH variation between both commercial formulations (pH 5.5 for Lucentis versus pH 6.2 for Avastin) might also be a factor contributing to the observed difference in stability. At pH 5.0, bevacizumab is very stable as well; for both bevacizumab alone and associated with dexamethasone sodium phosphate a reversion back into monomers is observed with time. Apparently, pH 5.0 is an optimal environment for bevacizumab; aggregates that are formed at pH 6.2 in the commercial product revert back into monomers at a lower pH. A similar reversion back into monomers is detected with the samples of 5 mg/ml and 10 mg/ml bevacizumab after 35 days of storage. The results are confirmed by

a study of Moore et al.,[21] who observed that the ideal pH for the native protein structure of bevacizumab is pH 5.5 and below. Furthermore, this work showed the capacity of bevacizumab to revert back into monomers upon dilution.

Based on the stability results of the present study, one could state that ranibizumab is a therapeutically better option compared to bevacizumab. However, since protein characteristics are very specific, it is unknown what the effect of the aggregation profiles of bevacizumab and ranibizumab will be *in vivo*. At this stage of investigation, it is uncertain whether bevacizumab with its higher aggregation state will have a higher clinical significance compared to the more stable ranibizumab. Besides, it must be taken into account that although the aggregated fraction for ranibizumab is very small, the aggregates observed are higher order aggregates, compared to dimers for bevacizumab. Since the last has the unique ability to revert back to the monomeric state upon dilution,[21] the formation of dimers might have advantages for the intravitreal usage of bevacizumab. As the formed dimers are probably too big to cross the retina, it might be possible that they will revert back into monomers in the vitreous, thereby causing a prolonged release effect *in vivo*. Thus, although ranibizumab is more stable than bevacizumab *in vitro*, it is uncertain how this affects their mechanisms of action *in vivo*. Further research will focus on the effects of the aggregation state of both antibodies *in vivo*.

The percentage of aggregation of bevacizumab alone and in the combination samples rises with higher pH and temperature. This can be explained by a low range in thermodynamic stability of the native protein structure.[26] Changes in external factors like pH or temperature can easily cause a destabilization in the structure of the protein, which leads to unfolding of parts of the protein. Partly unfolded proteins are more prone to aggregation than the native state of the protein.[26] For ranibizumab, similar effects are observed with an augmentation in temperature and less clear, for a rise in pH. All samples of ranibizumab alone and in combination that are stored at pH 5.0 and pH 5.5 show comparable results and their pHs probably lie too close together to show an effect. At pH 7.0 a rise in aggregation percentage is observed for all samples, except for the sample containing ranibizumab and dexamethasone. However, changes are minimal since all ranibizumab samples stay very stable.

For the combination samples, the most surprising effect observed is the stabilization of bevacizumab after addition of dexamethasone sodium phosphate. The influence of dexamethasone sodium phosphate was only observed at values of pH 6.2 and pH 7.0; at pH 5.0 bevacizumab is already very stable on its own. For the commercial formulation, a similar effect was observed after 7 and 14 days storage at 40ºC. However, after 35 days a fraction of large aggregates was detected for this combined formulation. The presence of large aggregates in the commercial formulation and the absence of these aggregates in the dialysed formulations show that the environment can highly influence the conformation of the antibody. Apparently, the ability of dexamethasone sodium phosphate to partly inhibit aggregation of the antibody only exists under certain circumstances. Consequently, optimisation of the formulation before starting clinical studies is a crucial step in combining therapeutic antibodies. It is unlikely that the stabilizing effect is caused by a pH change, since the pH was elevated after addition of dexamethasone sodium phosphate: a pH of 6.6 was measured for the sample of pH 6.2 and a pH 7.2 for the sample of pH 7.0. Since a higher pH leads to more aggregation, the stabilization is probably not due to changes in the pH.

The association of both antibodies with triamcinolone acetonide suspension is more stable than the combination with the triamcinolone acetonide phosphate solution. This might be caused by the fact that the pH of the triamcinolone acetonide phosphate solution alone is 7.4, whereas that of the suspension is 6.2. Therefore, the addition of triamcinolone acetonide phosphate solution causes a higher pH raise for all combinations than that of triamcinolone acetonide suspension, resulting in a higher aggregation state. Besides, where all other combined formulations are isotonic, a highly hypertonic formulation is formed after addition of triamcinolone acetonide solution to the antibody and this environmental change might also result in a destabilized antibody. Dexamethasone sodium phosphate was added as a solid form that was dissolved in the bevacizumab or ranibizumab formulation. Therefore, the association did not change the concentration of the antibodies. For triamcinolone acetonide, a solution and a suspension were used, thereby diluting the concentration of bevacizumab and ranibizumab. This may have influenced the stability of the antibodies, since less concentrated formulations are generally less prone to aggregation.

CONCLUSIONS

In this study, an *in vitro* comparison of the aggregation state of bevacizumab and ranibizumab was made and the effects of dexamethasone sodium phosphate and triamcinolone acetonide on their stability were investigated. The purpose of the study was not to determine whether bevacizumab or ranibizumab is a therapeutically better choice, but to provide a preliminary insight in the possible interactions between these antibodies and anti-inflammatory drugs. Ranibizumab is observed to be more stable than bevacizumab alone and in combination with dexamethasone sodium phosphate and triamcinolone acetonide suspension. Nevertheless, it is unknown how the *in vivo* activity of both antibodies is affected by the aggregates that are formed. Work is in progress to test the effects of the aggregation state of these antibodies *in vivo*. The results show that the stability profile of ranibizumab and bevacizumab is generally not decreased by the addition of dexamethasone sodium phosphate or triamcinolone acetonide suspension. A stabilizing effect of dexamethasone sodium phosphate on bevacizumab is even observed. However, combination of the commercial product Avastin® with dexamethasone phosphate shows higher order aggregates after 35 days storage at 40ºC, demonstrating the importance of optimising a combined formulation before starting clinical studies. Further research has to determine whether a combined formulation is able to prolong the injection interval.

REFERENCES

1. Andreoli CM, Miller JW. Anti-vascular endothelial growth factor therapy for ocular neovascular disease. *Curr Opin Ophthalmol* 2007; 18: 502-508.

2. Dadgostar H, Waheed N. The evolving role of vascular endothelial growth factor inhibitors in the treatment of neovascular age-related macular degeneration. *Eye* 2008; 22: 761-767.

3. Regillo CD, Brown DM, Abraham P, Yue H, Ianchulev T, Schneider S, Shams N. Randomized, double-masked, sham-controlled trial of ranibizumab for neovascular age-related macular degeneration: PIER study year 1. *Am J Ophthalmol* 2008; 145: 239-248.

4. Brown DM, Regillo CD. Anti-VEGF agents in the treatment of neovascular age-related macular degeneration: applying clinical trials results to the treatment of everyday patients. *Am J Ophthalmol* 2007; 144: 627-637.

5. Augustin AJ, Puls S, Offerman I. Triple therapy for choroidal neovascularisation due to age-related macular degeneration: verteporfin PDT, bevacizumab and dexamethasone. *Retina* 2007; 27: 133-140.

6. Conti SM, Kertes PJ. The use of intravitreal corticosteroids, evidence-based and otherwise. *Curr Opin Ophthalmol* 2006; 17: 235-244.

7. Gopal L, Sharma T. Use of intravitreal injection of triamcinolone acetonide in the treatment of age-related macular degeneration. *Indian J Ophthalmol* 2007; 55: 431-435.

8. Jonas JB. Intravitreal triamcinolone acetonide: a change in a paradigm. *Ophthalmic Res* 2006; 38: 218-245.

9. Oliver A, Ciulla TA. Corticosteroids as antiangiogenic agents. *Ophthalmol Clin North Am* 2006; 19: 345-351.

10. Ahmadieh H, Ramezani A, Shoeibi N, Bijanzadeh B, Tabatabaei A, Azarmina M, Soheilian M, Keshavarzi G, Mohebbi MR. Intravitreal bevacizumab with or without triamcinolone for refractory diabetic macular edema; a placebo-controlled, randomized clinical trial. *Graefes Arch Clin Exp Ophthalmol* 2008; 246: 483-489.

11. Ahmadieh H, Taei R, Soheilian M, Riazi-Esfahani M, Karkhaneh R, Lashay A, Azarmina M, Dehghan MH, Moradian S. Single-session photodynamic therapy combined with intravitreal bevacizumab and triamcinolone for neovascular age-related macular degeneration. *BMC Ophthalmol* 2007; 7: 10.

12. Colucciello M. Intravitreal bevacizumab and triamcinolone acetonide combination therapy for exudative neovascular age-related macular degeneration: Short-term optical coherence tomography results. *J Ocul Pharmacol Ther* 2008; 24: 15-24.

13. Soheilian M, Ramezani A, Bijanzadeh B, Yaseri M, Ahmadieh H, Dehghan MH, Azarmina M, Moradian S, Tabatabaei H, Peyman GA. Intravitreal bevacizumab (avastin) injection alone or combined with triamcinolone versus macular photocoagulation as primary treatment of diabetic macular edema. *Retina* 2007; 27: 1187-1195.

14. Demeule B, Gurny R, Arvinte T. Where disease pathogenesis meets protein formulation: Renal deposition of immunoglobulin aggregates. *Eur J Pharm Biopharm* 2006; 62: 121-130.

15. Hermeling S, Crommelin DJ, Schellekens H, Jiskoot W. Structure-immunogenicity relationships of therapeutic proteins. *Pharm Res* 2004; 21: 897-903.

16. Braun A, Kwee L, Labow MA, Alsenz J. Protein aggregates seem to play a key role among the parameters influencing the antigenicity of interferon alpha (IFN-alpha) in normal and transgenic mice. *Pharm Res* 1997; 14: 1472-1478.

17. Bucciantini M, Giannoni E, Chiti F, Baroni F, Formigli L, Zurdo J, Taddei N, Ramponi G, Dobson CM, Stefani M. Inherent toxicity of aggregates implies a common mechanism for protein misfolding diseases. *Nature* 2002; 416: 507-511.

18. Mahler HC, Friess W, Grauschopf U, Kiese S. Protein aggregation: Pathways, induction factors and analysis. *J Pharm Sci* 2009; 98: 2909-2934.

19. Demeule B, Gurny R, Arvinte T. Detection of protein aggregates: Methodologies for pharmaceutical development. Thesis dissertation, University of Geneva, 2006.

20. Martin A. Physical Pharmacy, 4th ed. Lea and Febiger, Philadelphia 1993, pp. 178-179.

21. Moore JM, Patapoff TW, Cromwell ME. Kinetics and thermodynamics of dimer formation and dissociation for a recombinant humanized monoclonal antibody to vascular endothelial growth factor. *Biochemistry* 1999; 38: 13960-13967.

22. Demeule B, Lawrence MJ, Drake AF, Gurny R, Arvinte T. Characterization of protein aggregation: The case of a therapeutic immunoglobulin. *Biochim Biophys Acta* 2007; 1774: 146-153.

23. Fraunhofer W, Winter G. The use of asymmetrical flow field-flow fractionation in pharmaceutics and biopharmaceutics. *Eur J Pharm Biopharm* 2004; 58: 369-383.

24. Furrer E, Berdugo M, Stella C, Behar-Cohen F, Gurny R, Feige U, Lichtlen PD, Urech DM. Pharmacokinetics and posterior segment biodistribution of ESBA105, an anti-TNF-{alpha} single-chain antibody, upon topical administration to the rabbit eye. *Invest Ophthalmol Vis Sci* 2009; 50: 771-778.

25. Wang W, Singh S, Zeng DL, King K, Nema S. Antibody structure, instability, and formulation. *J Pharm Sci* 2007; 96: 1-26.

26. Chi EY, Krishnan S, Randolph TW, Carpenter JF. Physical stability of proteins in aqueous solution: Mechanism and driving forces in non native protein aggregation. *Pharm Res* 2003; 20: 1325-1336.

Breaking the Aggregation of the Monoclonal Antibody Bevacizumab (Avastin®) by Dexamethasone Phosphate: Insights from Molecular Modelling and Asymmetrical Flow Field-Flow Fractionation

Marieke Veurink[1,2], Yvonne Westermaier[1,2], Robert Gurny[1], Leonardo Scapozza[1]

[1] School of Pharmaceutical Sciences, University of Geneva, University of Lausanne, Geneva, Switzerland
[2] Both authors contributed equally to this work

Published in: Pharmaceutical Research, 2013; 30: 1176-1187

Purpose: To investigate the mechanism behind the aggregation breaking properties of dexamethasone phosphate and related corticosteroids on the IgG1 antibody bevacizumab (Avastin®).

Methods: An *in silico* 3D dimer model is developed to identify the bevacizumab-bevacizumab interface, and different corticosteroids are docked onto the model to distinguish preferred binding sites. The *in silico* predictions are validated by *in vitro* stability studies, where the antibody is stressed in presence or absence of each corticosteroid and formed aggregates are quantified by asymmetrical flow field-flow fractionation.

Results: The dimer model features only one close crystal contact area: Lys445 on the Fc region interacts with one Fab arm of the second bevacizumab. Docking reveals an interaction between the phosphate group of dexamethasone phosphate and Lys445, while the rest of the molecule is hindering dimer formation. The predictions are confirmed *in vitro*, demonstrating that dexamethasone phosphate and betamethasone phosphate partly prevent antibody aggregation, whereas triamcinolone acetonide phosphate does not.

Conclusions: The results suggest that bevacizumab monomers follow a specific mechanism to form dimers in which a protein-protein interaction hotspot can be distinguished. The dimer formation can be hindered by corticosteroids in a specific way. This approach allows a simple way to stabilize IgG1 antibodies.

Keywords: monoclonal antibody, aggregation breaker, corticosteroids, molecular modelling, asymmetrical flow field-flow fractionation.

INTRODUCTION

Therapeutic antibodies are currently the fastest growing area of biopharmaceuticals with an average yearly market growth rate of 35% since 2001.[1] The recent development of chimeric and fully-humanized monoclonal antibodies has spawned an unprecedented interest in using these molecules as therapeutic agents, since they can specifically target molecules implicated in disease, thereby essentially side-stepping the secondary effects that may be associated with conventional drug therapies.

The development of stable antibody formulations is challenging, since they have the tendency to be physically and chemically instable in aqueous media. Antibodies are, for example, susceptible to denaturation, aggregation and covalent modifications.[2,3] Degradation of antibody formulations due to aggregation phenomena is a particular problem. The formation of aggregates might lead to a reduced efficacy of the protein drug. Since aggregates can increase the immunogenicity of the antibody,[4] clinical side-effects might occur. Antibody aggregation is also a source of batch-to-batch variations in the antibody production chain and its control leads to regulatory and quality control burdens with their associated costs. Furthermore, the propensity of antibodies to aggregate decreases the stability of the formulation, which negatively affects product shelf-life.[5]

Like for most other proteins, antibody stability depends on many factors, like protein concentration, pH, ionic strength, temperature and agitation. Predicting whether an antibody will aggregate is challenging, notably because each antibody may have a very specific and characteristic stability profile.[6] Moreover, due to the complexity of the antibody structure, identification of the precise nature of the antibody-antibody interaction and contact surfaces of aggregates remains challenging.[7] A number of approaches have been investigated to improve antibody stability, including the addition of "stabilizing" agents to the protein formulation. Examples of these agents are polysorbate-based surfactants,[8] amino acids,[9] glucose,[10] sorbitol,[10] and dextran sulphate.[9] Unfortunately, their success has been limited, mainly due to the fact that most of these agents are directed at optimising the environment surrounding the antibody, and not specifically at interfering with the interaction hotspot

involved in the formation of aggregates. Another concept to ameliorate the stability of the protein drug is to mutate single amino acids in Igs to specifically target hydrophobic patches implicated in aggregation.[7] However, such an approach necessarily modifies the structure of the Ig, possibly affecting both the clinical efficacy and immunogenicity of the protein drug.

The humanized monoclonal IgG1 antibody bevacizumab (Avastin®) is registered for the treatment of different forms of cancer and has also been widely used off-label for the ophthalmic indication age-related macular degeneration. It acts by blocking vascular endothelial growth factor A (VEGF-A), thereby inhibiting neovascularisation and leakage of blood vessels.[11] The present study is based on a clinical observation made earlier by our group,[12] in which the combination of bevacizumab with the anti-inflammatory drug dexamethasone disodium phosphate led to a decrease in aggregate formation. The rationale behind the combination of bevacizumab with dexamethasone phosphate is the fact that the latter also suppresses the formation of new leaky blood vessels. Thus, a synergistic effect might be obtained through combination therapy.[13]

The aims of this study are to clarify the mechanisms behind this protective process through a combination of *in silico* and *in vitro* studies. The formation of bevacizumab dimers is investigated by homology modelling and the interactions between several anti-inflammatory drugs and the antibody are studied by molecular docking. Outcomes of the *in silico* work are experimentally validated through *in vitro* stability studies on the combined formulations using Asymmetrical Flow Field-Flow Fractionation and Size Exclusion Chromatography coupled to Multi-Angle Light Scattering (AF4-MALS and SEC-MALS).

MATERIALS AND METHODS

Molecular modelling

Template identification and alignment

Bevacizumab is a humanized antibody formed by a Fab region responsible for recognizing antigens and a Fc region derived from IgG1. The Protein Data Bank (PDB) (http://www.rcsb.org)[14,15] was

surveyed for suitable crystal structures to be used as structural templates for homology modelling. Three structures were found: the bevacizumab Fab moieties in complex with the human VEGF (PDB id: 1BJ1)[16] and two full length IgG1 antibodies, a human (PDB id: 1HZH) and a murine one (PDB id: 1IGY). Because bevacizumab is a humanized antibody, the human antibody logically should be taken as template. However, the only full-length human IgG1 crystallized so far (PDB id: 1HZH) has an unusual crystal symmetry ($H3_2$) and strongly distorted orientations of the Fabs with respect to the axis of the Fc region.[17] In contrast, the intact murine IgG1κ is a template with a more usual overall 3D structure. With a resolution of 3.2 Å (PDB id: 1IGY), this structure is acceptable as template. To humanize its hinge-Fc region, the residues were mutated so as to match the sequence of the structure 1HZH. All sequence alignments were carried out with ClustalW[18,19] in the Biology Workbench 3.2 (San Diego Supercomputer Center; http://seqtool.sdsc.edu/CGI/BW.cgi). To nonetheless compare the symmetric murine configuration with an asymmetric model, the human template (1HZH) was used to build a second model.

3D model building and validation

The initial 3D model of bevacizumab was carried out using Sybyl 8.0 (Tripos Inc., St. Louis, MO, USA). The Fabs of IgG1 (1IGY) were structurally superposed and thereafter replaced with the ones of bevacizumab (1BJ1). Then, the bevacizumab Fabs were connected with the hinge-Fc of IgG1 (1IGY) and finally, the hinge-Fc region was humanized using the sequence of 1HZH. The connecting region of the model was submitted to energy minimization using Sybyl 8.0 default parameters while keeping the disulfide bridges intact. The quality of the resulting model was assessed using Procheck.[20] A Ramachandran plot analysis (in Procheck) of the amino acid conformations was carried out using a resolution mean between the crystal structures of both the Fc (resolution of 1IGY: 3.2 Å) and the Fabs (resolution of 1BJ1: 2.4 Å). Critical side chains were corrected for distortion in Sybyl 8.0 and the refinement procedure (manual adjustments and minimization) was repeated until reaching φ and ψ angles in the Ramachandran plot that were comparable to the input crystal structures. An analogous procedure was applied for the second model based on 1HZH.

3D (dimer) aggregation model

A 3D aggregation model was built to identify the bevacizumab-bevacizumab interface, with the idea in mind that crystal contacts represent privileged protein-protein interfaces. Based on the crystal symmetries of the IgG1 structure 1IGY and subsequently on the IgG1 structure 1HZH, putative crystal contacts between two full length bevacizumabs were defined using SwissPDBViewer 4.0.1.[21] For the 3D aggregation model based on 1IGY, the crystallographic symmetry ($P2_1$) of the IgG1 crystal structure was applied to obtain a layer, which was translated along the unit cell, and to recreate crystal contacts. The first translation, featuring the only close crystal contact between the monomers in the order of 4 Å, was saved in pdb format and the bevacizumab model overlaid according to the carbon α atom positions in Sybyl 8.0. The second model based on the crystal structure of 1HZH was obtained by applying the same procedure. Its translation according to the crystal symmetry of 1HZH was also displayed to verify whether close crystal contacts would occur in the same region for this asymmetric conformer as for the symmetric 1IGY.

Docking dexamethasone phosphate and similar anti-inflammatory drugs onto the bevacizumab monomer

Dexamethasone phosphate and two similar, commercially available anti-inflammatory drugs (betamethasone phosphate and triamcinolone acetonide phosphate) were docked onto the bevacizumab monomer to see where they were binding preferentially, whether binding took place in the aggregation zone and if so, how the observed binding propensities could be related to properties of the small molecules and the binding site, respectively. The small molecule setup for docking was done in Sybyl 8.0. Hydrogens were added to the small molecular weight molecule, the phosphate group was left unprotonated and Gasteiger-Huckel charges were calculated and added. Each resulting molecule was minimized using 100 steps of the default Powell minimization protocol of Sybyl 8.0. Systematic flexible docking with standard parameters was then performed with FlexX 3.1.3 (Biosolveit GmbH) all over the bevacizumab antibody surface (monomer: Fabs, hinge and Fc), previously divided into several segments of 10 Å around each arginine and lysine. By adopting this strategy, roughly 90% of the whole antibody surface and all major cavities were included in the docking study.

Based on the binding propensities of dexamethasone phosphate at the bevacizumab-bevacizumab interface and the physicochemical properties of the ligand and the binding site on one monomer, a putative mechanism of action was postulated. This mechanism was subsequently verified by docking betamethasone phosphate and triamcinolone acetonide phosphate in the same way as described for dexamethasone phosphate, in order to find out whether they would bind in the antibody-antibody contact region. Ten docking poses per molecule and docking site were kept, as this number revealed later to be sufficient to distinguish between aggregation breakers and non-aggregation breakers. The poses were scored with the FlexX scoring function. Evaluation of docking results was based on the attributed bevacizumab-small molecule interactions score, and the subsequent visual inspection was performed by considering the context of both the monomer and the dimer antibody models, using a cylindric "volume of interference" (Supplementary Material, Figure S1). The best-ranked poses projecting roughly orthogonally outwards from the bevacizumab surface and thus enclosed by this volume of interference, were retained.

***In vitro* experiments**

Three anti-inflammatory drugs were tested for their aggregation breaking properties, following the modelling outcomes:

i. Dexamethasone 21-phosphate disodium salt (Sigma-Aldrich, Lausanne, Switzerland),

ii. Betamethasone 21-phosphate disodium salt (Sigma-Aldrich, Lausanne, Switzerland), and

iii. Triamcinolone acetonide-21-phosphate dipotassium salt solution (Kenacort A Solubile, Dermapharm AG Arzneimittel, Grünwald, Germany).

All were combined with bevacizumab (Avastin®, Roche Pharma, Reinach, Switzerland) in a 1:150, 1:15 and/or 1:1.5 molar ratio (antibody:anti-inflammatory drug). Ratios were derived from clinical studies in which bevacizumab was combined with dexamethasone disodium phosphate in a molar ratio of 1 mol bevacizumab versus 150 mol dexamethasone disodium phosphate.[13]

Bevacizumab was used as commercial formulation, hereinafter referred to as Avastin®, in which the antibody is formulated in a 51 mM phosphate buffer pH 6.2 with 60 mg/ml α,α-trehalose dihydrate and 0.04% polysorbate 20, or was dialyzed overnight (Pierce Slide-A-Lyzer Dialysis Cassette, Reactolab, Servion, Switzerland) into 50 mM phosphate buffer at pH 7, hereinafter referred to as bevacizumab. The concentration of bevacizumab was kept at 25 mg/ml in all series to simulate the concentration of the commercial formulation, since dilution may lead to reversion of small aggregates into monomers.[6] After dialysis, the antibody formulation was combined directly with one of the three anti-inflammatory drugs or incubated at 40°C for one week, before addition of the anti-inflammatory drugs. Temperature and pH were chosen in order to accelerate the formation of aggregates, since an ongoing aggregation process is needed to observe a stabilizing effect of the different anti-inflammatory drugs in a reasonable time frame. Osmolality and pH were controlled and stayed constant over the duration of the study. The pH and osmolality of the samples containing antibody alone were similar to those in which the antibody was combined with a corticosteroid. Over time, all samples remained clear solutions and no insoluble aggregates were observed upon visible inspection.

It should be noted that the commercially available product Avastin® contains 0.04% polysorbate 20. Although the product was dialysed for a part of the studies, this does not lead to the complete removal of polysorbate.[22] Thus, it should be taken into account that all observed effects of the corticosteroids on the antibody occur in the presence of this surfactant.

Inter-sample variability was observed when different batches of Avastin were dialysed, with a maximum variability of 11%. In other words, the same treatment and stress did not always lead to the same amount of aggregates, possibly due to an inter-batch variability in the polysorbate concentration.[22] Therefore, comparisons were always made on the same batch, meaning that the sample to which the corticosteroid was added was always compared with a sample of the antibody alone from the same batch.

Series I: Effect of dexamethasone phosphate on aggregation formation induced by temperature stress

Three different concentrations of dexamethasone phosphate in 51 mM phosphate buffer pH 6.2 were added to the commercial formulation of Avastin® to obtain Avastin:dexamethasone disodium phosphate molar ratios of 1:1.5, 1:15 and 1:150. To the sample containing the antibody alone, the same volume of 51 mM phosphate buffer pH 6.2 was added, to avoid differences in antibody concentration between the samples with and without anti-inflammatory drug. After addition, Avastin® alone and the combined formulations were all stored for 35 days at 40°C. Samples were analysed directly after preparation (t_0) and after 7, 14 and 35 days. Based upon the outcomes of this series, in which the 1:15 molar ratio showed to be optimal, it was decided to perform all other series with this particular molar ratio.

Series II: Effect of dexamethasone phosphate on aggregation formation induced by mechanical stress

Bevacizumab was combined with dexamethasone phosphate in a 1:15 molar ratio, after dialysis of the antibody into 50 mM phosphate buffer at pH 7. The same volume of buffer was added to the sample containing antibody alone. Both samples were placed vertically in a Thermomixer (Thermomixer Comfort, Eppendorf AG, Hamburg, Germany) and were horizontally shaken at controlled room temperature for 48 hours at 1000 rpm. Samples were analysed at t_0 and at 1, 4, 24 and 48 hours.

Series III: Effect of three anti-inflammatory drugs on prestressed antibody

Bevacizumab was dialysed into 50 mM phosphate buffer at pH 7 and stored at 40°C for 7 days. After 7 days, dexamethasone phosphate, betamethasone phosphate and triamcinolone acetonide phosphate were added to the antibody in a 1:15 molar ratio. The same volume of buffer was added to the sample containing antibody alone. All samples were stored for 28 days at 40°C and analysed at t_0 and after 1, 7, 14 and 28 days.

Series IV: Effect of dexamethasone phosphate on prestressed Fab-fragment

The stabilizing properties of dexamethasone phosphate on the commercially available Fab-fragment ranibizumab (Lucentis®, Novartis Pharma Schweiz AG, Bern, Switzerland) were investigated as well.

Ranibizumab was dialysed overnight into a 50 mM phosphate buffer at pH 7 and concentrated to 10 mg/ml (based on the concentration of the commercial formulation). Since the fragment is very stable, the sample was stored for 1 year at 25°C before the addition of dexamethasone disodium phosphate in a 1:15 molar ratio. To the sample that contained the Fab fragment alone, a similar volume of buffer was added. Both the sample of ranibizumab alone and the combined formulation were stored for 28 days at 40°C. Samples were analysed at t_0 and after 1, 7, 14 and 28 days.

Sample analysis

Asymmetrical Flow Field-Flow Fractionation

All samples were analyzed by asymmetrical flow field-flow fractionation (AF4) (Wyatt Technology Europe GmbH, Dernbach, Germany), coupled to multi-angle light scattering (MALS) and UV spectroscopy at 280 nm.[23] This technique allows the measurement of aggregates up to the subvisible range.[24] Samples were injected undiluted; the injection volume per run depended on the concentration of the formulation and was 0.5 µl for bevacizumab (25 mg/ml) and 1.0 µl for ranibizumab (10 mg/ml). The applied mobile phase was similar to the buffer of the analyzed formulations, e.g. 51 mM phosphate buffer pH 6.2 for the commercial formulation and 50 mM phosphate buffer pH 7.0 for the dialysed samples. MALS detection allowed calculating the weight-average molar mass of the antibody fractions that were separated by AF4, thus providing information on the aggregation state of the particular fraction (a fraction with a molar mass of e.g. twice the monomer contains dimers, etc). Bevacizumab and ranibizumab concentrations were determined by UV spectroscopy, based upon an extinction coefficient of 1.7 and 1.8 cm ml/mg, respectively. Data collection and analysis were done using Astra software (version 5.1.9.1, Wyatt Technology Europe GmbH, Dernbach, Germany) and the different fractions were classified as monomers, dimers, trimers or higher order aggregates. Because of the low inter-sample variability observed over time using this method,[12] one sample container was stored for all samples and analyses were carried out in triplicates. All data were reported as average percentage of monomers/aggregates ± standard deviation (SD) (n=3). Pair-wise comparisons were carried out to compare the antibody alone with the combined formulations using a Mann-Whitney U test (exact one-tailed significance, $p \leq 0.05$).

Size Exclusion Chromatography

In order to confirm the data obtained by AF4 using an orthogonal technique, part of the samples was analysed by size exclusion chromatography (SEC) as well. A TSK G3000 SW_{XL} column, 7.8 x 300 mm (Tosoh Bioscience GmbH, Stuttgart, Germany) was combined with the same UV and MALS detectors used for the AF4 analyses. Separation was performed at 25°C at a flow rate of 0.5 ml/min, using a 200 mM potassium phosphate buffer with 250 mM KCl pH 7.0 as a mobile phase; 2 µl undiluted sample were injected per run. Data collection and analysis were performed as described for AF4.

RESULTS

Molecular modelling

3D monomer- and aggregation model

The geometric quality of the final "symmetric" monomer model based on 1IGY (Figure 1) consisting of the bevacizumab Fabs and the humanized hinge-Fc is comparable to that of the input template structures, with 74.9% of the residues in the model found in most favoured regions, 21.4% in additionally allowed regions, 2.2% in generously allowed regions and 1.5% in disallowed areas of the Ramachandran plot. The aggregation model obtained by replicating the monomer model according to the crystal symmetry ($P2_1$) of the murine IgG1 (PDB id: 1IGY) (Figure 1A) shows a single specific close contact area (least distance in the order of 4 Å) between the two monomers (Figure 1B). The bottom of one Fc comes to lie in between the two Fab regions of the other bevacizumab monomer. More specifically, this specific contact is characterized by the interaction of Ser202 (1BJ1 naming and numbering), belonging to one Fab arm of one bevacizumab, and Lys445 (1HZH and 1IGY naming and numbering), which is part of the Fc region of the second bevacizumab.

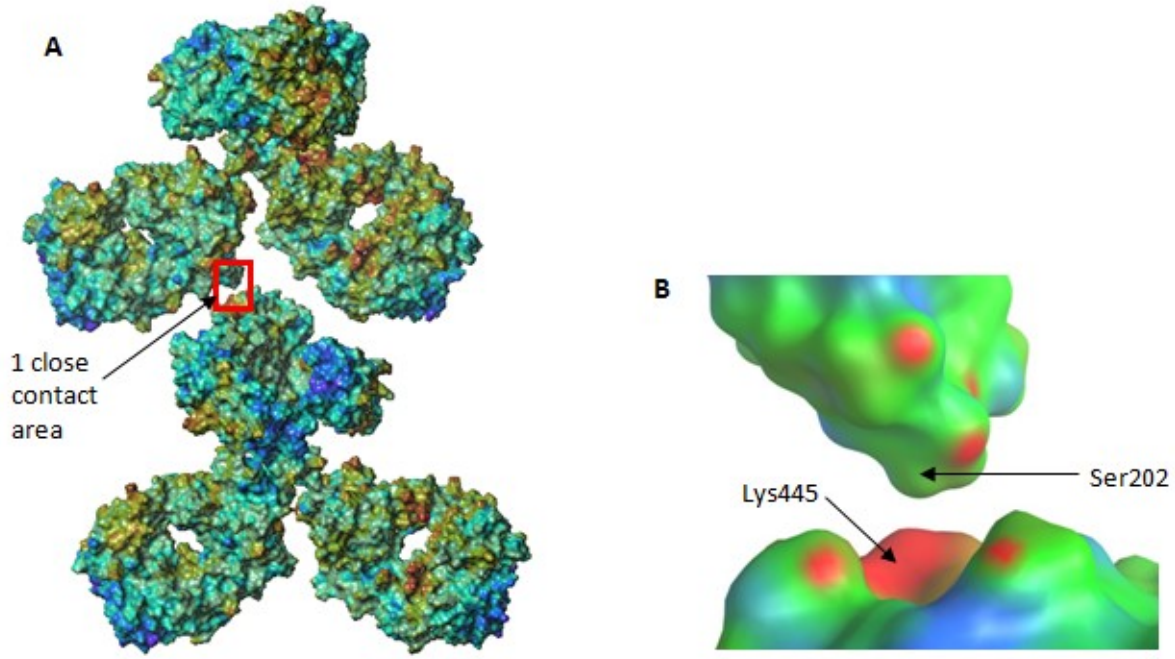

Figure 1. *The 3D aggregation model (A) of bevacizumab and a zoom on the contact region (B). The aggregation model was obtained by replicating the monomer model according to the crystal symmetry ($P2_1$) of the template IgG1. The least distance in the contact region between Lys445 (mouse and human IgG1 naming and numbering, PDB ids: 1IGY and 1HZH) and Ser202 (bevacizumab Fab naming and numbering, PDB id: 1BJ1) is in the order of 4 Å. The colouring gradient of the electrostatic potential surface goes from blue for negatively charged to red for positively charged atoms. Figures (A) and (B) were prepared using Sybyl 8.0 (Tripos Inc.) and MOE 2011 (Chemical Computing Group) respectively.*

Lys445 and Ser202 form the major interaction between the monomers and are fully conserved in engineered IgG1-based sequences (Supplementary Material, Figures S2-S6). The amino acids lining the contact area include for the Fab region His198 to Pro204 (1BJ1 naming and numbering) and for the Fc region Met381 to Val386 and Val443 to Glu449 (1IGY naming and numbering). Comparing the murine (PDB id: 1IGY) with the human Fc (PDB id: 1HZH), the residues surrounding and including Lys445 are well conserved from a sequence (Supplementary Material, Figure S2A) and structural (Supplementary Material, Figure S5) point of view. The non conserved amino acids are not involved in inter-antibody interactions and are thus thought to only marginally affect the prediction outcomes for potential aggregation breakers. The aggregation model based on the human framework shows, similar to the murine model, a close contact area between the region around Lys445 and the Fab

fragment, although due to the asymmetric Fab arrangement, another region on the Fab is involved. As expected for a Fab region, this region is not fully conserved among pharmaceutically relevant antibodies (Supplementary Material, Figure S7), but the hydrophilicity of the corresponding residues is conserved.

Docking of anti-inflammatory drugs

Concerning the docking of the steroids all over the monomer antibody model, highest docking scores (reflecting the antibody-small molecule interaction energy) are obtained for phosphate-containing steroids binding to Lys445 at the aggregation interface. Interactions with other lysines are less favourable, and the docking poses around different arginines receive even lower scores. For all shown docked compounds, a strong electrostatic interaction between the phosphate of the ligand and the Lys445 side chain is noted (Figure 2D for dexamethasone phosphate, Figure 2E for betamethasone phosphate and Figure 2F for triamcinolone acetonide phosphate). To provide an order of the strength of this interaction, an exposed salt bridge is known to be as strong as a neutral H-bond (5 ± 1 kJ/mol).[25,26] Additional H-bonds between residues adjacent to Lys445 and the phosphate further stabilize the steroid in the binding pocket. Among the steroids docked to this region, the propensity of the 10 generated poses to interfere with the adjacent antibody was highest for dexamethasone phosphate and betamethasone phosphate, with the higher scored docking poses all interfering. For triamcinolone acetonide phosphate, this propensity was only at 3 out of 10 poses. Because in our case, the docking scores were not informative with respect to their Ab-Ab breaking ability, we first displayed the docking poses of each small molecule on the aggregation model and then visually defined a « volume of interference » (Supplementary Material, Figure S1). The simplest geometric shape including all the dexamethasone phosphate or betamethasone phosphate aggregation breaking poses was defined using a cylinder. The centre of its base was put to the Cα atom of Lys445, with the plane of the base including the N atom of Lys445, and the radius was set to 7 Å. A height of 12 to 15 Å was drawn orthogonally from the base using Fc atoms situated approximately on the surface of the circle in vicinity of the adjacent Fab of the other antibody monomer. All docked steroids overlap in vicinity to the Fc, with their phosphates binding to the Lys445 side chain. While dexamethasone

phosphate and betamethasone phosphate are interfering with the Fab of the adjacent antibody, triamcinolone acetonide phosphate is generally not.

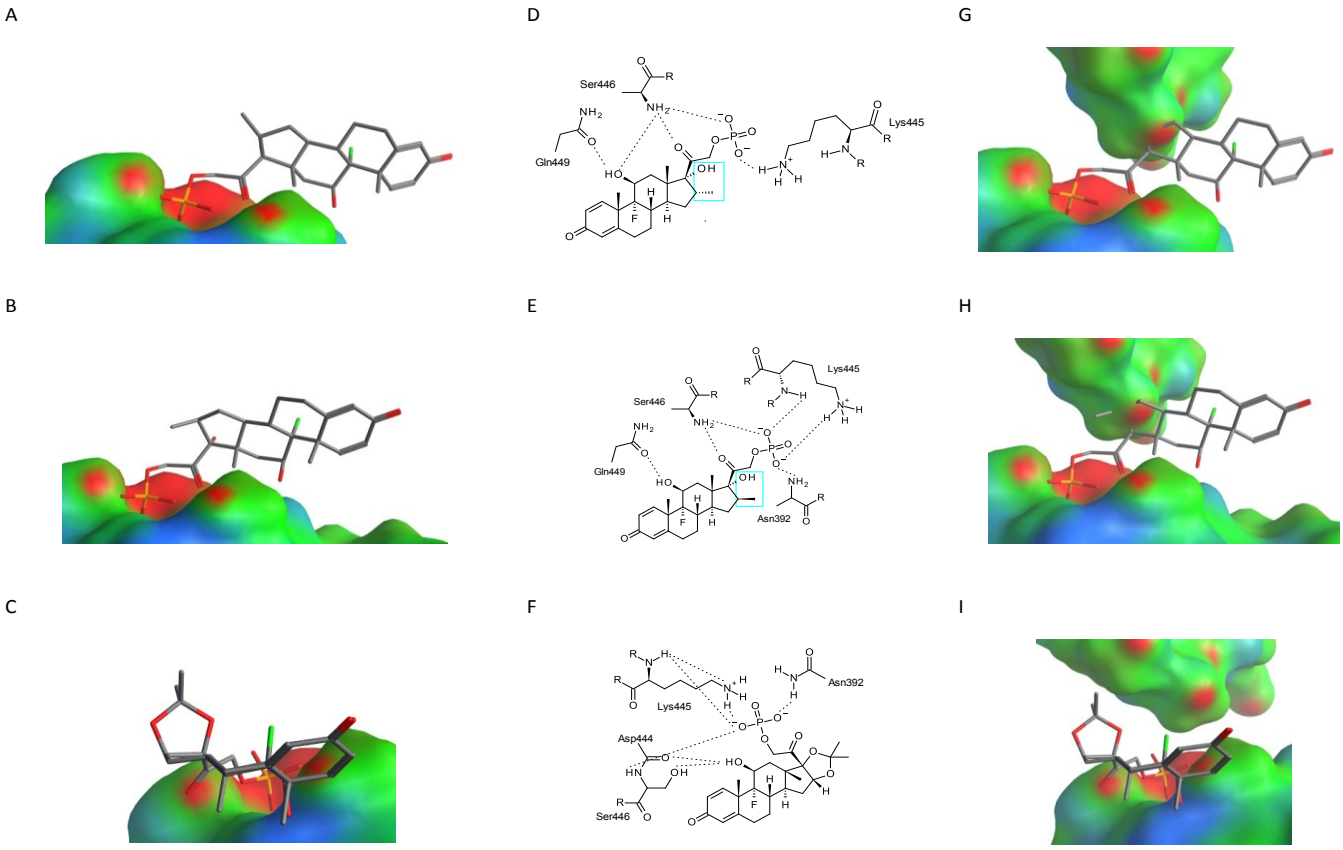

Figure 2. *Representative docking poses of dexamethasone phosphate (A, D and G), betamethasone phosphate (B, E and H) and triamcinolone acetonide phosphate (C, F and I), respectively. Docking poses on the bevacizumab monomer are displayed in A, B and C using MOE 2011 (Chemical Computing Group). Interactions between the docked steroid and the bevacizumab monomer are drawn in a schematic way in D, E and F using Symyx Draw 3.3. The dotted lines represent H-bonds or electrostatic interactions and the cyan box the parts of the steroid that clash with the second monomer of the aggregation model. The same poses are also represented in the aggregation model (G, H and I). MOE (Chemical Computing Group) was used for producing the monomer and dimer views, where the carbon atoms of the steroids are drawn in grey. The colour gradient for the electrostatic potential surface is the same as for Figure 1.*

A score of 5 was obtained for dexamethasone phosphate and betamethasone phosphate, while a score of 2 was obtained for triamcinolone acetonide phosphate. The same scores were also achieved when generating 100 docking poses. Figures 2A, 2B and 2C are representative figures showing how dexamethasone phosphate, betamethasone phosphate and triamcinolone acetonide phosphate are positioned on the monomer. The moieties of dexamethasone phosphate and betamethasone phosphate that are clashing with the second monomer in the aggregation model are clearly visible in Figures 2G and 2H, respectively. In contrast, triamcinolone acetonide phosphate does not clash into the second monomer (Figure 2I), which is probably due to the acetonide part that confers rigidity and a different spatial orientation to the compound.

In vitro **experiments**

Series I: Effect of dexamethasone phosphate on aggregation formation induced by temperature stress

Over time, storage at 40°C leads to differences in the decrease in monomer percentage for Avastin® alone or in presence of dexamethasone phosphate (Supplementary Material, Figure S8). The association of Avastin® with dexamethasone phosphate after 35 days of storage at 40°C is depicted in Figure 3 (and Supplementary Material, Table SI). The commercial product alone comprises 88.3 ± 0.2% of monomers, e.g. 11.7 ± 0.2% of the antibody has formed aggregates, consisting of dimers (10.16 ± 0.04%) and trimers (1.5 ± 0.2%). The stabilizing effect of dexamethasone phosphate is observed for all three molar ratios, being most pronounced for the 1:15 combination, which contains only 4.3 ± 0.5% dimers and 0.2 ± 0.2% trimers. All three combined formulations show a significant difference in aggregation percentages compared to Avastin® alone (Mann-Whitney U, one-tailed $p \leq 0.05$). Very low percentages of higher order aggregates (0.1 ± 0.2% decamers) were only observed for the 1:150 molar ratio.

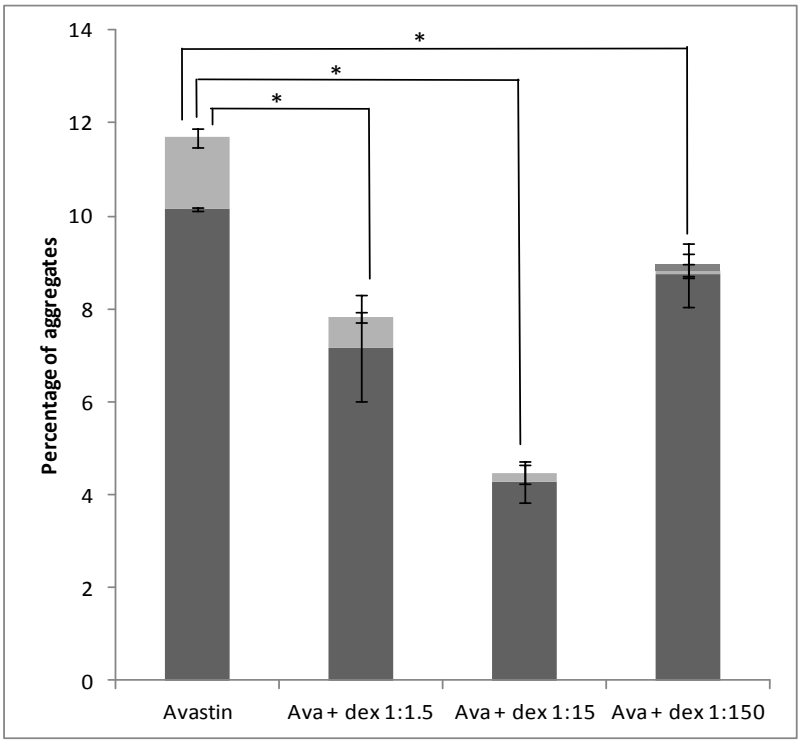

Figure 3. *Avastin® commercial formulation alone (Ava) and in combination with dexamethasone phosphate (dex) in a 1:1.5, 1:15, 1:150 molar ratio after 35 days of storage at 40°C. Quantification of aggregates was performed by AF4 coupled to MALS. Percentages of aggregates are expressed as average ± SD (n=3), dark grey = dimers, light grey = trimers, intermediate grey = higher order aggregates. * Significantly different from the percentage of aggregates of Avastin® alone (Mann-Whitney U test, p≤0.05, exact one-tailed significance).*

Series II: Effect of dexamethasone phosphate on aggregation formation induced by mechanical stress

Figure 4 shows the stabilizing effect of dexamethasone phosphate on bevacizumab during stress through agitation. Mechanical stress of the sample of bevacizumab alone leads to increased aggregation: The total percentage of aggregates doubles from 9.2 ± 0.6% after one hour of agitation to 18 ± 1% after 48 hours. In contrast, after one hour of agitation, the combined formulation (with a 1:15 molar ratio) shows an aggregation breaking effect, attributed to the presence of dexamethasone phosphate: Instead of 9.2 ± 0.6%, a total aggregate percentage of 4.2 ± 0.2% is measured. This percentage even slightly decreases to 3.8 ± 0.2% after 48 hours of agitation, indicating a stabilizing effect as well. The aggregation species that are observed are dimers and trimers for both samples. Differences in the amount of aggregates between the samples are significant (Mann-Whitney U, one-tailed p≤0.05) at all time points.

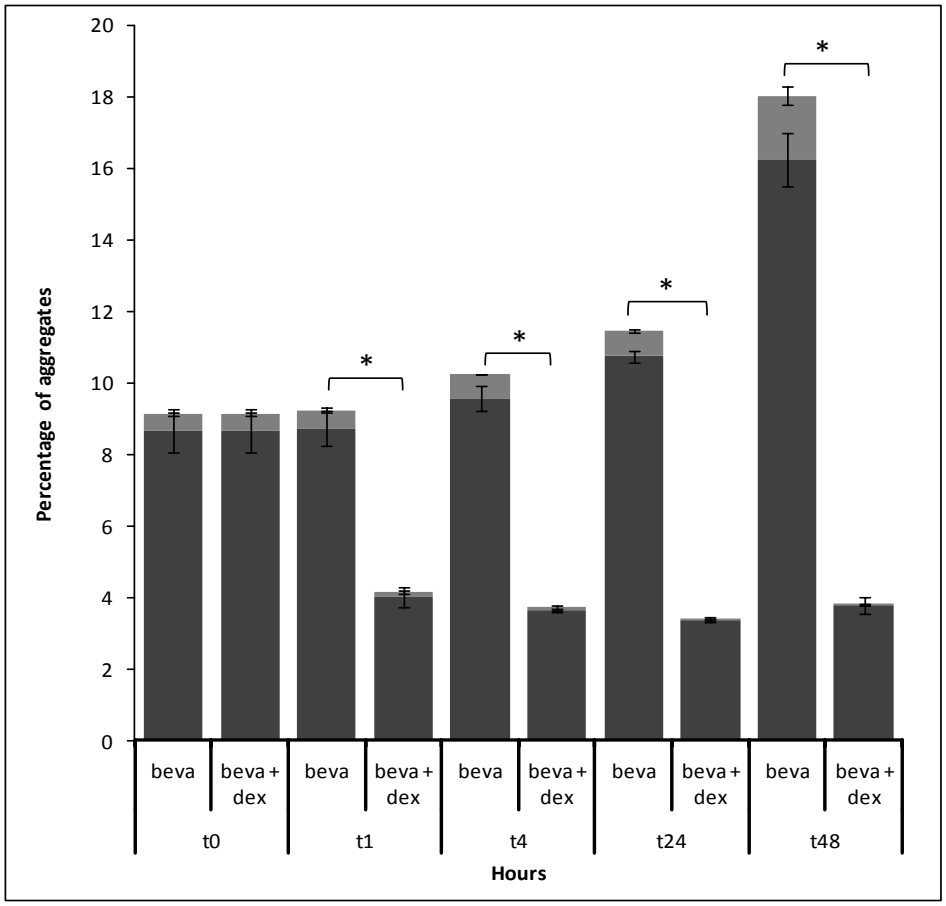

Figure 4. *Bevacizumab alone (beva) and in combination with dexamethasone phosphate in a 1:15 molar ratio (dex). Samples were stressed by agitation during 48 hours. Quantification of aggregates was performed by AF4 coupled to MALS. Percentages of aggregates are expressed as average ± SD (n=3), dark grey = dimers, light grey = trimers. *Significantly different from the percentage of aggregates of bevacizumab alone (Mann-Whitney U test, p≤0.05, exact one-tailed significance).*

Series III: Effect of three anti-inflammatory drugs on prestressed antibody

The addition of betamethasone phosphate in a 1:15 molar ratio to the prestressed antibody shows aggregation breaking properties of the corticosteroid (Figure 5). The results are comparable to the formulation in which dexamethasone phosphate is combined with the prestressed antibody (Table I, Figure 5). After 28 days, 63.3 ± 0.5% of monomers are present in the bevacizumab sample, compared to 80.73 ± 0.06% for the combination with dexamethasone phosphate (Table I) and 79.9 ± 0.3% for betamethasone phosphate (results not shown). Differences in aggregation between the antibody alone and the combined formulations are significant (Mann-Whitney U, one-tailed p≤0.05). Moreover, the aggregated fractions of both combined formulations only consist of dimers (19.27 ± 0.06% and 20.1 ±

0.3%, respectively), while the antibody alone forms both dimers (26.5± 0.1%) and trimers (10.3 ± 0.4%) (As depicted for bevacizumab alone or in combination with dexamethasone phosphate in Supplementary Material, Figure S9).

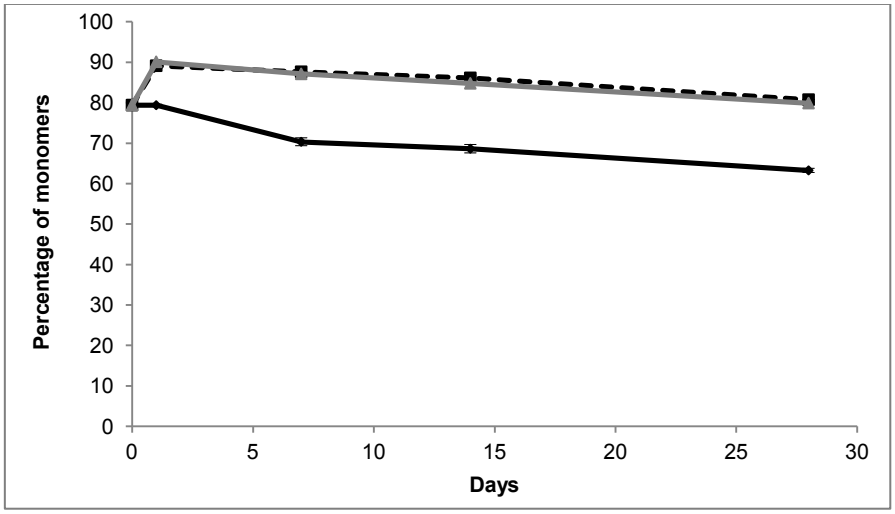

Figure 5. *Percentage of monomers for bevacizumab alone (black curve) and in combination with dexamethasone phosphate (black dashed curve) and betamethasone phosphate (grey curve) in a 1:15 molar ratio after 28 days at 40°C. Quantification of aggregates was performed by AF4 coupled to MALS. Bevacizumab was stressed for 7 days at 40°C before the addition of the steroid drugs. Percentages are expressed as average ± SD, shown as vertical bars (n=3).*

In order to check the data obtained by AF4 with an orthogonal technique, the combination of the prestressed antibody with dexamethasone phosphate was investigated by SEC. The percentages of monomers found by SEC are in agreement with those detected by AF4, especially considering the fact that both analyses were carried out on different vials (Table IB). Thus, these data confirm the aggregation breaking properties of dexamethasone phosphate on the IgG1 based antibody. It should be noted that SEC detects more separate fractions than AF4: Fragments and higher order aggregates are present in the samples analysed by SEC, but absent when the analyses are performed by AF4. It is unclear whether these fractions are created during the analysis, or whether SEC enables better separation.

Table I: *Prestressed bevacizumab (7 days at 40°C) alone and in combination with dexamethasone phosphate in a 1:15 molar ratio after 28 days at 40°C.*

IA. AF4	bevacizumab	bevacizumab + dexamethasone phosphate 1:15
Fragments (%)	Not detected	Not detected
Monomers (%)	63.3 ± 0.5	80.83 ± 0.06*
Dimers (%)	26.5 ± 0.1	19.27 ± 0.06
Trimers (%)	10.3 ± 0.4	Not detected
Higher order aggregates (%)	Not detected	Not detected

IB. SEC	bevacizumab	bevacizumab + dexamethasone phosphate 1:15
Fragment (%)	1.7 ± 0.1	2.3 ± 0.1
Monomers (%)	60.7 ± 1.1	82.9 ± 0.3*
Dimers (%)	26.5 ± 0.5	12.3 ± 0.3
Trimers (%)	8.5 ± 0.4	1.93 ± 0.04
Higher order aggregates (%)	2.6 ± 0.2	0.62 ± 0.02

*Quantification of monomers/aggregates was performed by AF4 coupled to MALS (IA) and by SEC coupled to MALS (IB). Percentages are expressed as average ± SD (n=3). *Significantly different from the percentage of monomers of bevacizumab alone (Mann-Whitney U test, p≤0.05, exact one-tailed significance).*

In contrast to the aggregation breaking effect seen with dexamethasone phosphate and betamethasone phosphate, the addition of triamcinolone acetonide phosphate only has an effect at t_1, thereafter the combination does not significantly affect the aggregation profile of the antibody (Supplementary Material, Figures S10 and S11). The samples with and without steroid drug show similar percentages of aggregates after 28 days of storage: In the bevacizumab sample, 20.8 ± 0.6% of dimers, 3.5 ± 0.2% of trimers and 0.9 ± 0.2% of higher order aggregates are present, compared to 20.2 ± 0.2% of dimers, 3.5 ± 0.2% of trimers and 0.95 ± 0.09% of higher order aggregates for the combined formulation.

Series IV: Effect of dexamethasone phosphate on prestressed Fab fragment

The percentages of formed aggregates after 28 days are represented in Table II, both for the prestressed ranibizumab alone and for the combination with dexamethasone phosphate in a 1:15 molar ratio. The addition of dexamethasone phosphate has no stabilizing effect on the Fab fragment; the

monomer percentages that are present in both samples are comparable (51.8 ± 0.5% for ranibizumab alone vs. 50.0 ± 0.4% for the combined formulation). All measured aggregation species (dimers, trimers and higher order aggregates) are also comparable between both samples.

Table II: *Prestressed ranibizumab (365 days at 25°C) alone and in combination with dexamethasone phosphate in a 1:15 molar ratio.*

AF4	ranibizumab	ranibizumab + dexamethasone phosphate 1:15
Monomers (%)	51.8 ± 0.5	50.0 ± 0.4
Dimers (%)	15.4 ± 0.4	14.9 ± 0.9
Trimers (%)	8 ± 1	7 ± 1
Higher order aggregates (%)	25 ± 1	27.6 ± 0.4

Quantification of monomers/aggregates was performed by AF4 coupled to MALS. Percentages are expressed as average ± SD (n=3). No significant difference was observed between the samples with and without dexamethasone phosphate (Mann-Whitney U test, p≤0.05, exact one-tailed significance).

DISCUSSION

In this study, the aggregation breaking properties of dexamethasone phosphate on the monoclonal antibody bevacizumab are investigated. Construction of a 3D aggregation model and small molecule docking allow comprehending the process through which aggregation might occur and how an aggregation breaker might interfere with this mechanism. Furthermore, the requirements that have to be met by a small molecule to be a breaker can be predicted (structure-activity relationship). The combination with *in vitro* stability studies provides a validation of the observations made *in silico.*

It should be noted that the 3D model focuses on the onset of aggregation; only the formation of dimers was investigated. Moreover, the native structure of the antibody was used, while it is generally assumed that especially partly unfolded antibodies are prone to aggregation.[27,28] Computational prediction of unfolding would however require time- and resource-intensive molecular dynamics, which would go beyond the scope of this work. Besides, reversible self-association of native state

proteins is possible through hydrophobic or electrostatic interactions; with or without subtle conformational changes.[6,29] The term "aggregation" that is used throughout the paper therefore refers to "self association of native state monomers" in this particular context.

Based on the symmetry and space group found in the crystal structures of 1IGY and 1HZH, respectively, a « symmetric » (replicated according to the crystal symmetry of 1IGY) and an « asymmetric » (replicated according to the crystal symmetry of 1HZH) bevacizumab model were built. Both aggregation models reveal a contact zone situated on the Fc tip region around Lys445 of the first bevacizumab and a variable interacting region on one Fab of the second bevacizumab. The contact zone on the Fab depends on the overall antibody configuration (symmetric vs. asymmetric). To understand the stabilizing effect of dexamethasone phosphate, the ligand was docked all over the monomer antibody model. The highest docking scores were obtained for the binding of the phosphate group to Lys445 at the aggregation interface. Additional H-bonds between residues adjacent to Lys445 and the phosphate further stabilize the steroid in the binding pocket. Thus, dexamethasone phosphate masks the interaction interface between two monomers and consequently hinders dimer formation through the strong electrostatic interaction between the phosphate and the side chain of Lys445. *In vitro* investigations support these observations: Dexamethasone phosphate is able to partly prevent or reverse aggregation of the antibody during the stability studies.

It is shown that the 1:15 molar ratio bevacizumab:dexamethasone phosphate is optimal to stabilize the protein in the commercial formulation at pH 6.2. Apparently, in a formulation with a 1:1.5 ratio, the number of dexamethasone molecules is too low to interact with all antibodies present, whereas the 1:150 ratio leads to the formation of higher order aggregates. For betamethasone phosphate, the 1:15 combination was also observed to be the optimal molar ratio (results on other molar ratios are not shown). A similar importance for molar ratios was reported by Cleland et al., who studied the stabilizing effects of sugar on a lyophilized monoclonal antibody: The molar ratio between stabilizing agent and antibody was found to be a critical parameter in the stabilizing process.[30] It should be noted that the 1:15 molar ratio was observed to be optimal only for this particular formulation. Since the

dialysed formulation at pH 7 is different from the commercial one, it might not be the optimal ratio at pH 7. This should be investigated in further work.

Because an aggregation breaking effect of dexamethasone phosphate is observed during both thermal stress and agitation, the assumption can be made that the form of stress applied has no influence on the ability of the steroid drug to hinder dimer formation. This observation may suggest that the formation of bevacizumab aggregates is similar for both thermal and mechanical stresses, at least in the initial process of aggregation. *In vitro* measurements show that the first aggregates observed are dimers (and low percentages of trimers in the case of agitation) for both stressing processes; higher order aggregates are only measured in later stages of the stress studies. Thus, in addition to the 3D dimer model, these data imply that aggregation takes place through a primary formation of dimers, which might act as active nuclei for further aggregation. This said, it should be noted that there is an important difference between aggregation formation due to thermal stress and agitation. In the case of thermal stress, the corticosteroid is able to cause reversion of formed aggregates back to monomers (Figure 5). However, the slope of the curve is comparable to that of bevacizumab alone, i.e. the aggregation kinetics are similar and the addition of the breaker does not slow down the rate at which aggregates are formed. In contrast, during agitation a clear stabilization of the aggregation kinetics is observed: Figure 4 shows that over time, the percentage of aggregates increases for the sample containing bevacizumab only, whereas it stays almost the same if dexamethasone phosphate is present.

To validate the aggregation model and to verify whether the Fc region is indeed indispensable for aggregation, as shown in the aggregation model, a negative control is performed *in vitro*. Ranibizumab is a Fab fragment that has the same sequence as a single Fab fragment of bevacizumab. If the prediction of the aggregation model is correct, than the assumption could be made that ranibizumab is less prone to aggregation than the complete antibody bevacizumab, since it lacks the Fc region that is involved in the aggregation process. This is confirmed by comparing the aggregation profiles of bevacizumab and ranibizumab induced by temperature stress: Ranibizumab is already more stable than bevacizumab at t_0 and stays more stable over the whole study period, as was observed in

earlier work.[12] Furthermore, the absence of the Fc region implies that dexamethasone phosphate is unable to stabilize ranibizumab: If dexamethasone phosphate interacts with Lys 445 as proposed in the 3D model, than it would be impossible to stabilize the aggregated Fab fragment, which lacks this particular and surrounding amino acids. Indeed, no significant difference is observed between the aggregate percentages of ranibizumab alone and in combination with dexamethasone phosphate, thereby confirming the assumption.

A second validation of the aggregation model and the assessment of the capacity of the procedure to distinguish between aggregation breakers and non breakers in a predictive way were performed by docking several steroids onto the Fc contact region of the monomer. Subsequently, the second monomer of the aggregation model was displayed and the molecules were selected or rejected based on their propensity of interfering with dimer formation while binding to the first monomer. It seems that phosphate is fundamental for the interaction, since this negatively charged functional group can form an electrostatic interaction with the (at physiological pH) positively charged terminal amide of Lys445. Of the tested steroids, betamethasone phosphate is predicted to be a bevacizumab-bevacizumab interaction breaker, since its phosphate group is in a similar configuration as in dexamethasone phosphate. Indeed, betamethasone phosphate shows a similar binding mode as dexamethasone phosphate. The *in vitro* examination of betamethasone phosphate shows that this molecule has a similar aggregation breaking effect on bevacizumab as was observed for dexamethasone phosphate, supporting the predictability of the model.

Triamcinolone acetonide phosphate serves as a further control for corroborating the model and the predictiveness of the compound selection procedure. In comparison with both dexamethasone phosphate and betamethasone phosphate, it is observed *in vitro* that triamcinolone acetonide phosphate lacks the protective properties on this particular antibody. By just looking at the presence of a phosphate group, one might expect that triamcinolone acetonide phosphate also has an aggregation breaking effect on bevacizumab. However, when comparing the docking results on the Fc contact region of triamcinolone acetonide phosphate with the aggregation-breaking steroids, it is shown that

(i) the presence of the acetonide moiety restricts the conformational flexibility so that Lys445 is still able to interact with the phosphate, but that (ii) the steroid part is oriented parallel to the Fc surface and therefore (iii) not interfering with the adjacent antibody, since only the acetonide group is pointing towards the other monomer, not being voluminous enough to hinder dimer formation.

CONCLUSION

In this paper, the mechanism behind the aggregation breaking properties of dexamethasone phosphate on the monoclonal IgG1-based antibody bevacizumab has been investigated. In the proposed *in silico* model, interfering with dimer formation is based on the ability of dexamethasone phosphate (or betamethasone phosphate) to hinder the interaction between the Fc part of the first, and the Fab arm of the second bevacizumab monomer. *In vitro*, bevacizumab dimers revert partly into monomers after addition of dexamethasone phosphate, independently of the form of stress applied. This observation supports the idea that the mechanism behind the initial dimer formation of bevacizumab is similar for these two forms of stress testing. As we have shown, it is possible to predict whether a molecule has aggregation breaking properties: In order to hinder the dimer formation, a flexibly bending phosphate group is required to accurately position the rest of the steroid. Such flexibility is guaranteed in dexamethasone phosphate and betamethasone phosphate, but impossible in triamcinolone acetonide phosphate due to the rigidity conferred by its acetonide moiety.

This approach allows a simple way to stabilize therapeutic antibodies without the need to modify the Ig structure through mutation of specific amino acids, which might lead to a loss in efficacy. The therapeutic activity of the corticosteroids might be an advantage in the development of a combination product. However, further research will focus on the discovery of safe and therapeutically inactive molecules with similar aggregation breaking properties. Besides, supplementary studies on unformulated bevacizumab need to be carried out to investigate the contribution of polysorbate to the aggregation breaking effect of the anti-inflammatory drugs. The effects shown for the specific antibody bevacizumab might be applicable to other IgG1 antibodies as well, which might be advantageous for the future development of stable IgG1-derived antibodies.

ACKNOWLEDGMENTS

The authors wish to thank Ms. Sylvie Guinchard for her help on the *in vitro* studies and the Swiss National Science Foundation for financial support (#320030-122190/1).

REFERENCES

1. Aggarwal S. What's fueling the biotech engine? *Nat Biotechnol* 2007; 25: 1097-1104.

2. Wang W, Singh S, Zeng DL, King K, Nema S. Antibody structure, instability and formulation. *J Pharm Sci* 2007; 96: 1-26.

3. Manning MC, Chou DK, Murphy BM, Payne RW, Katayama DS. Stability of protein pharmaceuticals: an update. *Pharm Res* 2010; 27: 544-575.

4. Demeule B, Gurny R, Arvinte T. Where disease pathogenesis meets protein formulation: renal deposition of immunoglobulin aggregates. *Eur J Pharm Biopharm* 2006; 62: 121-130.

5. Harris RJ, Shire SJ, Winter C. Commercial manufacturing scale formulation and analytical characterization of therapeutic recombinant antibodies. *Drug Dev Res* 2004; 61: 137-154.

6. Wang W, Nema S, Teagarden D. Protein aggregation-pathways and influencing factors. *Int J Pharm* 2010; 390: 89-99.

7. Chennamsetty N, Voynov V, Kayser V, Helk B, Trout BL. Design of therapeutic proteins with enhanced stability. *Proc Natl Acad Sci USA* 2009; 106: 11937-11942.

8. Kerwin BA. Polysorbates 20 and 80 used in the formulation of protein biotherapeutics: structure and degradation pathways. *J Pharm Sci* 2008; 97: 2924-2935.

9. Bolli R, Woodtli K, Bärtschi M, Höfferer L, Lerch P. L-Proline reduces IgG dimer content and enhances the stability of intravenous immunoglobulin (IVIG) solutions. *Biologicals* 2010; 38: 150-157.

10. Szenczi A, Kardos J, Medgyesi GA, Zavodszky P. The effect of solvent environment on the conformation and stability of human polyclonal IgG in solution. *Biologicals* 2006; 34: 5-14.

11. Ciulla TA, Rosenfeld PJ. Antivascular endothelial growth factor therapy for neovascular age-related macular degeneration. *Curr Opin Ophthalmol* 2009; 20: 158-165.

12. Veurink M, Stella C, Tabatabay C, Pournaras CJ, Gurny R. Association of ranibizumab (Lucentis®) or bevacizumab (Avastin®) with dexamethasone and triamcinolone acetonide: an in vitro stability assessment. *Eur J Pharm Biopharm* 2011; 78: 271-277.

13. Augustin AJ, Puls S, Offermann I. Triple therapy for choroidal neovascularization due to age-related macular degeneration: verteporfin PDT, bevacizumab, and dexamethasone. *Retina* 2007; 27: 133-140.

14. Berman HM, Westbrook J, Feng Z, Gilliland G, Bhat TN, Weissig H, Shindyalov IN, Bourne PE. The Protein Data Bank. *Nucleic Acids Res* 2000; 28: 235-242.

15. Berman HM, Battistuz T, Bhat TN, Bluhm WF, Bourne PE, Burkhardt K, Feng Z, Gilliland GL, Iype L, Jain S, Fagan P, Marvin J, Padilla D, Ravichandran V, Schneider B, Thanki N, Weissig H, Westbrook JD, Zardecki C. The Protein Data Bank. *Acta Crystallogr D Biol Crystallogr* 2002; 58: 899-907.

16. Muller YA, Christinger HW, Keyt BA, de Vos AM. The crystal structure of vascular endothelial growth factor (VEGF) refined to 1.93 A resolution: multiple copy flexibility and receptor binding. *Structure* 1997; 5: 1325-1338.

17. Saphire EO, Parren PW, Pantophlet R, Zwick MB, Morris GM, Rudd PM, Dwek RA, Stanfield RL, Burton DR, Wilson IA. Crystal structure of a neutralizing human IGG against HIV-1: a template for vaccine design. *Science* 2001; 293: 1155-1159.

18. Thompson JD, Higgins DG, Gibson TJ. CLUSTAL W: improving the sensitivity of progressive multiple sequence alignment through sequence weighting, position-specific gap penalties and weight matrix choice. *Nucleic Acids Res* 1994; 22: 4673-4680.

19. Larkin MA, Blackshields G, Brown NP, Chenna R, McGettigan PA, McWilliam H, Valentin F, Wallace IM, Wilm A, Lopez R, Thompson JD, Gibson TJ, Higgins DG. Clustal W and Clustal X version 2.0. *Bioinformatics* 2007; 23: 2947-2948.

20. Laskowski RA, MacArthur MW, Moss DM, Thornton JM. PROCHECK : A program to check the stereochemical quality of protein structures. *J Appl Cryst* 1993; 26: 283-291.

21. Guex N, Peitsch MC. SWISS-MODEL and the Swiss-PdbViewer: an environment for comparative protein modeling. *Electrophoresis* 1997; 18: 2714-2723.

22. Mahler HC, Printz M, Kopf R, Schuller R, Muller R. Behaviour of polysorbate 20 during dialysis, concentration and filtration using membrane separation techniques. *J Pharm Sci* 2008; 97: 764-774.

23. Fraunhofer W, Winter G. The use of asymmetrical flow field-flow fractionation in pharmaceutics and biopharmaceutics. *Eur J Pharm Biopharm* 2004; 58: 369-383.

24. Mahler HC, Fries W, Grauschopf U, Kiese S. Protein aggregation: pathways, induction factors and analysis. *J Pharm Sci* 2009; 98: 2909-2934.

25. Schneider HJ, Schiestel T, Zimmermann P. The incremental approach to noncovalent interactions: Coulomb and van der Waals effect in organic ion pairs. *J Am Chem Soc* 1992; 114: 7698-7703.

26. Tissot AC, Vuilleumier S, Fersht AR. Importance of two buried salt bridges in the stability and folding pathway of barnase. *Biochemistry* 1996; 35: 6786-6794.

27. Roberts CJ. Non-native protein aggregation kinetics. *Biotechnol Bioeng* 2007; 98: 927-938.

28. Chi EY, Krishnan S, Randolph TW, Carpenter JF. Physical stability of proteins in aqueous solution: mechanism and driving forces in non-native protein aggregation. *Pharm Res* 2003; 20: 1325-1336.

29. Philo JS, Arakawa T. Mechanisms of protein aggregation. *Curr Pharm Biotechnol* 2009; 10: 348-351.

30. Cleland JL, Lam X, Kendrick B, Yang J, Yang T-H, Overcashier D, Brooks D, Hsu C, Carpenter JF. A specific molar ratio of stabilizer to protein is required for storage stability of a lyophilized monoclonal antibody. *J Pharm Sci* 2001; 90: 310-321.

SUPPLEMENTARY MATERIAL

AF4	Avastin®	Avastin® + dexamethasone phosphate 1:1.5	Avastin® + dexamethasone phosphate 1:15	Avastin® + dexamethasone phosphate 1:150
Monomers (%)	88.3 ± 0.2	92 ± 1	95.6 ± 0.3	91.0 ± 0.5
Dimers (%)	10.16 ± 0.04	7.2 ± 1.2	4.3 ± 0.5	8.7 ± 0.7
Trimers (%)	1.5 ± 0.2	0.7 ± 0.1	0.2 ± 0.2	0.1 ± 0.2
Higher order aggregates (%)	Not detected	Not detected	Not detected	0.1 ± 0.2

Table SI: *Avastin® commercial formulation alone and in combination with dexamethasone phosphate in a 1 :1.5, 1 :15, 1 :150 molar ratio after 35 days of storage at 40°C. Quantification of aggregates was performed by AF4 coupled to MALS. Percentages of aggregates are expressed as average ± SD (n=3).*

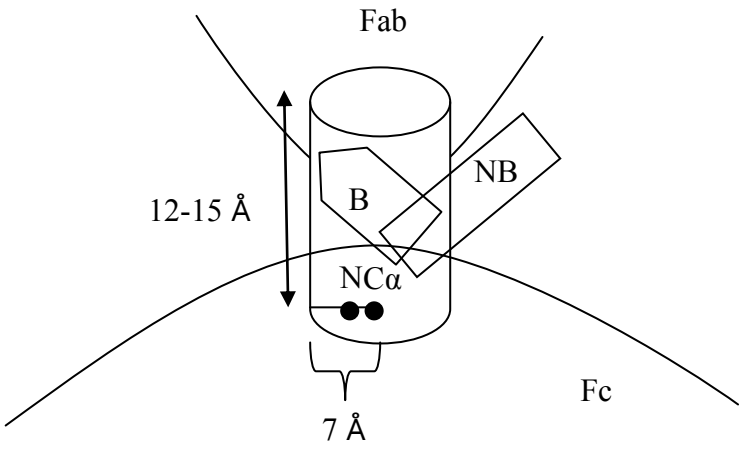

Figure S1. *Definition of a cylindric « volume of interference » between the Fc of one bevacizumab and an adjacent Fab of the next bevacizumab to be able to distinguish between potential aggregation breakers (B), and non-breakers (NB).*[1] *N-Cα corresponds to the Cα atom of Lys445, with the plane of the base including the N atom of Lys445. The following scoring scheme was applied:*

- *5: Majority of poses interfering, all poses completely inside the cylinder and root mean square deviation (RMSD) of heavy atoms ≤ 2 Å*
- *4: Majority of poses interfering, majority of poses completely inside the cylinder*
- *3: 5/10 poses interfering, 5/10 poses not completely inside the cylinder*
- *2: 3/10 to 4/10 interfering or 3/10 to 4/10 completely inside the cylinder*
- *1: 1/10 to 2/10 interfering or 1/10 to 2/10 completely inside the cylinder*
- *0: None of the poses either interfering or inside the cylinder*

A

B

Figure S2. *Sequence alignment of the Fc region of crystallised (deposited in PDB) (A) and pharmaceutically relevant monoclonal antibodies (sequences from DrugBank) (A, B). The alignment was performed with the ClustalW tool[2,3] of the BiologyWorkbench and coloured with TexShade.[4] Complete residue matches are highlighted on a black, similar residues on a light grey and non matching residues on a white background. The consensus sequence for a full match (upper case letters) and a conserved amino acid property (lower case letters) between the 2 compared sequences are indicated as well. The sequence alignment starts at the first residue which is common to all sequences. Lys445 (red arrow) is conserved in all sequences. A complete sequence conservation is observed for Lys445 and the residues preceding and following it in sequence in the pharmaceutically relevant antibodies (B). All of the antibodies in (B) contain the human Fc region. Rituximab is a genetically engineered chimeric murine/human monoclonal IgG1 kappa antibody directed against the CD20 antigen. Basiliximab and daclizumab are also IgG1 kappa antibodies, but are directed against the interleukin-2 receptor α (CD25). Cetuximab and trastuzumab are directed against the epidermal growth factor receptor. Alemtuzumab is directed against a cell surface glycoprotein known as CD52. Etanercept binds to the tumor necrosis factor receptor. The crystallised proteins include: 1HZH, an intact human IgG1 B12, 2DTQ (in the meantime superseeded by 3AVE), the Fc fragment from human IgG1, and 3D6G, the Fc fragment of IgG1 Herceptin® (trastuzumab).*

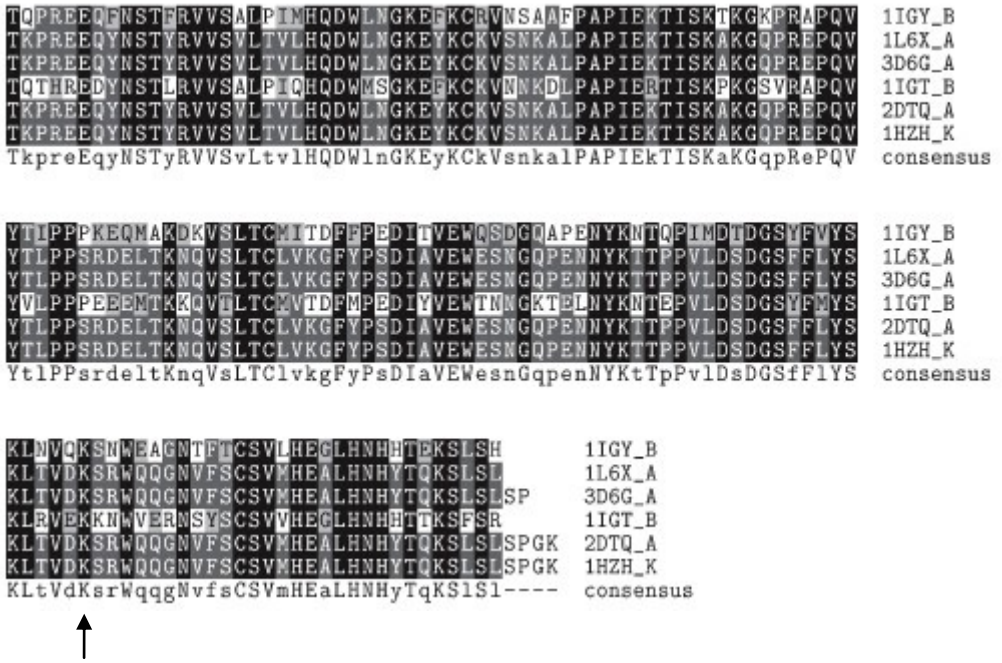

Figure S3. *Sequence alignment of the murine Fc of IgG1 (PDB id: 1IGY, chain B), the corresponding part of rituximab (an IgG1, PDB id: 1L6X, chain A), trastuzumab (an IgG1, PDB id: 3D6G, chain A), an IgG2a (PDB id: 1IGT, chain B), an IgG1 (PDB id: 2DTQ, chain A) and the human Fc of IgG1 (PDB id: 1HZH, chain K). The sequence colouring is the same as in Figure S2. As seen in Figure S2, the sequence of all IgG1 based antibodies is fully conserved.*

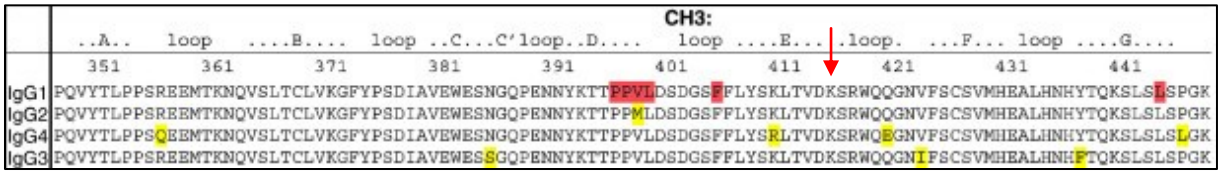

Figure S4. *Sequence comparison of different IgG subclasses: The aggregation prone motifs identified for IgG1 in Chennamsetty et al.*[5] *are marked in red and the sequence differences between different IgGs in yellow. These motifs are included in the aggregation prone region identified in our study (red arrow marking Lys445 which corresponds to Lys414 in the sequences above, due to the fact that we use the 1HZH numbering). In our study, this residue was identified to be the anchor point for small molecular weight antibody aggregation breakers.*

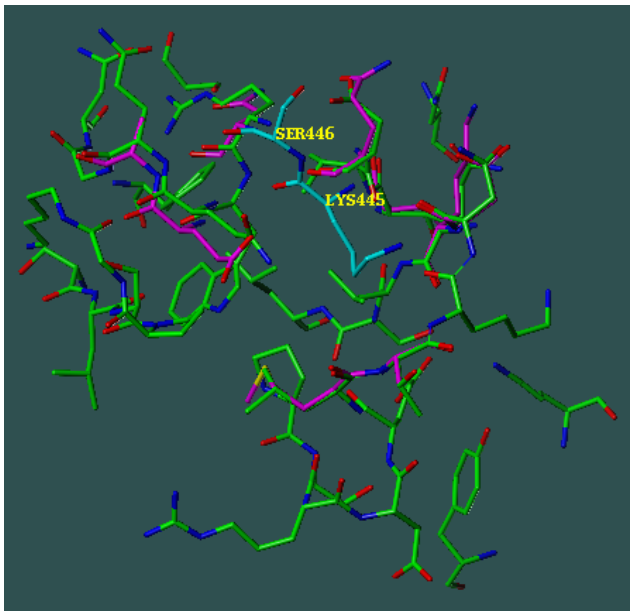

(A)

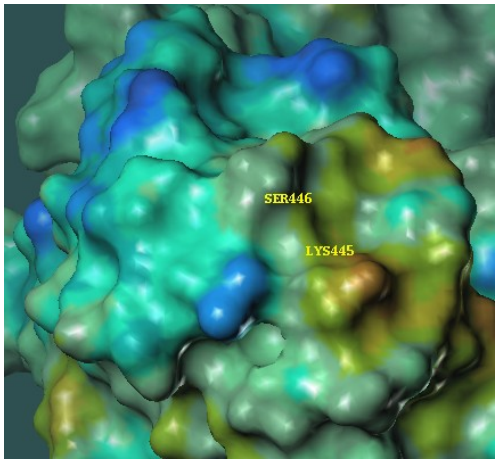

(B)

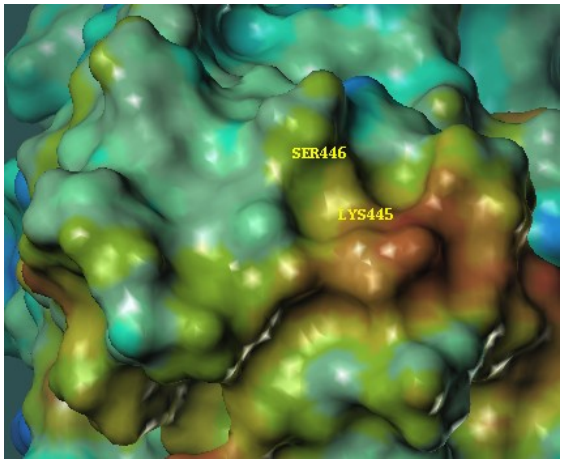

(C)

Figure S5. *Superposition of the Fc aggregation zone of the mouse IgG1 (PDB id: 1IGY) with the corresponding human IgG1 (PDB id: 1HZH). (A) Amino acid view of the superposition. Both Lys445 and the nearby Ser446 (shown with cyan carbon atoms) are conserved and mainly surrounded by conserved amino acids. The amino acids displayed with green carbons correspond to the humanized bevacizumab model. Only a few residues (shown with magenta carbons) are different in the murine crystal structure. The electrostatic surface of the Fc crystal contact region around Lys445 as found in the murine Fc is drawn in (B) and the human Fc in (C). (C) was used as the Fc of the bevacizumab model.*

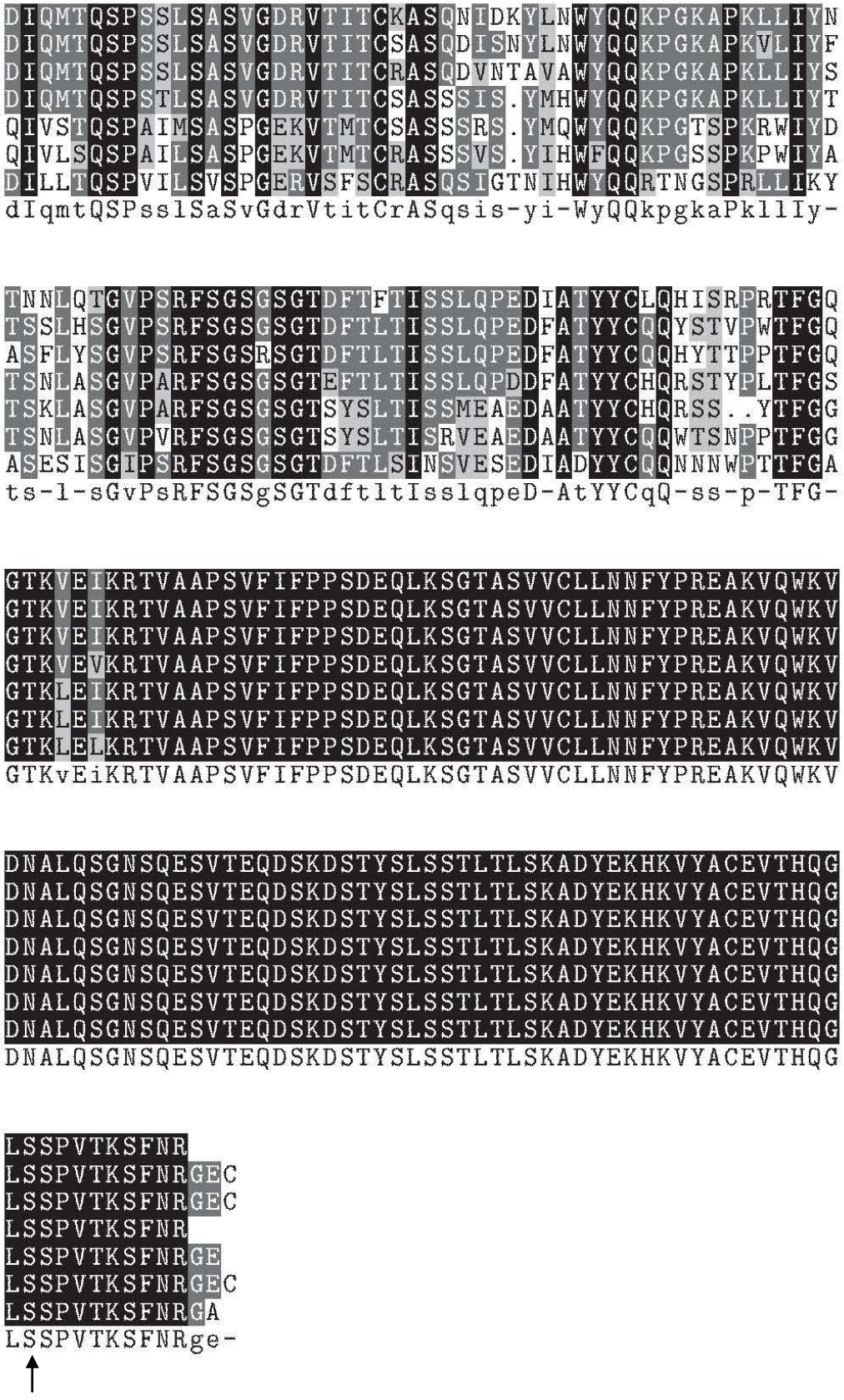

Figure S6. *Ser202 (marked in red) conservation: From top to bottom, the alignment of alemtuzumab, 1BJ1 (chain J), trastuzumab, daclizumab, basiliximab, rituximab, and cetuximab.*

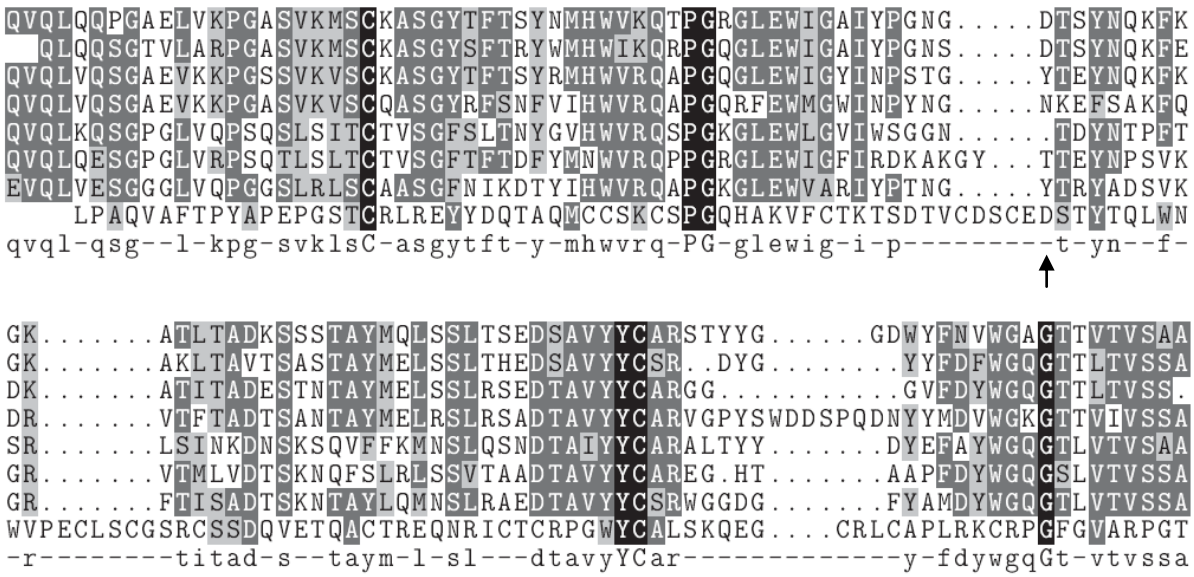

Figure S7. *Sequence alignment of the region around Asn56 (1HZH) and the corresponding regions of pharmaceutically relevant antibodies. The sequences from top to bottom correspond to: Rituximab, basiliximab, daclizumab, 1HZH, cetuximab, alemtuzumab, trastuzumab, etanercept, consensus sequence.*

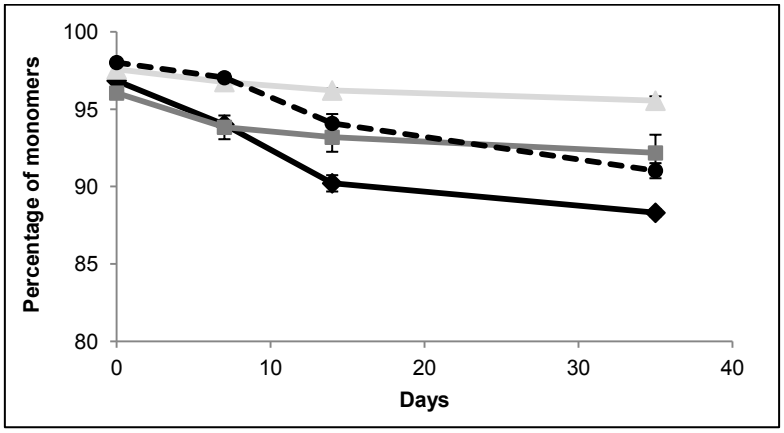

Figure S8. *Percentage of monomers for Avastin® commercial formulation alone (black line) and in combination with dexamethasone phosphate in a 1:1.5 (dark grey line), 1:15 (light grey line), 1:150 molar ratio (black dashed line), storage at 40°C. Quantification of monomers was performed by AF4 coupled to MALS. Percentages are expressed as average ± SD, shown as vertical error bars (n=3).*

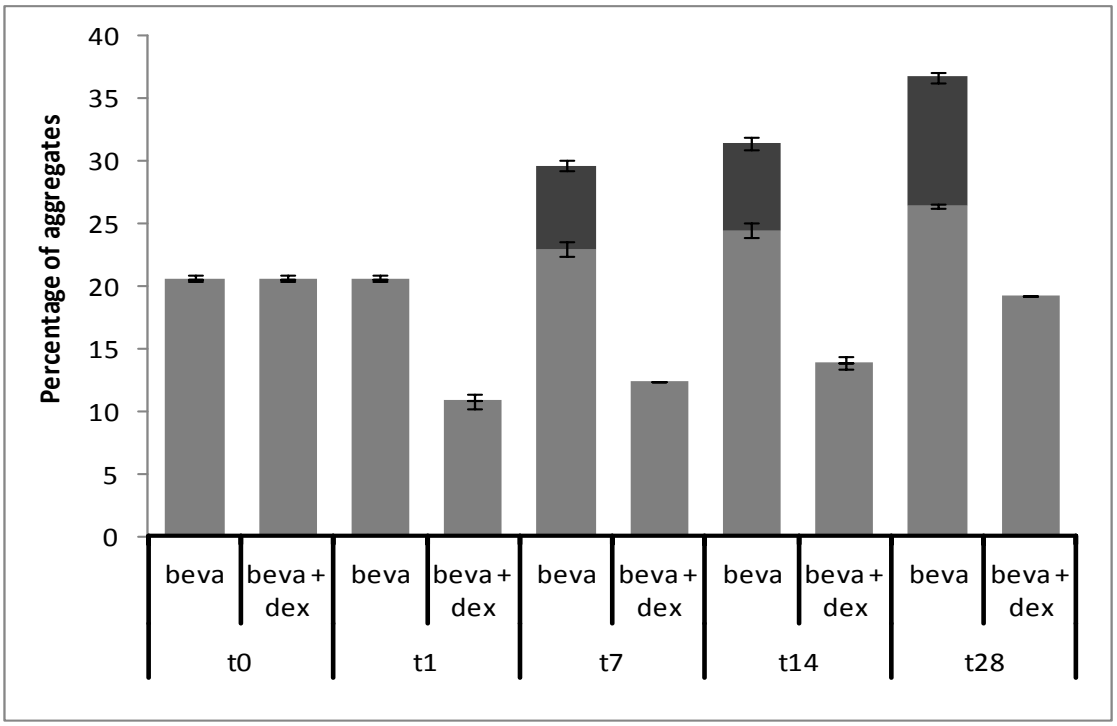

Figure S9. *Percentage of aggregates for bevacizumab (beva) alone and in combination with dexamethasone phosphate (dexa) in a 1:15 molar ratio, storage at 40°C for 28 days. Light grey bar= % of dimers, dark grey bar= % of trimers. Quantification of aggregates was performed by AF4 coupled to MALS. Bevacizumab was stressed for 7 days at 40°C before the addition of the steroid drug. Percentages are expressed as average ± SD, shown as vertical bars (n=3).*

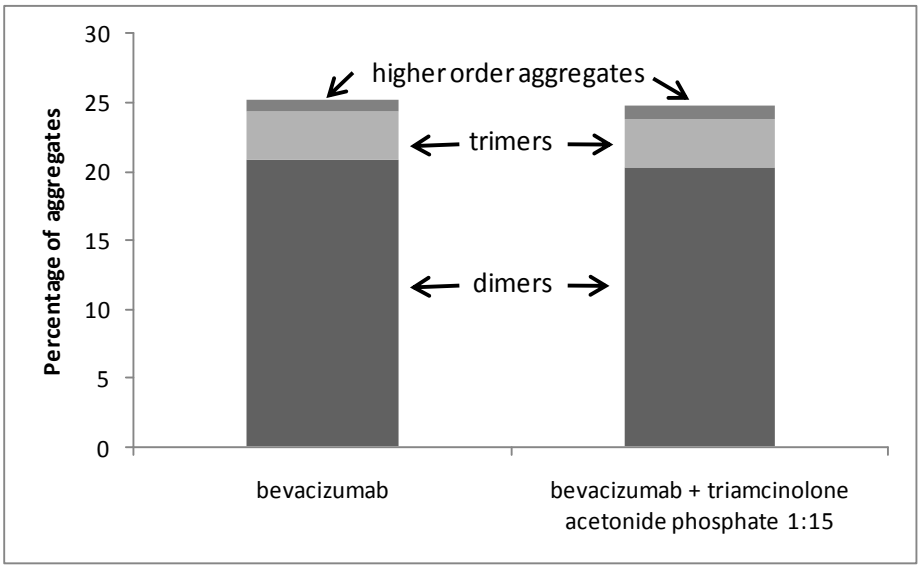

Figure S10. *Bevacizumab alone and in combination with triamcinolone acetonide phosphate in a 1:15 molar ratio after 28 days at 40°C. Quantification of aggregates was performed by AF4 coupled to MALS. Percentages of aggregates are expressed as average (n=3). No significant difference was observed between the samples with and without triamcinolone acetonide phosphate.*

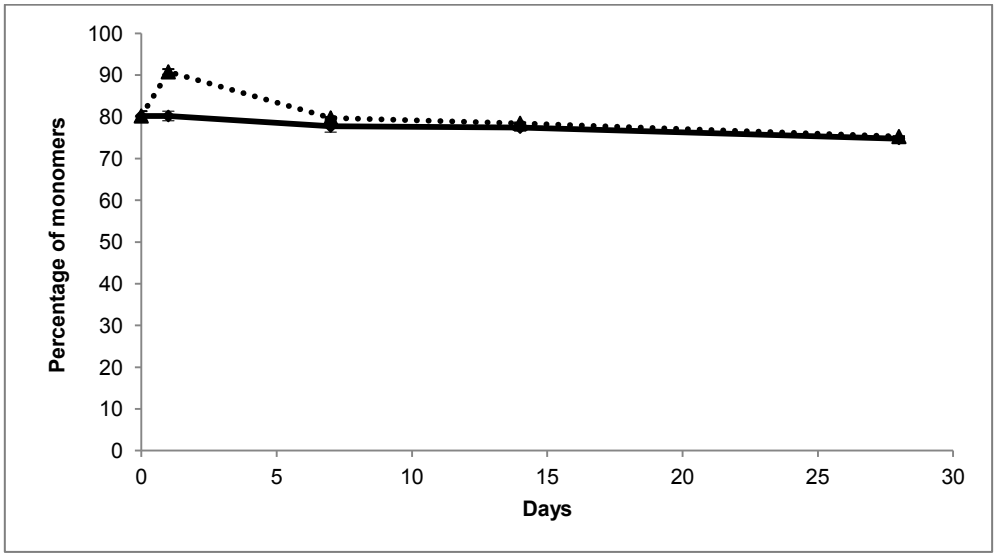

Figure S11. *Percentage of monomers for bevacizumab alone (black curve) and in combination with triamcinolone acetonide phosphate (black dashed curve) in a 1:15 molar ratio, storage at 40°C. Quantification of aggregates was performed by AF4 coupled to MALS. Bevacizumab was stressed for 7 days at 40°C before the addition of the steroid drug. Percentages are expressed as average ± SD, shown as vertical bars (n=3).*

REFERENCES FOR SUPPLEMENTARY MATERIAL

1. Veurink M, Westermaier Y, Scapozza L, Gurny R. Stabilized intact antibody formulations, related methods and uses thereof. World Intellectual Property Organization PCT/IB2011/051373 2011.

2. Thompson JD, Higgins DG, Gibson TJ. CLUSTAL W: improving the sensitivity of progressive multiple sequence alignment through sequence weighting, position-specific gap penalties and weight matrix choice. *Nucleic Acids Res* 1994; 22: 4673-4680.

3. Larkin MA, Blackshields G, Brown NP, Chenna R, McGettigan PA, McWilliam H, Valentin F, Wallace IM, Wilm A, Lopez R, Thompson JD, Gibson TJ, Higgins DG. Clustal W and Clustal X version 2.0. *Bioinformatics* 2007; 23: 2947-2948.

4. Beitz E. TEXshade: shading and labeling of multiple sequence alignments using LATEX2 epsilon. *Bioinformatics* 2000; 16: 135-139.

5. Chennamsetty N, Helk B, Voynov V, Kayser V, Trout BL. Aggregation-prone motifs in human immunoglobulin G. *J Mol Biol* 2009; 391: 404-413.

Inhibitory effect of adenosine monophosphate on bevacizumab (Avastin®) self-association: Identification of aggregation breakers through similarity searching and interaction studies

Y. Westermaier[1,2], M. Veurink[1,2], T. Riis-Johannessen[1], S. Guinchard[1], R. Gurny[1], L. Scapozza[1]

[1]School of Pharmaceutical Sciences, University of Geneva, University of Lausanne, Quai Ernest-Ansermet 30, CH-1211 Geneva 4, Switzerland. [2]Both authors contributed equally to this work.

Submitted to European Journal of Pharmaceutics and Biopharmaceutics

Aggregation is a common challenge in the optimisation of therapeutic antibody formulations. Since initial self-association of two monomers is typically a reversible process, the aim of this study is to identify different excipients that are able to shift this equilibrium to the monomeric state. The hypothesis is that a specific interaction between excipient and antibody may hinder two monomers from approaching each other, based on previous work in which dexamethasone phosphate showed the ability to partially reverse formed aggregates of the monoclonal IgG1 antibody bevacizumab back into monomers. The current study focuses on the selection of therapeutically inactive compounds with similar properties. Adenosine monophosphate, adenosine triphosphate, sucrose-6-phosphate and guanosine monophosphate were selected *in silico* through similarity searching and docking. All four compounds were predicted to bind to a protein-protein hotspot on the Fc region of bevacizumab and thereby inhibiting dimer formation. The predictions were supported *in vitro*: An interaction between AMP and bevacizumab with a dissociation constant of 9.59 ± 0.15 mM was observed by microscale thermophoresis. The stability of the antibody at elevated temperature (40°C) in a 51 mM phosphate buffer pH 7 was investigated in presence and absence of the excipients. Quantification of the different aggregation species by asymmetrical flow field-flow fractionation and size exclusion chromatography demonstrates that all four excipients are able to partially overcome the initial self-association of bevacizumab monomers.

Keywords: antibody self-association, aggregation breaker, similarity searching, microscale thermophoresis, asymmetrical flow field-flow fractionation, size exclusion chromatography.

INTRODUCTION

The development and application of therapeutic antibodies have widely increased in the past decade.[1] An important step in the optimisation of antibody formulations is the prevention of aggregation. This is of clinical relevance since aggregates may cause immunogenicity and a diminished efficacy of the protein drug.[2] Because therapeutic antibodies are large and complex proteins, aggregation is a complicated process that may follow different pathways. The protein may partly unfold, leading to exposure of its inner hydrophobic regions, which promotes intramolecular interactions between two monomers.[3,4] Alternatively, chemical degradations of the protein, like oxidation or deamidation, may result in the formation of aggregates.[3,4] This study focuses on a third mechanism; namely, the reversible self-association of the native state of the protein, in which an equilibrium exists between monomers and small oligomers.[3,4]

Since this pathway is a reversible process, an interesting option to investigate is the possibility to shift the equilibrium towards a monomeric state. This could be envisaged through the addition of an excipient to the formulation which is able to prevent monomeric species from approaching each other and forming dimers. Because of the low predictability of the aggregation process, a variety of excipients[5-8] has been investigated on a trial and error base in the past, without applying a specific selection process. The majority of them act by optimising the environment around the antibody, by inhibiting interface-dependent aggregation, or by forming a layer that surrounds the protein through non-specific associations with its hydrophobic patches, thereby avoiding two monomers from approaching each other.[6-8]

In this work, different excipients are screened for their ability to specifically interfere with the initial self-association of the antibody by binding to a protein-protein interaction hotspot, which we hypothesized to be involved in dimer formation.[9] The study is a follow-up on earlier work by our group in which the glucocorticoid dexamethasone phosphate was observed to possess aggregation breaking properties on the monoclonal IgG1 antibody bevacizumab (Avastin®).[9,10] Besides its aggregation breaking effect on bevacizumab, dexamethasone phosphate is a compound with anti-

inflammatory and immunosuppressant activity.[11] Therefore, although a combination product in which bevacizumab and dexamethasone act synergistically may be beneficial for certain treatments,[12] this study focuses on finding molecules that have similar aggregation breaking properties on bevacizumab, but no therapeutic activity or side effects. Two separate mechanisms in the hindrance of dimerization can be distinguished: First, an aggregation breaking effect, referring to the reversion of formed dimers and other small aggregates to monomers. Secondly, a stabilizing effect, dealing with a decrease in the overall reaction rate at which aggregates are formed over time.

Based on dexamethasone phosphate and a corticosteroid with a similar structure, i.e. betamethasone phosphate, a similarity search was performed *in silico* to select safe and therapeutically inactive excipients. After selection of these molecules, validation of the *in silico* predictions was performed in two steps: First, microscale thermophoresis (MST) assays were performed to investigate binding events occurring between the excipient and bevacizumab. Second, the bevacizumab stability in absence and presence of the excipient was studied under stress conditions. The fractions of monomers and aggregates in the samples were quantified by asymmetrical flow field-flow fractionation (AF4) and size exclusion chromatography (SEC).[9,10]

MATERIAL AND METHODS

In silico similarity screening

An *in silico* 3D dimer model was developed in earlier work.[9] In short, a protein-protein interaction hotspot was identified in which the Fc region surrounding Lys445 (numbering according to the crystal structure with the PDB code 1HZH) of a first bevacizumab is interacting with one Fab arm of a second bevacizumab. Docking of dexamethasone phosphate all over the bevacizumab monomer surface using FlexX 3.1.3 (Biosolveit GmbH, Sankt Augustin, Germany) showed a strong electrostatic interaction between the phosphate group of the glucocorticoid and the Lys445 side chain.[9] Therefore, it was postulated that the anti-inflammatory drug masks the interaction interface, thereby specifically preventing the formation of a dimer.[9] With the aim of finding a therapeutically inactive excipient, which is able to break the primary event of bevacizumab dimerisation, as was observed for

dexamethasone phosphate, other low molecular weight compounds have been searched by a similarity search/scaffold hopping approach. Similarity searches usually rely on similar physicochemical properties (pharmacophores) or shapes. Scaffold hopping deals with finding isofunctional, but structurally dissimilar molecular entities.[13-16] Ideally, screening methods that perform successful scaffold hops would not only find a maximum number but also a maximally diverse set of active compounds from a given chemical structure.[17]

ROCS 2.4.2 (OpenEye Scientific Software, Windows version, Santa Fe, USA) was used for fast shape comparison, with the assumption that molecules do have similar shapes if their volumes overlay well. Any volume mismatch was treated as a measure of dissimilarity. Similarity searches were performed using one conformer of dexamethasone phosphate and of betamethasone phosphate each. A multi mol2 file containing the two molecules was defined as query together with a sdf database file containing the small molecules to screen in ROCS. A database including almost 4800 FDA-approved molecules (DrugBank Library) was used.[18,19] Results were visualized and browsed in Vida 4.0.0 (OpenEye Scientific Software) for molecules that were likely to bind to Lys445 on the bevacizumab monomer model. The selection criteria included were: (i) At least two negative charges (preferentially a phosphate group), (ii) a spacer separating the negatively charged moiety, (iii) a part which provides bulk to the molecule, and (iv) high ranks (out of 500). Because in our case, the docking scores were not informative enough with respect to the antibody-antibody breaking ability, we used a cylindric « volume of interference » as published in our previous paper[9] to clearly distinguish between aggregation breaking and non-breaking docking poses. A second round of similarity searches was performed with the hit adenosine monophosphate (AMP) on the same input database. After selection of the molecules, docking was performed using the same protocol as described earlier,[9] targeting a region of 10 Å surrounding Lys445.

Interactions measured by MST

To assess whether a specific interaction occurs between AMP and bevacizumab, a study was performed using microscale thermophoresis (NanoTemper Technologies GmbH, Munich, Germany).

Besides, the binding affinity between two bevacizumab monomers was investigated. This technique, as described in detail by Jerabek-Willemsen et al.,[20] studies the movement of molecules induced by temperature gradients. It can be applied to investigate intermolecular interactions, since the effect is sensitive to the small changes in conformation, charge and size which occur during a binding event.[19]

Experiments were performed on label-free and labeled bevacizumab. For the former, the intrinsic fluorescence of tryptophan present in label-free bevacizumab (in 51 mM phosphate buffer pH 7) was used as a means of monitoring thermophoretic movement. A serial dilution of AMP (1.5 µM - 50 mM) in the same buffer was prepared and mixed 1:1 with a 20 µM solution of unlabeled antibody. A negative control was performed with the same serial dilutions of AMP in a 1:1 mixture with 20 µM tryptophan in 51 mM phosphate buffer pH 7. All measurements were carried out using hydrophilic glass capillaries and a Monolith NT.LabelFree (NanoTemper Technologies GmbH, Munich, Germany). The background signal caused by the blank buffer was subtracted.

In a second study, bevacizumab was labeled. To 100 µl of 20 µM antibody in a 51 mM phosphate buffer pH 7 three equivalents of a red fluorescent dye (NT-647) were added following a standard protocol of the manufacturer (NanoTemper Technologies GmbH). Excess dye was removed by gel filtration. Serial dilutions of the unlabeled interaction partners AMP (1.5 µM - 50 mM) or bevacizumab (5 nM - 86 µM) were prepared in the same buffer as the labeled bevacizumab. Hydrophilic glass capillaries were filled with a 1:1 mixture of labeled antibody and unlabeled partner for a final concentration of 20-40 nM labeled bevacizumab. Measurements were carried out in triplicates using a Monolith NT.115 (NanoTemper Technologies). Data analyses and curve fitting were carried out using the Nanotemper Analysis software.

***In vitro* stability studies**

Bevacizumab was dialysed into a 51 mM sodium phosphate buffer at pH 7 using a Slide-A-Lyzer Dialysis Cassette (Pierce, Reactolab, Servion, Switzerland). This buffer system was selected since it promotes the formation of aggregates, which are needed in order to observe an aggregation breaking

effect of the small molecule.[9] After dialyis, the concentration of the antibody was determined by UV spectroscopy (Nanodrop, Thermo Fisher Scientific Inc, Wilmington, USA) using an extinction coefficient of 1.7 cm ml/mg[21] and adjusted by centrifugation to a final concentration of 25 ± 1 mg/ml. To investigate the ability of the small molecule to revert formed aggregates back to monomers, the antibody was stored alone for 1 week at 40°C before addition of the aggregation breaker in order to increase the amount of aggregates present. The following compounds were added to the antibody in a 1:1, 1:10 and 1:100 molar ratio (antibody:small molecule): (i) Adenosine monophosphate (AMP), (ii) adenosine triphosphate (ATP), (iii) guanosine monophosphate (GMP), and (iv) sucrose-6-phosphate. For all samples, one sample container was stored and measurements were carried out in triplicates as in our previous study.[9]

The pH was kept constant at pH 7 and isotonicity of all samples was adjusted to be between 250 and 350 mOsmol/kg by adding NaCl. All samples were stored at 40°C over a period of 28 days. Because of observed differences in the amounts of aggregates between different batches, the comparison between the amount of aggregates in the sample of the antibody alone and in presence of the aggregation breaker was always performed on the same batch.[9]

The aggregation breaking effect of AMP on the commercial Avastin® formulation was investigated by stressing the formulated antibody in absence or presence of the aggregation breaker for 28 days at 40°C. The formulation had a pH of 6.1 (experimentally determined) and contained 60 mg/ml α,α-trehalose dihydrate and 0.04% polysorbate 20 in a 51 mM sodium phosphate buffer. In all the experiments, AMP was added to obtain an antibody:aggregation breaker molar ratio of 1:1, 1:10 and 1:100.

Quantification of monomers and aggregates by AF4 and SEC

Quantification of different aggregate species in each sample was performed using two orthogonal techniques, i.e. asymmetrical flow field-flow fractionation (AF4) (Wyatt Technology Europe GmbH, Dernbach, Germany) and size exclusion chromatography (SEC) using a TSK G3000 SW_{XL} column,

7.8 x 300 mm (Tosoh Bioscience GmbH, Stuttgart, Germany). The samples were injected undiluted with an injection volume of 0.5 µl for AF4 and of 2 µl for SEC, each run was carried out in triplicate. As a mobile phase, 51 mM sodium phosphate buffer with 94 mM NaCl pH 7.0 was used for AF4, whereas the SEC mobile phase was composed of 200 mM potassium phosphate buffer with 250 mM KCl pH 7.0. For the latter, a flow rate of 0.5 ml/min was applied at 25°C. Detection was achieved by UV spectroscopy (Agilent Technologies, Santa Clara, USA) at 280 nm and multi-angle light scattering (MALS) (Dawn EOS, Wyatt Technology Europe GmbH, Dernbach, Germany). The combination of the two detection methods allowed the calculation of the weight-averaged molar mass as well as the ratio of the different aggregate species separated by AF4 or SEC, respectively. Astra software (version 5.1.9.1, Wyatt Technology Europe GmbH, Dernbach, Germany) was used for data collection and analysis, whereby the different measured fractions were defined as average percentages of monomers, dimers, trimers or tetramers ± standard deviation (SD). Group-wise comparisons were carried out to compare the antibody alone with the combined samples in a 1:1, 1:10, and 1:100 molar ratio, using a Kruskal-Wallis test with post-hoc Bonferroni analysis ($p<0.05$).

RESULTS

In silico similarity search

Using betamethasone phosphate or dexamethasone phosphate as queries for the ligand-based screening of the DrugBank library, identical hit lists in terms of Tanimoto coefficients[22,23] were obtained. Taking the two queries together, fludarabine, fosphenytoin, AMP, tenofovir and cidofovir were identified as hits. AMP was used as a query to rescreen the DrugBank library, yielding as new hits ATP, tiludronate, amifostine and pyridoxal phosphate in decreasing Tanimoto coefficient rank order.

Every identified hit was docked onto the Fc contact region around Lys445 of the monomer. The second monomer of the aggregation model was then displayed and the molecules were selected or rejected based on the degree to which they overlapped with the second monomer. Fosphenytoin and pyridoxal phosphate could be discarded because the former was only seldom clashing and the latter

was too small to interfere with aggregation. Docking results suggested that fludarabine, tenofovir, cidofovir, tiludronate, and amifostin would interfere with dimer formation; however, since these molecules possess therapeutic activity, they were not considered for the present study. Figure 1 depicts the remaining molecules, AMP and ATP, docked onto the bevacizumab monomer. Only poses which are located completely inside our previously defined "volume of interference"[9] are shown.

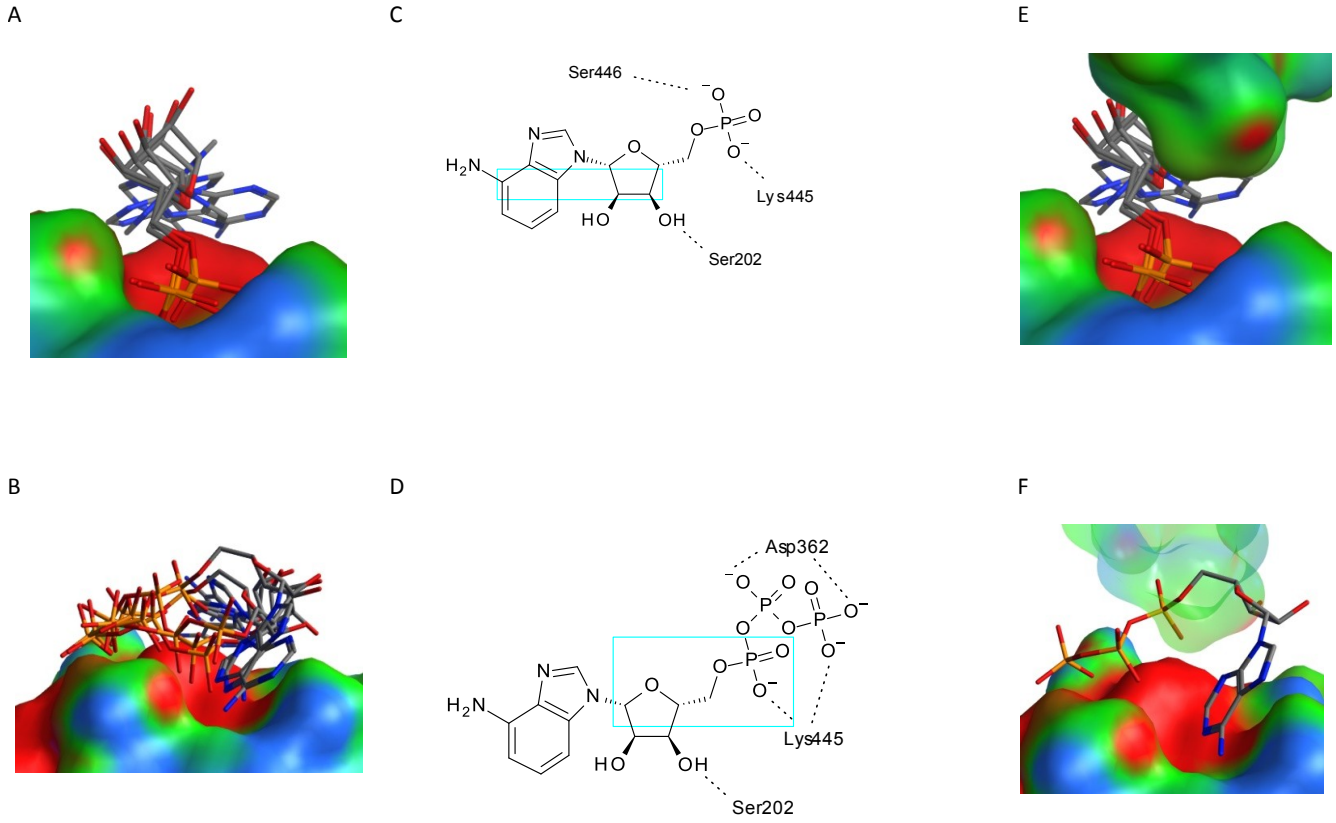

Figure 1. *Representative docking poses of AMP (A, C and E) and ATP (B, D and F). Docking poses on the bevacizumab monomer are displayed in A and B. Interactions between the docked molecule and the bevacizumab monomer are drawn in a schematic way in C and D. The dotted lines represent H-bonds or electrostatic interactions and the cyan box the parts of the small molecule that clash with the second monomer of the aggregation model. Representative poses for each compound are also represented in the dimer aggregation model (E and F). FlexX 3.1.3 (Biosolveit GmbH, Sankt Augustin, Germany) was used for docking and MOE (Chemical Computing Group, Montréal, Canada) for producing the monomer and dimer views, where the carbon atoms of the excipients are drawn in grey. The colour gradient of the electrostatic potential surface goes from blue for negatively charged to red for positively charged atoms. For the sake of clarity, a slightly different viewpoint has been chosen for ATP than for AMP.*

This volume was defined between the Fc of one bevacizumab and an adjacent Fab as a means to distinguish between potential aggregation breakers and non-breakers. As can be observed, AMP binds perfectly and preferably in the region of Lys445 on the bevacizumab monomer and interferes strongly with the formation of the dimer, as measured by the number and orientation of the poses inside the "volume of interference" and interfering with dimer formation. For both AMP and ATP, a majority of the poses were indeed within the "volume of interference" (10 out of 10 poses for both ligands) and interfering. Docking predicted that AMP has better aggregation breaking properties than ATP. While in the case of AMP, all poses had heavy atom root mean square (RMSD) deviations below 2Å, this was less the case for ATP. In other words, the rotatable bonds of the triphosphate in ATP render the molecule more flexible than the monophosphate in AMP and allow it to adopt many different conformations, influencing the orientation of adenosine, which is the bulky part of the molecule contributing to the aggregation breaking effect.

Based on the DrugBank screening results, we also investigated the role of the sugar-phosphate and the bulk "clashing" moieties, respectively. Several mono- and disaccharides were docked onto the monomer to assess whether the sugar-phosphate moiety is sufficient for binding into the pocket surrounding Lys445 and clashing into the adjacent antibody or if an additional spacer attached to the sugar moiety would be needed. Whereas monosaccharide phosphates were rejected as potential aggregation breakers, disaccharide phosphates were designated as candidate protein-protein interaction breakers due to their size and shape. Thus, to confirm the aggregation breaking properties of disaccharide phosphates, sucrose-6-phosphate was selected for *in vitro* investigation. Finally, guanosine monophosphate was included to study whether changing the nucleoside from adenosine to guanosine would influence the aggregation breaking properties of the molecule.

Binding assays by MST

The results of the binding assay using MST revealed a specific interaction between AMP and label-free bevacizumab, for which a dissociation constant (K_d) of 9.59 ± 0.15 mM was observed (Figure 2A). The negative control (Figure 2B), i.e. the interaction between tryptophan and AMP, showed a

weak unspecific "background binding", with a minimum K_d value greater than 116 mM. For the binding between labeled bevacizumab and AMP a K_d value of 22.6 ± 0.94 mM was found (Figure 3A), which is in line with the value determined for the label-free bevacizumab. A slightly weaker interaction may reflect the lower number of free Lys445 residues on labeled bevacizumab, since the labeling process indiscriminately targets all surface-accessible lysine residues. A higher affinity was observed for the self-association between labeled-bevacizumab and bevacizumab, with a K_d of 0.40 ± 0.02 μM. Visible aggregates appeared for the three highest bevacizumab concentrations and thus these three samples were excluded from the curve fitting procedure (Figure 3B).

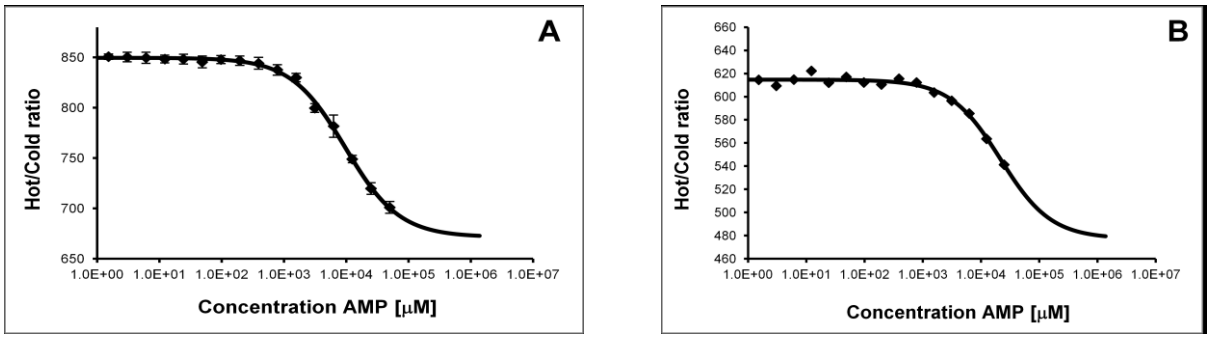

Figure 2. *AMP binding to unlabeled bevacizumab* ***(A)*** *or to the negative control tryptophan* ***(B)****. Concentrations of bevacizumab and tryptophan in 51 mM phosphate buffer pH 7 were kept constant at 10 μM with increasing concentrations of AMP.* ***(A)*** *For the interaction between bevacizumab and AMP a* K_d *of 9.59 ± 0.15 mM was determined, with a coefficient of determination* (r^2) *of 0.76 for the fitted curve. A LED power of 5% and a laser power of 20% were used.* ***(B)*** *The negative control (tryptophan-AMP) shows a "background binding" with a* $K_d \geq 116$ *mM. The fitted curve has an* r^2 *of 0.42 and the LED and laser powers were 10% and 20%, respectively. The hot/cold ratio measures the difference in fluorescence signal before switching on the laser (cold) and after a defined period of heating (hot). A change in this ratio is caused by a change in thermophoretic motion due to a binding event.*

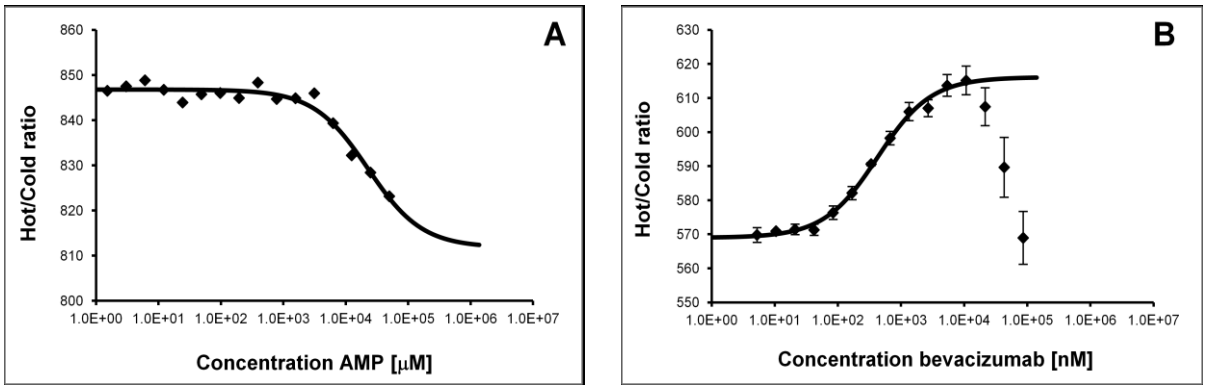

Figure 3. *AMP binding to bevacizumab* ***(A)*** *and bevacizumab-bevacizumab binding* ***(B)*** *using labeled bevacizumab. The bevacizumab concentration in 51 mM phosphate buffer pH 7 was kept constant at 20 nM* ***(A)*** *and 40 nM* ***(B)*** *with increasing concentrations of AMP and of bevacizumab, respectively. A K_d value of 22.6 ± 0.94 mM was determined for AMP binding to bevacizumab, while the bevacizumab-bevacizumab dimer formation reveals a K_d value of 0.40 ± 0.02 μM.* ***(A)*** *The fitted curve has a coefficient of determination (r^2) of 0.91; the used LED and laser powers were 50% and 40% respectively.* ***(B)*** *The fitted curve has a r^2 of 0.99, the used LED and laser power were 20% and 80%, respectively.*

Table 1: *Effect of AMP on bevacizumab aggregation. Addition of AMP leads to a concentration-dependent increase in the percentage of bevacizumab monomers after 28 days at 40°C. The antibody was dialysed into 51 mM phosphate buffer pH 7 and prestressed for 7 days at 40°C. Thereafter, AMP was added in different molar ratios. The increase in monomer percentage is presented as average ± SD. Separation was performed by AF4 and SEC.*

	Increase in monomer percentage at $t_{28\ days}$[1] (%)			Relative recovery[2] (%)		
Method of separation	bevacizumab + AMP 1:1	bevacizumab + AMP 1:10	bevacizumab + AMP 1:100	bevacizumab + AMP 1:1	bevacizumab + AMP 1:10	bevacizumab + AMP 1:100
AF4	-0.4 ± 0.5	3.0 ± 0.1*	11.6 ± 0.8*	107 ± 4	105 ± 1	105 ± 5
SEC	3.7 ± 0.7*	8 ± 1*	12 ± 2*	109.1 ± 0.6	107 ± 2	106 ± 1

** Significantly different from antibody alone ($p<0.05$, Kruskal-Wallis test with post-hoc Bonferroni analysis).*
[1] Calculated as follows: $((\%_{beva+AMP})_{t28} - (\%_{beva\ alone})_{t28} / (\%_{beva\ alone})_{t28}) \times 100$
[2] Calculated as follows: $(AUC_{bevacizumab\ alone\ at\ t0} / AUC_{sample\ at\ t28}) * 100\%$, in which AUC is the area under the curve detected by UV.

***In vitro* stability studies**

After 28 days of storage at 40°C, a partial prevention of aggregation due to the addition of AMP to bevacizumab is measured by AF4 and SEC (Table 1). The formed aggregates present in the different samples are depicted in Figure 4. This analysis clearly shows that dimers and trimers are the prevailing aggregates and that an AMP concentration-dependent reduction of aggregates occurred (Figure 4). Both techniques showed a similar trend: The higher the molar ratio, the lower the percentage of aggregates and the more pronounced the observed increase in monomer percentages (Table 1). By SEC, all molar ratios of AMP had a positive effect on the antibody, with an increase in monomer percentages of 3.7 ± 0.7%, 8 ± 1%, and 12 ± 2% for the 1:1, 1:10 and 1:100 molar ratio, respectively. Similar effects were observed with AF4, except for the 1:1 molar ratio, exhibiting a slightly negative effect on bevacizumab: An increase in monomer percentages of -0.4 ± 0.5%, 3.0 ± 0.1%, and 11.6 ±0.8% was detected for the 1:1, 1:10 and 1:100 molar ratio, respectively. The difference obtained with these two orthogonal techniques may be explained by the fact that a fragile equilibrium exists between monomers and aggregates. It is therefore possible that aggregates are formed or disrupted during the analysis.[24] The commercial formulation Avastin® at pH 6.1 in combination with AMP demonstrated similar effects as bevacizumab at pH 7. However, the antibody was more stable in both absence and presence of AMP at this lower pH and the aggregation breaking effect was less pronounced (data not shown).

The analysis of the percentage of monomers over time for bevacizumab alone and in presence of AMP or ATP in a 1:100 molar ratio showed that both small molecules were able to interfere with the initial monomer self-association, causing the reversion of small aggregates to monomeric species (Figure 5). The increase in monomer percentages compared to bevacizumab alone was maintained over 28 days, and was comparable for AMP and ATP during the whole study. The slopes of the curves were similar with or without the small molecule. Similar effects were observed after addition of sucrose-6-phosphate and GMP to the antibody (data not shown).

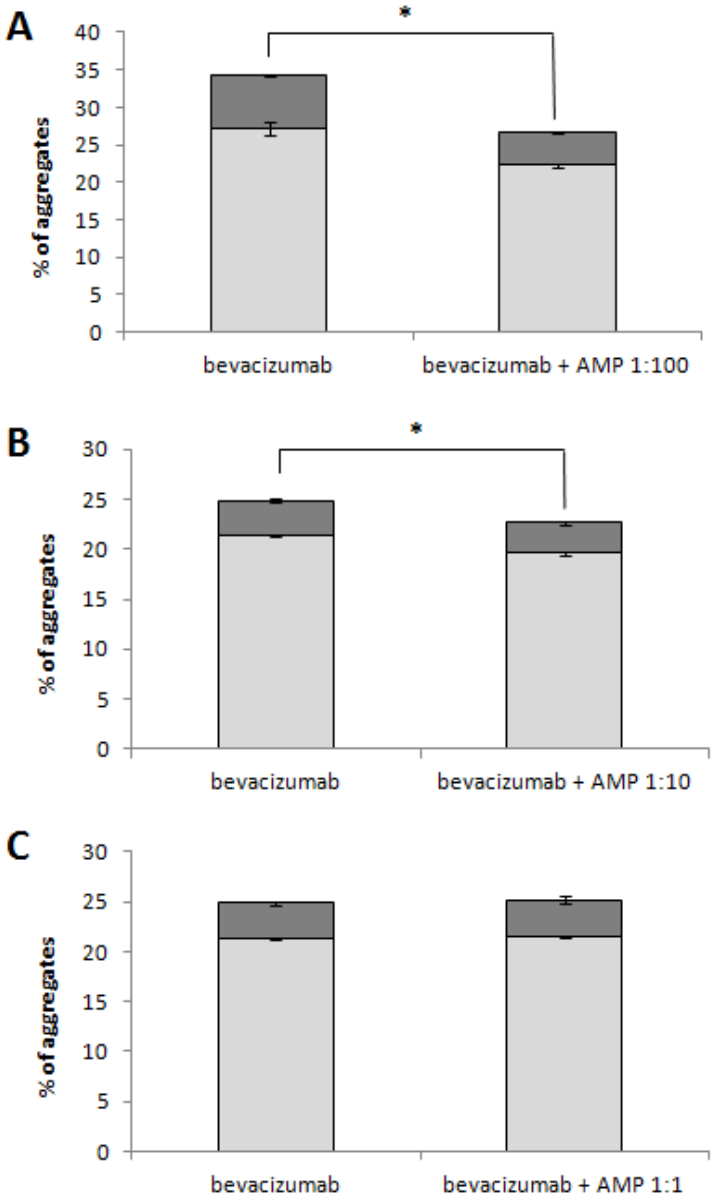

Figure 4. *Presence of AMP in a 1:100* ***(A)****, 1:10* ***(B)*** *and 1:1* ***(C)*** *molar ratio decreases the amount of small aggregates in the bevacizumab sample at* $t_{28\ days}$ *in a concentration dependent way. The percentages of dimers and tetramers are represented as light grey and dark grey bar, respectively. The antibody alone was dialysed in 51 mM phosphate buffer pH 7 and prestressed for 7 days at 40°C. Thereafter, AMP was added and samples are stored at 40°C for 28 days. To overcome inter-batch differences, control (absence of AMP) and experiment (presence of AMP) were always run in triplicate on the same batch. The percentage of aggregates are presented as average ± SD, measured by AF4. * Significant difference (p<0.05, Kruskal-Wallis test with post-hoc Bonferroni analysis).*

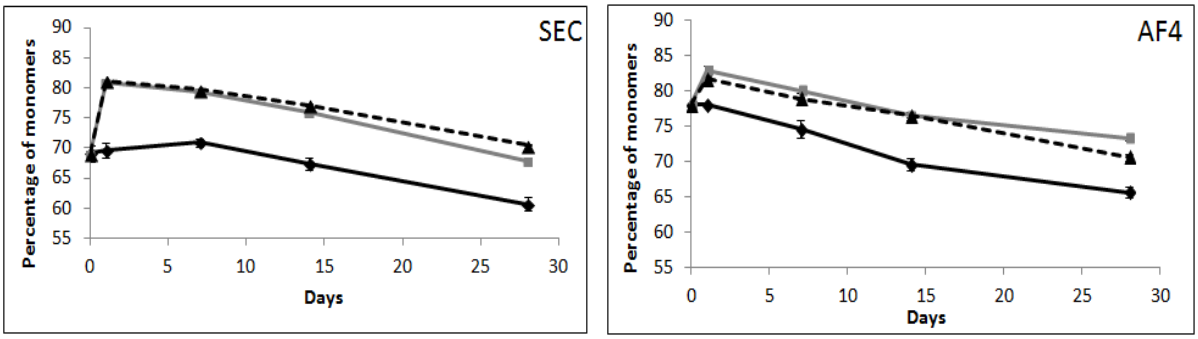

Figure 5. *Aggregation breaking effect of AMP and ATP on bevacizumab in a 1:100 molar ratio, monitored over time. Bevacizumab alone is represented as a black line, bevacizumab and AMP (1:100 molar ratio) as a grey line, and bevacizumab with ATP (1:100 molar ratio) as a black dashed line. The antibody alone was prestressed for 7 days at 40°C in 51 mM phosphate buffer pH 7. Thereafter, the aggregation breakers were added and samples were stored at 40°C for 28 days. The percentage of monomers is presented as average ± SD, measured by SEC and AF4.*

Comparing the different aggregate species present in the bevacizumab formulation alone, or together with GMP, sucrose-6-phosphate, or ATP revealed that all samples contained dimers and tetramers after 28 days at 40°C (Figure 6). All molar ratios of GMP caused a significant decrease in the total amount of aggregates compared to the sample of bevacizumab alone. The effect was concentration-dependent: The sample of bevacizumab alone contained 32.1 ± 0.7% of aggregates, compared to 29.8 ± 0.2%, 27.4 ± 0.9% and 22.21 ± 0.05% for the 1:1, 1:10 and 1:100 GMP molar ratios, respectively. For sucrose-6-phosphate, only the 1:10 and 1:100 molar ratios were observed to significantly diminish the amount of aggregates in the sample (24.2 ± 0.4% and 23.6 ± 0.3%) compared to bevacizumab alone (27.1 ± 0.6%). The difference in aggregate percentage between the sample of bevacizumab alone and combined with ATP was only significant for the 1:100 molar ratio, with 27.6 ± 0.5% for bevacizumab alone and 27.1 ± 0.2%, 27.8 ± 0.1% and 22.0 ± 0.4% for the 1:1, 1:10 and 1:100 molar ratios, respectively.

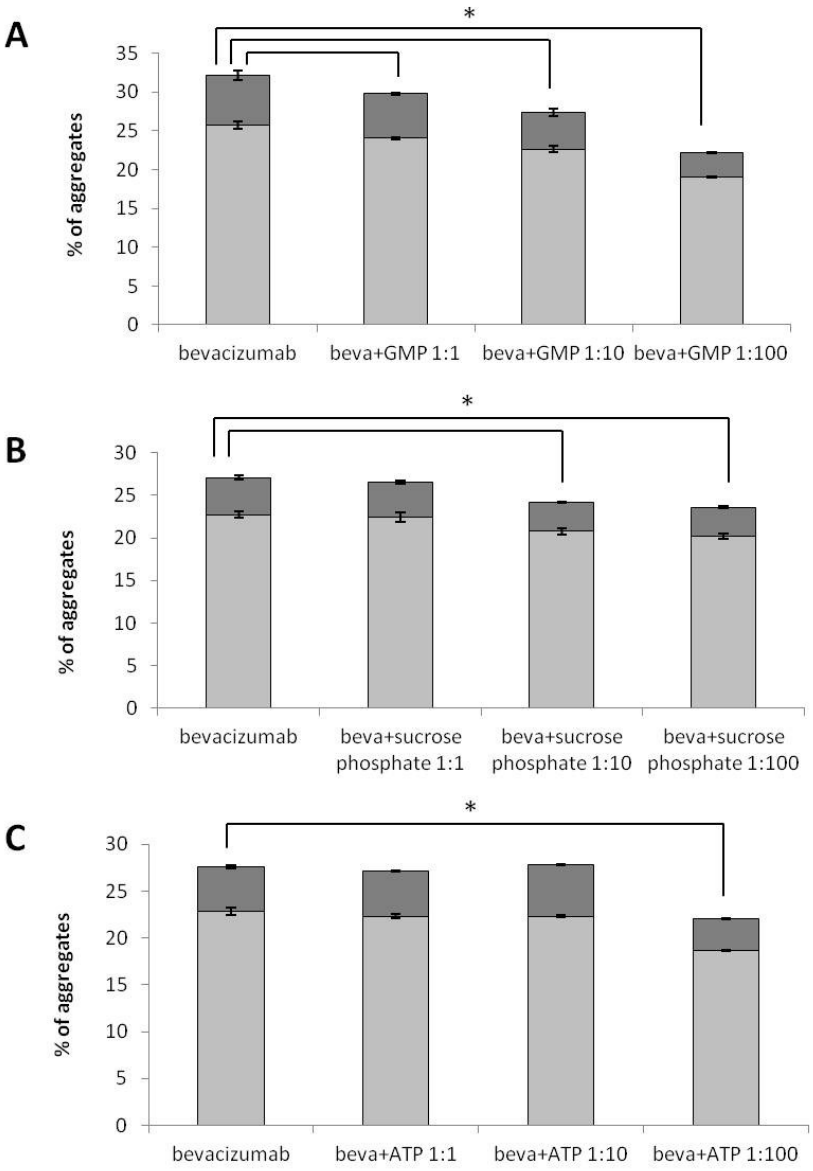

Figure 6. *Presence of GMP* ***(A)****, sucrose phosphate* ***(B)*** *or ATP* ***(C)*** *decreases the amount of small aggregates in the bevacizumab (beva) sample at* $t_{28\ days}$*. The percentages of dimers and tetramers are represented as light grey and dark grey bar, respectively. The antibody alone was dialysed in 51 mM phosphate buffer pH 7 and prestressed for 7 days at 40°C. Thereafter, the aggregation breakers were added and samples were stored at 40°C for 28 days. The percentage of aggregates are presented as average ± SD, measured by AF4.* ******* *Significant difference (*$p<0.05$*, Kruskal-Wallis test with post-hoc Bonferroni analysis).*

DISCUSSION

The main aim of this study was to identify safe and therapeutically inactive compounds that have an aggregation breaking and/or stabilizing effect on the IgG1-based antibody bevacizumab. AMP and

ATP were identified as hits and meet our requirements, having no therapeutic activity and both naturally occurring in the human body. Additionally, AMP is used as a food additive and is generally recognized as safe (GRAS) by the FDA.[25] The other two molecules, sucrose-6-phosphate and GMP, also have the potential of being safe excipients, the first being a key intermediate in the synthesis of sucrose in plants,[26] and the latter a food additive[27] like AMP.

The choice for using MST to study binding events between bevacizumab and AMP was based upon several considerations. First of all, interactions between small molecules and proteins are difficult to measure, due to their difference in molecular weight.[28] Here, AMP has a molecular weight of 347 Da and bevacizumab of 149000 Da. Consequently, no pronounced change in size of the protein will occur upon interaction with AMP, making the use of mass-based techniques challenging.[29] In contrast, microscale thermophoresis has a high sensitivity for binding between small molecules and proteins, as was demonstrated by Wienken et al.[28] Besides, measurements are performed in the buffer of choice with both interaction partners in free solution[20] and the required sample volumes are low, in contrast to more conventional techniques like isothermal titration calorimetry.[28]

The dissociation constant for the self-interaction between two bevacizumab monomers was studied earlier by the group of Moore et al.,[21] who found a K_d of 230 μM in a 10 mM phosphate buffer at pH 7. An approximate 500-fold higher affinity was observed in our study (K_d of 0.40 μM), which may be due to the fact that the buffer systems differ in respect to ionic strength: instead of a 10 mM, a 51 mM phosphate buffer was used in our study. Kameoka et al.[30] described that the increase in ionic strength of a phosphate buffer led to increased aggregation of a humanized IgG antibody. Thus, the elevated ionic strength influences the equilibrium between monomers and small aggregates, causing a shift to the aggregated state. Possibly, this shift results in an increase in binding affinity between two monomers, which is driven by the changes in the environment surrounding them and influences the strength of each single interaction. Subsequently, their presence as aggregates in the formulation will be prolonged, before they will revert back to a monomeric state. Hence, the observed difference in

binding affinity between our study and the one by Moore et al. may be explained by the rise in ionic strength from 10 mM to 51 mM.

The *in vitro* stability studies revealed that all four selected compounds were able to break the initial aggregation of the antibody, although they differed in efficacy. The observed aggregation breaking effect involved an inhibition of the initial dimer formation and the reversion of already formed dimers back to monomers. However, none of the studied compounds influenced the overall reaction rate at which aggregates were formed, in other words, they did not have a stabilizing effect on the antibody. If the aggregation breaker would have been a stabilizer, the slope in Figure 5 in presence of the small molecule would have been less steep than for the curve of the antibody alone. Nevertheless, all four excipients (in a 1:100 molar ratio) caused a significant rise in monomer percentage that was still present after 28 days storage at 40°C. The *in silico* prediction, in which AMP was identified as a better aggregation breaker than ATP, was confirmed *in vitro*. Although the 1:100 molar ratio of AMP and ATP both showed rather similar effects on bevacizumab, comparison of the results at lower concentrations of excipient showed that there is a difference in efficacy between them. After 28 days, AMP showed a significant difference for both the 1:10 and 1:100 molar ratios, whereas ATP only had a significant effect at a 1:100 molar ratio. Thus, 10 times less AMP than ATP is needed to maintain a significant aggregation breaking effect over 28 days.

The fact that a concentration-dependent effect was observed, with higher molar ratios being more effective in breaking the aggregation, is in agreement with the difference in affinity that was distinguished between AMP interacting with bevacizumab and bevacizumab interacting with itself. According to the *in silico* model, AMP competes with a second bevacizumab monomer for the binding-spot on the Fc region. Since the bevacizumab-bevacizumab interaction was found to be much stronger than the binding between AMP and bevacizumab, a 1:1 molar ratio of AMP:bevacizumab would unlikely be sufficient to effectively hinder two monomers from approaching each other, as was shown experimentally.

Based on the results, it is postulated that an effective aggregation breaker should comply with a general "bulky group-spacer-phosphate" principle as depicted for AMP in Figure 7. The molecule should possess a phosphate group to enhance electrostatic components of the interaction with the Lys445 side chain. It should also contain a base or bulky group that is able to interfere with the Fab of an approaching monomer. And the spacer should at least partially bridge the 4 Å gap defining the minimal distance in the Fc-Fab interface. This model could be useful to systematically identify other therapeutically inactive and safe aggregation breakers.[31]

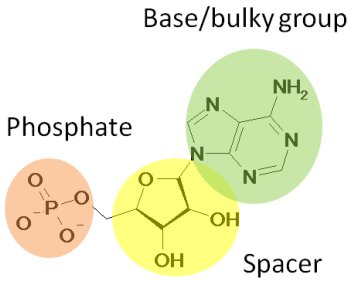

Figure 7. *The "bulky group-spacer-phosphate" principle applied to AMP.*

The present work was intended as an initial investigation of the concept that small molecules with similar structures are able to inhibit self-association in a similar way and not to study their aggregation breaking properties while changing parameters. Extensive investigation of different buffer systems, pHs, ionic strength, stress methods and other antibodies were considered outside the scope of this work. Thus, it was decided to use only one IgG1-based engineered antibody, in one buffer system. Certainly, future investigations need to be undertaken to verify whether the observed effects are more widely applicable. Furthermore, the herein used bevacizumab formulation was obtained through dialysis of the commercially available formulation Avastin®. This formulation contains polysorbate 20, which cannot be completely removed from the sample by dialysis.[32] Therefore, we cannot exclude that the detected aggregation breaking effect is enhanced by the presence of polysorbate.

To conclude, a specific binding with a dissociation constant of 9.59 ± 0.15 mM, is observed between AMP and bevacizumab, leading to an aggregation breaking effect. These data strengthen our

hypothesis that a specific interaction between excipient and antibody specifically hinders the initial self-association of two monomers; although it has to be proven that the region around Lys445 is indeed involved. Moreover, this work provides a systematic approach in the discovery of new excipients for antibody formulations. Since aggregation may lead to adverse events and the search for stabilizing agents has so far been driven by trial and error, a rational selection process might be of clinical importance in the future development of stable antibody formulations. AMP was found by *in silico* similarity screening of 4800 approved drug molecules and was successfully predicted to be able to break the self-association of bevacizumab, demonstrating the potential value of similarity searches in this field. Based upon the results of the stability studies, AMP and GMP, both being food additives and the first being a GRAS compound, show promising properties as safe and therapeutically inactive aggregation breakers.

ACKNOWLEDGMENTS

The authors wish to thank Dr François Xavier Ogi from Nanotemper Technologies for putting the Monolith NT.LabelFree and Monolith NT.115 at their disposal and the Swiss National Science Foundation for financial support (#320030-122190/1). They also acknowledge Openeye Scientific Software for providing an academic license for the programs ROCS and Vida, respectively.

REFERENCES

1. Aggarwal S. What's fueling the biotech engine-2009-2010. *Nat Biotechnol* 2010; 28: 1165-1171.

2. Wang W, Singh SK, Ning L, Toler MR, King KR, Nema S. Immunogenicity of protein aggregates – concerns and realities. *Int J Pharm* 2012; 431: 1-11.

3. Philo JS, Arakawa T. Mechanisms of protein aggregation. *Curr Pharm Biotechnol* 2009; 10: 348-351.

4. Wang W, Nema S, Teagarden D. Protein aggregation – pathways and influencing factors. *Int J Pharm* 2010; 390: 89-99.

5. Szenczi A, Kardos J, Medgyesi GA, Zavodszky P. The effect of solvent environment on the conformation and stability of human polyclonal IgG in solution. *Biologicals* 2006; 34: 5-14.

6. Bolli R, Woodtli K, Bärtschi M, Höfferer L, Lerch P. L-Proline reduces IgG dimer content and enhances the stability of intravenous immunoglobulin (IVIG) solutions. *Biologicals* 2010; 38: 150-157.

7. Lee HJ, McAuley A, Schilke KF, McGuire J. Molecular origins of surfactant-mediated stabilization of protein drugs. *Adv Drug Deliv Rev* 2011; 63: 1160-1171.

8. Bee JS, Randolph TW, Carpenter JF, Bishop SM, Dimitrova MN. Effects of surfaces and leachables on the stability of biopharmaceuticals. *J Pharm Sci* 2011; 100: 4158-4170.

9. Veurink M, Westermaier Y, Gurny R, Scapozza L. Breaking the aggregation of the monoclonal antibody bevacizumab (Avastin®) by dexamethasone phosphate: insights from molecular modelling and asymmetrical flow field-flow fractionation. *Pharmaceutical Research (in press)*

10. Veurink M, Stella C, Tabatabay C, Pournaras CJ, Gurny R. Association of ranibizumab (Lucentis®) or bevacizumab (Avastin®) with dexamethasone and triamcinolone acetonide: an in vitro stability assessment. *Eur J Pharm Biopharm* 2011; 78: 271-277.

11. Rhen T, Cidlowski JA. Antiinflammatory action of glucocorticoids – new mechanisms for old drugs. *N Engl J Med* 2005; 353: 1711-1723.

12. Andreoli CM, Miller JW. Anti-vascular endothelial growth factor therapy for ocular neovascular disease. *Curr Opin Ophthalmol* 2007; 18: 502-508.

13. Schneider G, Neidhart W, Giller T, Schmid G. "Scaffold-hopping" by topological pharmacophore search: a contribution to virtual screening. *Angew Chem Int Ed Engl* 1999; 38: 2894-2896.

14. Schneider G, et al. Virtual screening for bioactive molecules by evolutionary de novo design. *Angew Chem Int Ed Engl* 2000; 39: 4130-4133.

15. Boehm HJ, Flohr A, Stahl M. Scaffold hopping. *Drug Discov Today* 2004; 1: 217-224.

16. Jenkins JL, Glick M, Davies JW. A 3D similarity method for scaffold hopping from known drugs or natural ligands to new chemotypes. *J Med Chem* 2004; 47: 6144-6159.

17. Renner S, Schneider G. Scaffold-hopping potential of ligand-based similarity concepts. *ChemMedChem* 2006; 1: 181-185.

18. Wishart DS, Knox C, Guo AC, Cheng D, Shrivastava S, Tzur D, Gautam B, Hassanali M. DrugBank: a knowledgebase for drugs, drug actions and drug targets. *Nucleic Acids Res* 2008; 36: D901-906.

19. Wishart DS, Knox C, Guo AC, Shrivastava S, Hassanali M, Stothard P, Chang Z, Woolsey J. DrugBank: a comprehensive resource for in silico drug discovery and exploration. *Nucleic Acids Res* 2006; 34: D668-672.

20. Jerabek-Willemsen M, Wienken CJ, Braun D, Baaske P, Duhr S. Molecular interaction studies using microscale thermophoresis. *Assay Drug Dev Technol* 2011; 9: 342–353.

21. Moore JM, Patapoff TW, Cromwell ME. Kinetics and thermodynamics of dimer formation and dissociation for a recombinant humanized monoclonal antibody to vascular endothelial growth factor. *Biochemistry* 1999; 38: 13960-13967.

22. Tanimoto TT. IBM Internal Report 17th Nov 1957.

23. Jaccard P. Distribution de la flore alpine dans le bassin des Dranses et dans quelques régions voisines. *Bulletin del la Société Vaudoise des Sciences Naturelles* 1901; 37: 241-272.

24. Carpenter JF, Randolph TW, Jiskoot W, Crommelin DJA, Middaugh CR, Winter G. Potential inaccurate quantitation and sizing of protein aggregates by size exclusion chromatography: essential need to use orthogonal methods to assure the quality of therapeutic protein products. *J Pharm Sci* 2010; 99: 2200-2208.

25. http://www.fda.gov/ucm/groups/fdagov-public/@fdagov-foods-gen/documents/document/ucm267832.pdf

26. Avigad G, Dey PM. Carbohydrate metabolism: storage carbohydrates. In: P.M. Dey, J.B. Harborne (Eds.), Plant Biochemistry, Academic Press, San Diego, 1997, pp. 143-203.

27. http://www.fda.gov/food/foodingredientspackaging/foodadditives/foodadditivelisting/ucm091048.htm

28. Wienken CJ, Baaske P, Rothbauer U, Braun D, Duhr S. Protein-binding assays in biological liquids using microscale thermophoresis. *Nat Commun* 2010; 1: 100.

29. Corin K, Baaske P, Ravel DB, Song J, Brown E, Wang X, Geissler S, Wienken CJ, Jerabek-Willemsen M, Duhr S, Braun D, Zang S. A robust and rapid method of producing soluble, stable, and functional G-protein coupled receptors. *PLoS One* 2011; 6: e23036.

30. Kameoka D, Masuzaki E, Ueda T, Imoto T. Effect of buffer species on the unfolding and the aggregation of humanized IgG. *J Biochem* 2007; 142: 383-391.

31. Gurny R, Scapozza L, Westermaier Y, Veurink M. Stabilized intact antibody formulations, related methods and uses thereof, World Intellectual Property Organization PCT/IB2011/051373 (2011).

32. Mahler HC, Printz M, Kopf R, Schuller R, Müller R. Behaviour of polysorbate 20 during dialysis, concentration and filtration using membrane separation techniques. *J Pharm Sci* 2008; 97: 764-774.

Conclusions and Perspectives

Vision loss and blindness are often caused by conditions in which the retinal vasculature is affected. Due to the isolated structure of the eye, drug delivery to the retina presents a challenge. Intravitreal injections are a straight forward approach to target the posterior segment; however frequent re-injections may lead to severe side-effects and thus affect patient compliance. The objective of this work was therefore to ameliorate intravitreal formulations targeting the retinal vasculature, in order to improve the therapeutic efficacy and to reduce the number of injections needed for optimal treatment. Two different strategies were investigated to reach these goals. A first approach focused on injectable drug delivery systems, acting as carrier or as prodrug for the sustained release of small vasodilative molecules to the retinal tissues. A second strategy aimed at the development of a stable intravitreal antibody formulation, through the development of a combined formulation with corticosteroids or through the addition of excipients, acting as aggregation breakers.

For the first approach, injectable and biocompatible poly(2-hydroxy esters) were used, based on the hypothesis that they will form intravitreal drug depots that slowly release therapeutic doses of the vasodilator. The rationale behind such a vasodilative system is to overcome retinal vascular occlusions, in order to prevent angiogenesis and a cascade of secondary effects leading to vision loss. Poly(2-hydroxyoctanoic acid) and poly(L-lactic acid-*co*-2-hydroxyoctanoic acid) were selected as drug delivery systems, since both degrade slowly through hydrolysis while present in an aqueous medium like the vitreous humour. This biodegradation is required, in order to prevent the need to surgically remove the system from the eye. Moreover, these polymers can be administered as conventional intravitreal injection, thus avoiding high costs and invasiveness that are associated with ocular implants.

The main advantage of poly(L-lactic acid-*co*-2-hydroxyoctanoic acid) is the fact that no drug incorporation was needed: hydrolysis of the system will automatically lead to the presence of free L-

lactate in the vitreous humor. To our knowledge, this is the first time that such an “all in one” copolymer system for intravitreal injection was investigated. Similar to this straightforward “all in one” approach, the principle behind the development of the poly(2-hydroxyoctanoic acid) formulation was based on simplicity: although incorporation of the active substance is required in this case, this was done by simple mixing without the need of heat or solvents. Moreover, to neither of the polymer systems additional excipients were added.

The initial step in the development of these intravitreal drug depots showed encouraging results, with a zero order release over a period varying between 7 and 14 days, good injectability and biocompatibility with the retinal tissues. An initial proof of concept was obtained *in vivo*, demonstrating the potential of these polymers to act as intraocular sustained release systems. Thus, both poly(L-lactic acid-*co*-2-hydroxyoctanoic acid) and poly(2-hydroxyoctanoic acid) are promising systems for intravitreal drug delivery. In the future, these polymers may offer an alternative for intravitreal injections of micro- and nanoparticles. Their application for the sustained release of other drugs targeting the retinal tissues, like corticosteroids, may be considered as well.

For the second approach, the development of a stable intravitreal formulation, in which the therapeutic antibodies bevacizumab and ranibizumab were combined with a corticosteroid, was envisaged. Simultaneous injections of an antibody and a corticosteroid separately were investigated in clinics; however their potential interaction in the limited volume of the eye was not taken into consideration. Therapeutic antibodies are prone to aggregation, which may lead to immunogenicity problems or reduce the efficacy of the protein drug. Therefore, it is essential to be aware that the addition of a corticosteroid to the formulation may affect the aggregation profile of the antibody. For the case of bevacizumab this is particularly important, since the commercial formulation Avastin® was formulated for intravenous infusion and was never intended for intraocular administration. Besides, it is unknown to what extent bevacizumab will aggregate during its residence in the vitreous humor at 37°C.

The importance of testing combined formulations before using them in clinics was demonstrated in this part of the thesis: Combination of both ranibizumab and bevacizumab with triamcinolone acetonide phosphate solution should be avoided, whereas a combined formulation with triamcinolone acetonide suspension could be considered, as well as with dexamethasone phosphate. To our surprise, addition of dexamethasone phosphate to bevacizumab even leads to a reversion of formed aggregates back to the monomeric state. Thus, a combo-formulation of dexamethasone phosphate and bevacizumab has not only the advantage of a possible synergistic effect, but the antibody formulation will also have an improved stability. Future *in vivo* studies need to be conducted to disclose whether a combo-formulation of bevacizumab and dexamethasone phosphate will indeed be beneficial compared to the antibody alone.

Based on the structure of dexamethasone phosphate, 4800 molecules were screened *in silico* in order to identify safe excipients with similar aggregation breaking properties. AMP was successfully selected as aggregation breaker, having no therapeutic activity and being Generally Recognized as Safe (GRAS) by the FDA. This compound specifically binds to the antibody and has aggregation breaking properties like dexamethasone phosphate. We postulate that this specific binding interferes with the initial step in self-association of two bevacizumab monomers. Addition of AMP as excipient to the protein formulation may provide a simple way to stabilize bevacizumab, without the need to modify the Ig structure through mutation of specific amino acids.

To our knowledge, no such systematic approach in which *in silico* and *in vitro* studies are combined to select stabilizing agents has been described up to now. Instead, due to the fact that the aggregation process is highly unpredictable, excipients have been chosen on a trial and error base. Therefore, the proposed strategy may be of great interest for future research in stabilizing antibody formulations, offering a rational selection process to distinguish aggregation breakers from non-breakers. Further work needs to clarify whether the observed effect is antibody specific, or whether it might be applicable to other IgG1 antibodies as well. In addition, the role of the buffer system and other excipients in the formulation needs to be resolved.

Overall, we conclude that formulation development plays an important role in the optimisation of drug delivery to the posterior segment. Both the use of injectable drug delivery systems and the stabilization of intravitreal antibody formulations are promising strategies to improve the therapeutic efficacy of pharmacotherapy targeting the retinal vasculature.

Summary

The focus of this work lies on ophthalmic formulations targeting the retinal vasculature, aiming at a reduction in the number of intravitreal injections needed for optimal treatment.

Part A of the thesis is dedicated to formulations designed to prevent angiogenesis through the intravitreal administration of vasodilative substances. These compounds are able to overcome retinal arteriolar occlusions, which may prevent the formation of new leaky blood vessels and a cascade of secondary effects. Since their vasodilative effect is short-lived after single injection, injectable and biodegradable polymers were investigated as drug delivery systems for these vasodilators. In **Chapter 1**, an "all in one" concept for the sustained release of L-lactic acid from poly(L-lactic acid-*co*-L,D-2-hydroxyoctanoic acid) was investigated. The copolymer acts not only as a carrier, but also as L-lactate prodrug, since its hydrolysis automatically leads to the sustained release of L-lactic acid, which will be converted to L-lactate at physiological pH. An *in vitro* sustained release over a period of 14 days was achieved and good *ex vivo* biocompatibility was observed when short oligomer chains were absent in the formulation. A copolymer with low polydispersity and low molecular weight showed a zero order release profile, good biocompatibility and injectability. The use of poly(2-hydroxyoctanoic acid) as a carrier for another vasodilative substance, the endothelin receptor antagonist BQ123, was studied in **Chapter 2**. *Ex vivo* release studies in porcine vitreous humor demonstrated a zero order release of BQ123 over 7 days. A proof of concept was obtained *in vivo*: the system was well tolerated in a mini pig model and a sustained release up to 7 days was demonstrated. Moreover, the formulation caused an immediate vasodilative effect in mini pigs that was observed over a period of 3 hours, which is a 6-fold increase compared to a single BQ123 injection. In conclusion, **Part A** of the present work shows the potential of injectable polymer systems based on 2-hydroxyoctanoic acid as intravitreal drug delivery systems.

Part B deals with formulations that suppress angiogenesis through inhibition of VEGF-A, focussing on the stability of therapeutic antibodies used for intravitreal injection. In **Chapter 3**, the therapeutic antibodies bevacizumab and ranibizumab were combined with corticosteroids, in order to develop a stable combined formulation that avoids multiple injections during combination treatment. Moreover, due to a synergistic effect, a combined formulation may prolong the interval between two subsequent injections. The Fab-fragment ranibizumab was observed to be more stable than the full-length antibody bevacizumab, in presence and absence of the anti-inflammatory drugs. Surprisingly, addition of dexamethasone phosphate to the bevacizumab formulation caused a reversion of formed aggregates back to monomers. The mechanism behind this protective effect was further studied in **Chapter 4**. An *in silico* 3D dimer model identified one close crystal contact area between two bevacizumab monomers. Docking of dexamethasone phosphate onto the protein predicted that the corticosteroid masks the interaction interface between two monomers and consequently hinders dimer formation. Indeed, *in vitro* stability studies showed that the addition of dexamethasone phosphate caused a significant reduction in the formation of small soluble aggregates. Thus, dexamethasone phosphate might be considered as an aggregation breaker for IgG1 antibodies. In **Chapter 5** other potential aggregation breakers were investigated, having a similar structure as dexamethasone phosphate, but without any therapeutic activity. The idea behind this search was to identify safe compounds that may serve as excipients for stable antibody formulations. AMP was selected by similarity searching as a potential candidate. *In vitro* investigations supported the prediction: a weak interaction between bevacizumab and AMP was observed and the small molecule showed to have aggregation breaking properties on the antibody. To conclude, **Part B** demonstrates that combining bevacizumab with dexamethasone phosphate increases the stability of the antibody and therefore the combo-formulation should be considered for further *in vivo* investigations. Moreover, a specific binding between the GRAS compound AMP and bevacizumab partially prevents aggregation of the antibody, thus providing a new strategy to stabilize antibody formulations.

Résumé

La perte partielle de la vision ou la cécité sont souvent la conséquence d'atteintes dans lesquelles la vascularisation rétinienne est affectée. Du fait de la structure isolée de l'œil, le transport du médicament vers le segment postérieur représente un défi. Une voie d'administration directe et efficace est l'injection intra-vitréenne; toutefois des injections fréquentes peuvent affecter la compliance du patient en causant des effets secondaires. L'objectif de ce travail consiste, de ce fait, à développer et améliorer des formulations intra-vitréennes, afin de réduire le nombre d'injections, dans le but d'optimiser le traitement des affections du réseau vasculaire rétinien.

La partie A de la thèse est dédiée aux formulations visant la prévention de l'angiogenèse, basée sur l'administration intra-vitréenne des petites molécules ayant un effet vasodilatateur. Ces composés pourraient être envisagés pour traiter certaines pathologies dans lesquelles les vaisseaux rétiniens sont obstrués. Malheureusement, l'effet thérapeutique est de très courte durée après une injection unique de ces molécules. De ce fait, un système à libération prolongé pourrait s'avérer bénéfique. Dans **le Chapitre 1**, la libération contrôlée de L-lactate à partir d'un copolymère de poly (acide lactique) et de poly (acide 2-hydroxyoctanoïque) est étudiée *in vitro*. Ce nouveau copolymère joue à la fois le rôle de véhicule et de L-lactate pro-drogue, du fait de la libération contrôlée de L-lactate au fil du temps par hydrolyse. Durant 14 jours, une libération prolongée de L-lactate à partir d'un tel système est observée *in vitro* avec une bonne biocompatibilité. Le copolymère à faible polydispersité et à basse masse moléculaire a montré une libération à vitesse constante, une bonne biocompatibilité et une injectabilité adéquate. **Le Chapitre 2** décrit l'incorporation d'un autre vasodilatateur, l'antagoniste de l'endothéline BQ123, dans poly(acide 2-hydroxyoctanoïque). Une cinétique d'ordre zéro a été observée dans l'humeur vitrée porcine pendant une semaine, de même qu'une biocompatibilité adéquate avec les tissus rétiniens. *In vivo*, la preuve du concept a été obtenue dans un modèle mini-cochon et l'effet vasodilatateur immédiat a été constaté pendant une période de trois heures. La durée de l'effet est ainsi multipliée par six comparé à l'effet pharmacologique obtenu après une seule

injection. En outre, dans le meme modèle mini-cochon une libération prolongée de BQ123 du système a été observée pendant une période de 7 jours. En conclusion, **la partie A** de ce travail montre le potentiel des polymères injectables basé sur acide 2-hydroxyoctanoïque pour l'administration intraoculaire.

Dans **la partie B**, des formulations intra-vitréennes réprimant l'angiogenèse par l'inhibition de VEGF-A sont étudiées. Le but **du Chapitre 3** était le développement d'une formulation stable, dans laquelle une combinaison entre les anticorps bevacizumab et ranibizumab avec un corticostéroïde est envisagée. Cette formulation pourrait s'avérer bénéfique en ce qui concerne une réduction du nombre d'injections ou encore un effet synergique potentiel de la combinaison. Les résultats ont montré que le fragment Fab ranibizumab est plus stable que l'anticorps complet bevacizumab, seul ou en combinaison avec les corticostéroïdes. Etonnamment, un retour des agrégats en état monomérique a été observé après adjonction de dexaméthasone phosphate à la formulation de bevacizumab. Le mécanisme sous-jacent à cet effet protecteur a été étudié de façon approfondie dans **le Chapitre 4**. Un modèle 3D du dimère a été développé *in silico*, identifiant une région de contact spécifique entre les deux monomères du bevacizumab. Le « docking » de la dexaméthasone phosphate sur la surface de la protéine révèle que le corticostéroïde est capable d'interagir avec des acides aminés dans cette région de contact, ce qui empêche la formation du dimère. En effet, suite à l'addition de dexaméthasone phosphate, une réduction significative dans la formation des petits agrégats solubles était observée. **Le Chapitre 5** décrit l'identification des autres « disjoncteurs d'agrégats » potentiels, ayant une structure similaire à la dexaméthasone phosphate, mais sans activité thérapeutique. L'AMP a été sélectionnée comme candidat potentiel par « similarity searching ». La prédiction a été supportée par des investigations *in vitro*: une interaction faible entre le bevacizumab et l'AMP a été observée et la petite molécule s'est révélée capable de perturber la formation initiale des agrégats. En conclusion, **la partie B** montre que la combinaison du bevacizumab avec la dexaméthasone phosphate améliore la stabilité de l'anticorps et par conséquent, une formulation combinée pourrait être considérée pour des investigations *in vivo*. En outre, les molécules thérapeutiquement inactives avec un effet stabilisant potentiel, peuvent être envisagées comme excipients pour des formulations d'anticorps.

Abbreviations

AFFF (AF4)	Asymmetrical Flow Field-Flow Fractionation
AMD	Age-Related Macular Degeneration
AMP	Adenosine Monophosphate
ARPE-19 cells	Human Retinal Pigment Epithelial Cells
ATP	Adenosine Triphosphate
BRVO	Branch Retinal Vein Occlusion
ET-1	Endothelin-1
ET_A	$Endothelin_A$
FDA	Food and Drug Administration
GCL	Ganglion Cell Layer
GMP	Guanosine Monophosphate
GPC	Gel Permeation Chromatography
GRAS	Generally Recognized As Safe
Ig	Immunoglobulin
INL	Inner Nuclear Layer
IOP	Intraocular Pressure
IPL	Inner Plexiform Layer
IS	Inner Segments
kDa	Kilo-Dalton
MALS	Multi-Angle Light Scattering
MST	Microscale Thermophoresis
M_n	Number-Average Molecular Weight
MTT	3-(4,5-dimethylthiazol-2-yl)-2,5-Diphenyltetrazolium Bromide
M_w	Weight-Average Molecular Weight
NOS	Nitric Oxide Synthase

ONL	Outer Nuclear Layer
OPL	Outer Plexiform Layer
OS	Outer Segments
PDB	Protein Data Bank
PDI	Polydispersity Index
PLA	Poly(Lactic Acid)
PLGA	Poly(Lactic-*co*-Glycolic Acid)
POE	Poly(Ortho Ester)
RVO	Retinal Vein Occlusion
RVA	Retinal Vessel Analyser
SD	Standard Deviation
SEC	Size Exclusion Chromatography
UPLC	Ultra Performance Liquid Chromatography
VEGF-A	Vascular Endothelial Growth Factor A